Title
Disturbance Regimes and Landscape Heterogeneity in the Boreal Forest

Author
Lyons, Evan Albert

Publication Date
2015

Peer reviewed|Thesis/dissertation

UNIVERSITY OF CALIFORNIA

Los Angeles

Disturbance Regimes and Landscape Heterogeneity in the Boreal Forest

A dissertation submitted in partial satisfaction of the
requirements for the degree Doctor of Philosophy
in Geography

by

Evan Albert Lyons

2015

ABSTRACT OF THE DISSERTATION

Disturbance Regimes and Landscape
Heterogeneity in the Boreal Forest

by

Evan Albert Lyons
Doctor of Philosophy in Geography
University of California, Los Angeles, 2015
Professor Yongwei Sheng, Chair

The boreal forest circles the high northern latitudes but it is far from a continuous carpet of evergreen trees. Rather, the boreal forest is a patchwork of land cover types in constant flux as they recover from wildfire and then are burned again. This fast turnover of land cover makes the boreal forest particularly susceptible to rapid change in response to climate. Furthermore, the boreal forest is an important component of the climate system that pumps heat into the atmosphere and significantly raises northern hemisphere temperatures year-round. As both a major component of the climate system and a sensitive indicator of climate change, the boreal forest is in a feedback loop. The direction of that feedback loop, positive or negative, depends largely on the strength of the land-atmosphere exchange of heat and momentum driven by forest cover and its spatial structure. That spatial structure has yet to be comprehensively measured.

This dissertation used newly available, high resolution, satellite based forest cover data to quantify the heterogeneity of the boreal forest in North America. First, at the local scale, the pattern of forest cover patches within fires were found to be larger, more regularly shaped, and clustered than in unburned forest. The heterogeneity metrics also returned to pre-fire levels relatively quickly. At the continental scale, the landscape heterogeneity maps were analyzed by region, with respect to the northern extent of trees, and disturbance regimes. The boreal forest regions had smaller, more complicated forest patches, and no single dominant forest cover class which was significantly different than the temperate forests that border the region to the south. When compared to two preexisting maps of the boreal treeline, the patch cohesion metric indicated that the tundra ecoregion extended further south into the forested Central and Eastern Canada. Based on this finding, a new patch cohesion-based treeline was drawn which divides the boreal forest and tundra in a standard and repeatable way. Lastly, fires and lakes had the opposite influence on the heterogeneity metric contagion. Fires tended to decrease heterogeneity in the landscape because they were larger than the preexisting forest patches while lakes were smaller and broke up the landscape increasing heterogeneity. The heterogeneity maps produced as a part of this dissertation will continue to provide insight into the spatial pattern of the boreal forest in the future.

The dissertation of Evan Lyons is approved.

Yongkang Xue

Laurence C. Smith

Steven A. Margulis

Yongwei Sheng, Committee Chair

University of California, Los Angeles

2015

This dissertation is dedicated to my wife and companion Jennifer

TABLE OF CONTENTS

LIST OF FIGURES

Figure

LIST OF TABLES

Table

ACKNOWLEDGMENTS

This work was funded in part by the National Science Foundation Office of Polar Programs Grant # ARC-0713903, the National Aeronautics and Space Administration Terrestrial Hydrology Program Grant # NNX08AE51G, and the U.S. Geological Survey (USGS) Landsat Science Team Program Grant # G12PC00071. I thank my advisor Professor Yongwei Sheng for his support and patience, and my committee members Professors Larry Smith, Yongkang Xue, and Steven Margulis.

For starting me on the academic path that brought me here, I thank Professor James Randerson. For his guidance in the field, I thank Professor Ken Hinkel. My fellow graduate students have been inspiring, helpful, and challenging. Without them I could not have made it, so I wish to thank Vena Chu, Jida Wang, Colin Gleason, Scott Stevenson, Andrew Fricker, Andrew Grant, Will Hobbs, Lorna Apper, Timur Hammond, Kebonyethata Dintwe, Tuyen Le, Austin Madson, Marcus Thomson, Nathan Healey, and Barry Winston. From the Geography Department, I wish to thank Kasi MacMurray and Brian Won.

I thank my parents, Margarete and Royal Lyons, my sister Austen Rose Thompson, and brother-in-law Nathaniel Thompson for their belief in me. Lastly, I thank my wife Jennifer Pihlak, to whom I dedicate this dissertation, for being wonderful, patient, tough, and loving through this long process.

VITA

EDUCATION:

- Master of Arts, Geography, 2010. University of California, Los Angeles.
  "Analysis of Error Contributing Factors in Landsat-Based Multitemporal Lake Mapping"
- Bachelor of Science, Earth and Environmental Science, 2005. University of California, Irvine.

RESEARCH:

- PhD Dissertation Research, UCLA Dept. of Geography, 2011 - present
  Landscape heterogeneity in the boreal forest. Advisor: Prof. Yongwei Sheng
- Graduate Student Mentorship, UCLA Dept. of Geography, 2010 - 2011
  Ice-push ridges as a driver of permafrost thaw lake orientation. Advisor: Prof. Yongwei Sheng
- Graduate Student Researcher, UCLA Dept. of Geography, 2007-2010
  Remote sensing of arctic lakes and global lake monitoring. Advisor: Prof. Yongwei Sheng
- Junior Specialist (Remote Sensing), UC Irvine, Dept. of ESS, Jan/2006-Sep/2007
  Diurnal variations in global fire emissions. Advisor: Prof. James Randerson
- Undergraduate Research Assistant, UC Irvine, Dept. of ESS, Jun/2005-Dec/2005.
  Remote sensing of the effects of wildfires in Alaska. Advisor: Prof. James Randerson

AWARDS and HONORS:

- Nominated for UCLA Distinguished Teaching Assistant Award, 2015.
- Third Place, Trivia Contest, Lebowskifest Los Angeles, 2015.
- Geography Department Outstanding Teaching Assistant, 2014.
- University of California, Los Angeles, Graduate Student Mentorship 2010 ($18,000, 2010-2011)
- Outstanding Student Paper Award for Hydrology, AGU Fall Meeting, December 2009.
- Physical Sciences Dean's List, 2003-2005, University of California, Irvine.

PUBLICATIONS:

- Sheng, Yongwei, Chunqiao Song, Jida Wang, Evan A Lyons, Benjamin Knox, Joshua Cox, Feng Gao, (2015) Comprehensive Lake Dynamics Mapping at Continental Scales Using Landsat 8. Submitted to Remote Sensing of Environment.

- Lyons Evan A., Yongwei Sheng. (2015) LakeTime: Automated Seasonal Landsat Scene Selection for Global Terrestrial Hydrology. In Review at Remote Sensing of Environment.

- Lyons Evan A., Yongwei Sheng, Laurence C. Smith, Junli Li, Kenneth M. Hinkel, John D. Lenters, Jida Wang (2013) Quantifying sources of error in multitemporal multisensor lake mapping, International Journal of Remote Sensing Vol. 34, Iss. 22.

- Hinkel, K.M., Y. Sheng, J.D. Lenters, E.A. Lyons, R.A. Beck, W.R. Eisner, and J. Wang. 2012. Thermokarst lakes on the Arctic coastal plain of Alaska: geomorphic controls on bathymetry, Permafrost and Periglacial Processes, 23 (2012): 218–230.

-Hinkel, K. M., J. D. Lenters, Y. W. Sheng, E. A. Lyons, R. A. Beck, W. R. Eisner, E. F. Maurer, J. D. Wang, and B. L. Potter (2012), Thermokarst Lakes on the Arctic Coastal Plain of Alaska: Spatial and Temporal Variability in Summer Water Temperature, Permafrost and Periglacial Processes, 23(3), 207-217.

- Hinkel K. M., Zheng Lin, Yongwei Sheng & Evan A. Lyons (2012): Regional lake ice meltout patterns near Barrow, Alaska, Polar Geography, DOI:10.1080/1088937X.2011.654355

- Wang, Jida, Yongwei Sheng, Kenneth M. Hinkel, Evan A. Lyons, Drained thaw lake basin recovery on the western Arctic Coastal Plain of Alaska using high-resolution digital elevation models and remote sensing imagery, Remote Sensing of Environment, Available online 15 December 2011, ISSN 0034-4257, 10.1016/j.rse.2011.

- Chen, Y., Li, Q., Randerson, J. T., Lyons, E. A., Kahn, R. A., Nelson, D. L., and Diner, D. J.: The sensitivity of CO and aerosol transport to the temporal and vertical distribution of North American boreal fire emissions, Atmos. Chem. Phys., 9, 6559-6580, 2009.

- Lyons, E. A., Y. Jin, and J. T. Randerson (2008), Changes in surface albedo after fire in boreal forest ecosystems of interior Alaska assessed using MODIS satellite observations, J. Geophys. Res., 113, G02012, doi:10.1029/2007JG000606.

- Randerson J. T. et al. The Impact of Boreal Forest Fire on Climate Warming, Science 17 November 2006: Vol. 314. no. 5802, pp. 1130 – 1132 DOI: 10.1126/Science.1132075

Chapter 1

Introduction

The boreal forest is one of the largest biomes on Earth but is often misunderstood as it is radically different from the temperate and tropical forests that we are most familiar with. I began researching the boreal forest before I had ever been there and was confident that the image of the forests in my mind was accurate because I had been looking at satellite images of the region for months. It was only when I arrived, looking out the window of the airplane as we approached Fairbanks, Alaska, that I realized how incorrect I had been. What I saw from that plane was not the continuous carpet of tall evergreen trees that I had expected, but a complex patchwork of meadows, lakes, deciduous and evergreen forest stands of all shapes and sizes. The evergreen trees were nothing like the majestic California Redwoods that I had grown up with, but tough, scraggly black spruce trees not much taller than myself. My first thought, as I looked down at the landscape was, "there is no way that I can get away with using 1 km MODIS pixels here."

Ultimately, I used MODIS anyways because it was the best albedo dataset available at the time and it worked well enough but there were some nagging problems (Lyons et al. 2008). We spent significant time and effort to establish control regions of unburned boreal forest for comparison to forest stands in various stages of post-fire succession. Despite our best efforts, we were never able to find a large region that matched the low albedo values reported by field studies. The problem was that the field studies had selected sites in the middle of small unburned evergreen patches that were not representative of the broader landscape as observed

from the top-down in satellite imagery. I wanted to express and quantify the complexity of the landscape that I had seen from the airplane window and understand the drivers of that complexity.

This goal of a more nuanced understanding of the boreal forest was also motivated by its importance in the global climate system and its potential for feedbacks with future climate change. It has been established that the boreal forest pumps heat into the atmosphere and is therefore responsible for maintaining higher temperatures across the northern hemisphere (Bonan et al. 1992; Bonan et al. 1995; Pielke and Vidale 1995; Liess et al. 2012). The exact mechanisms of this land surface-atmosphere heat flux are not completely understood because many of the processes occur at the scale between field observations and coupled climate models (Zeng and Pielke 1995; Dalu et al. 2000). An improved understanding and parametrization of the spatial structure of the land surface is required first in order to bridge this gap.

This dissertation sets out to map the spatial heterogeneity of the boreal forest and uses that new dataset to answer several science questions. First, how much change does the boreal forest experience within the relatively short time period of satellite data availability and what is driving the change? How does the spatial heterogeneity of forest cover vary within the boreal forest and compared to neighboring regions. Can any landscape pattern metrics be used for mapping the border between the boreal forest and tundra ecoregions as an alternative to manual methods currently used? How do fires and lakes influence the measured heterogeneity of the boreal forest? My hypotheses for these questions were that the boreal forest would have distinct regions with measurably different spatial patterns of forest cover, patch cohesion could be used

to produce a better map of the border between boreal forest and tundra, and that fires and lakes would both act to increase the heterogeneity and complexity of the boreal forest landscape.

The research began at the local scale with mapping land cover changes near Thompson, Manitoba, in central Canada. Here I found rapid changes occurring to the land cover largely caused by fire. Both the direct and indirect effect of fire and successional changes from past fires were significant drivers of the observed land cover change. The forest patches within recently burned were broadly larger, more regularly shaped, and clustered than patches in forest that burned before the observation period.

After the small scale study, I moved up to the continental scale and mapped different heterogeneity metrics across Alaska and Canada. This analysis was based on the Global Forest Cover 2000 dataset which was available at 30 m resolution (Hansen et al. 2013). The resolution and landscape extent of the landscape heterogeneity analysis was carefully chosen to maximize the resolution of the results while avoiding problems of spatial autocorrelation and maintain statistical significance. The boreal forest was more diverse in forest cover classes than neighboring regions with more, smaller forest patches. Most ecoregions within the boreal forest had fairly similar values for most metrics except for one that was dominated by mountains and therefore not representative. Because the patch cohesion values reached above the percolation threshold within the tundra ecoregion, patch cohesion of the sparsest land cover class made an effective tool mapping the border between the tundra and boreal forest. The resulting borderline performed differently than pervious treeline maps but was superior because it was automated rather than relying on manual image interpretation, based on satellite data, and standard and repeatable.

The next task was to analyze the influence of fires and lakes on the heterogeneity of the boreal forest. Fortunately, North American boreal forest fires have been very closely monitored and documented since approximately 1950 by the United States and Canadian governments. Open water was already included as a land cover class in the Global Forest Cover 2000 dataset and available. Comparisons of burned area and lake area with heterogeneity metrics proved inconclusive but the number of fires and number of lakes per 100 km^2 grid cell produced opposite responses in the contagion. Ultimately the scale difference between fires and lakes lead to the divergent responses as the few, large fires homogenized the landscape, increasing contagion values while many small lakes broke up the landscape decreasing contagion.

This dissertation is organized into six chapters. Following this introduction, is an extensive review of the boreal and tundra ecosystems and their role in the global climate system. The gaps in current understanding are highlighted there to explain the motivation for the study. Chapter three describes the local scale study performed in central Canada that laid the groundwork for the continental scale mapping project explained in chapter four. Chapter four also includes some analysis heterogeneity maps that were produced. The variability between ecoregions and the new treeline analysis are explained here. Chapter five focusses on fire and lakes as the drivers of boreal forest heterogeneity. Last is chapter six which contains a summary of the preceding material and conclusions.

References

Bonan, G. B., F. S. Chapin, et al. (1995). "Boreal Forest and Tundra Ecosystems as Components of the Climate System." Climatic Change **29**(2): 145-167.

Bonan, G. B., D. Pollard, et al. (1992). "Effects of boreal forest vegetation on global climate." Nature **359**(6397): 716-718.

Dalu, G. A., R. A. Pielke, et al. (2000). "Heat transport and weakening of atmospheric stability induced by mesoscale flows." Journal of Geophysical Research-Atmospheres **105**(D7): 9349-9363.

Hansen, M., P. Potapov, et al. (2013). "High-resolution global maps of 21st-century forest cover change." Science **342**(6160): 850-853.

Liess, S., P. K. Snyder, et al. (2012). "The effects of boreal forest expansion on the summer Arctic frontal zone." Climate Dynamics **38**(9-10): 1805-1827.

Lyons, E. A., Y. F. Jin, et al. (2008). "Changes in surface albedo after fire in boreal forest ecosystems of interior Alaska assessed using MODIS satellite observations." Journal of Geophysical Research-Biogeosciences **113**(G2).

Pielke, R. A. and P. L. Vidale (1995). "The boreal forest and the polar front." Journal of Geophysical Research-Atmospheres **100**(D12): 25755-25758.

Zeng, X. B. and R. A. Pielke (1995). "Landscape-Induced Atmospheric Flow and its Parameterization in Large-Scale Numerical Models." Journal of Climate **8**(5): 1156-1177.

Chapter 2

Land Cover in the High Latitudes and its Influence on Climate, a Review

Abstract

This literature review discusses the boreal forest and Arctic tundra's function within the broader global climate system, the role of land cover in land atmosphere interactions and circulation, and the driving factors for high latitude land cover change within and between biomes. In order to understand the northern high latitudes, the boreal forest, tundra, and the border between them must be studied together. This comprehensive approach considers these biomes' influence on climate and their responses to climate. Specifically, climate has been shown to strongly influence the position of the boundary between the boreal forest and tundra. Furthermore, dark evergreen trees of the boreal forest have been increasing air temperatures broadly in the northern hemisphere throughout the Holocene and helping to establish the very climatological patterns that are responsible for its position in the first place. The relationship between the tundra and boreal forest is a complex one that is regulated by climate mechanisms that are not sufficiently understood. Coupled climate models are currently unable to resolve mesoscale processes and therefore underestimate the flux of heat from the surface to the atmosphere in the boreal forest. The key to understanding these mechanisms and parameterizing them in a way that can be incorporated into general climate models is in land cover heterogeneity measured at a fine spatial resolution and at the continental to pan-Arctic extent.

2.1 Introduction

Circling the northern high latitudes, the boreal forest, sometimes called taiga, covers 12.2 X 10^8 ha (Landsberg and Gower 1997). Far from a homogeneous carpet of trees, the boreal forest is a patchwork of land cover types including evergreen and deciduous trees, meadows, lakes, and wetlands (Stow et al. 2004; Thof and Fraser 2007). Immediately to the north of this forest is the arctic tundra which features starkly different characteristics dominated by low stature shrubs and grasses (Chapin et al. 2000b). The border between these two biomes is called the boreal treeline or tundra-taiga ecotone (Bryson 1966). Large-scale ecological changes are expected in the Arctic tundra and sub-Arctic boreal forest ecoregions as consequences of continuous anthropogenic climate change (Christensen et al. 2007). These changes can be divided into two categories, changes within each ecoregion and changes in their distribution or movement of the border between them. The region, however, does not simply respond to climate changes, it also actively feeds back to the global climate system to speed up or slow down the rate of warming in the region (Bonan et al. 1995; Chapin et al. 2000b; Euskirchen et al. 2009).

High latitudes biomes are important components of the global climate because of their spatial extent, the persistence and reflective properties of snow and ice (Larsen 1980; Betts and Ball 1997; Kuang and Yung 2000; Loranty et al. 2013), the large variation in the annual cycle of solar radiation (Pinker and Laszlo 1992), and extensive carbon pools (Goodale et al. 2002; Hinkel et al. 2003; Sheng et al. 2004). Much interest is therefore placed on understanding and predicting the region's response to climate change and how that response will impact the climate in turn. The importance of this area of study was highlighted by the Steering Committee of the International Arctic Science Committee (IASC) project on the Dynamics of the Tundra Taiga Boundary who outlined some approaches including four priorities (Callaghan et al. 2002):

Priority 1. Where is the circumarctic treeline now, what are its characteristics, and what is changing?
Priority 2. How has the circumarctic treeline responded to environmental change in the last 100 yrs?
Priority 3. How will circumarctic treelines respond to predicted environmental change, and what are the mechanisms?
Priority 4. What are the environmental impacts of changes in the location and the characteristics of the tundra taiga boundary?

These priorities alone only cover half of the treeline story. The reverse relationship, the treeline's influence on climate and atmospheric circulation, must be included in order to fully understand the region. To accomplish these goals, the boreal forest and tundra must be studied together because they influence each other so strongly (Pielke and Vidale 1995; Liess et al. 2012). This approach to high latitude land surface interactions with climate is novel because it incorporates data from multiple fields across sub-disciplines and across regions.

2.1.1 Topics Covered in this Review

First, this review will discuss the biophysical mechanisms by which the high latitude land surface directly influences climate. Seminal papers by Reed and Kunkel (1960), Bryson (1966), and Bonan et al. (1992) first quantified the impact that boreal forest vegetation has on climate using meteorological data and later using computer models. North of the treeline, changes to the snow season length dominate the observed current climate forcing (Chapin et al. 2005) with increasing shrub populations contributing as well (Sturm et al. 2005a).

In addition to direct climate forcing, there are hypothesized interactions between the tundra-taiga ecotone and atmospheric circulation. The discussion focusses on the paper "The boreal forest and the polar front" (Pielke and Vidale 1995) and attempts by others to reproduce their results (Beringer et al. 2001; Lynch et al. 2001; Liess et al. 2012).

Lastly, land cover change is divided into internal changes in the makeup and pattern of land cover within a biome and large scale migrations of the borders between biomes. In this way the two concepts can be compared in terms of their spatial and temporal scales. Fire and permafrost are analyzed as the direct drivers of land cover change within the boreal forest (Kasischke et al. 2002; Christensen et al. 2004). Migration between biomes largely is driven by climactic changes and occur at much longer time scales (Epstein et al. 2007).

This review treats high latitude land cover's relationship with climate in both directions. Land cover's direct impact on climate is explored through biophysical interactions between the land surface and atmosphere. This is followed by a discussion of the hypothesized dynamic equilibrium of the tundra-taiga ecotone with the Polar Front. Lastly, an analysis of potential responses of high latitude land cover to climate change is presented.

2.1.2 High Latitude Biomes

In spatial extent, the boreal forest is circumpolar. The northernmost extent of forests in North America range from 68 °N latitude in the Brooks Range of Alaska and stretches southeast to 58 °N latitude at the west coast of the Hudson Bay (Larsen 1980) (Figure 1). In Eurasia, the treeline runs East-West at approximately 67 °N latitude from Scandinavia to Central Siberia where it becomes less distinct and runs to the Pacific Coast at approximately 67 °N latitude (Krebs and Barry 1970). The southern extent of the boreal forest is less well defined than the northern ecotone as it gradually transitions into broadleaf deciduous forests, parkland, grassland, and agriculture.

The boreal forest, and high latitudes in general, are characterized by low temperatures and cold tolerant plant species. Plant species diversity is broadly lower than temperate and

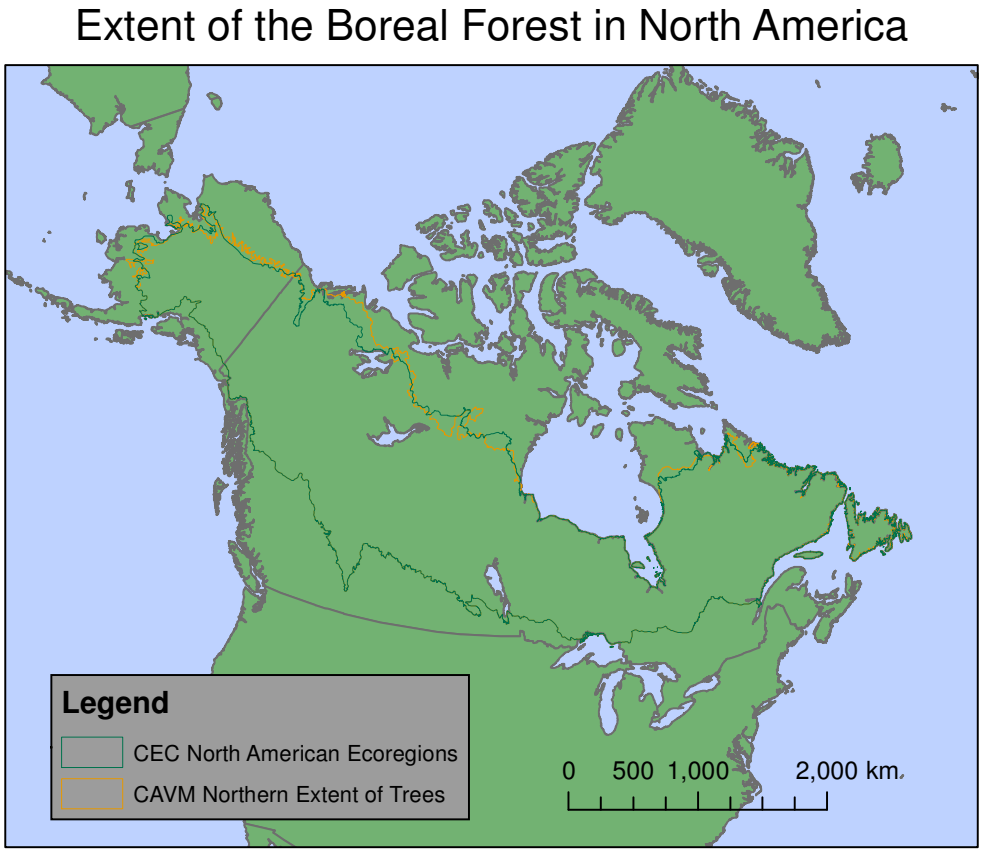

Figure 2.1. Two estimates of the boreal treeline, or the extreme northern extent of trees in North America. The orange line is from the Circumpolar Arctic Vegetation Map (CAVM) and the green line is from the Center for Environmental Cooperation (CEC) map of North American Ecoregions ((CEC) 1997; Nowacki et al. 2001; CAVM_Team 2003).

tropical forests because of the history of glacial and interglacial cycles which have reduced opportunities for specialization (McGlone 1996). The Alaskan and Canadian boreal forest is broadly composed of mixed stands of evergreen conifer species including black spruce (*Picea mariana*), white spruce (*Picea glauca*), and Jack pine (*Pinus banksiana*) and deciduous broadleaf species including quaking aspen (*Populus tremuloides*) and paper birch (*Betula papyrifera*) (Dyrness et al. 1986; Landsberg and Gower 1997). While this review focusses on North America, it is worth noting some similarities and differences between the North American and Eurasian forests. Shrub, moss, and lichen species have generally circumpolar distributions but tree species are much more localized and constrained to a single continent. Thus the primary Eurasian tree species include the conifers Siberian spruce (*Picea* obovata), Manchurian Fir (*Abies nephrolepi*), Scots pine (*Pinus silvestris*), the deciduous conifer Dahurian larch (*Larix gmelinii*), the broadleaf deciduous Eurasian aspen (*Populus tremula*), and Erman's birch (*Betula ermanii*) (Hare and Ritchie 1972). The most conspicuous difference in tree community is the greater extent of larch species in Eurasia than North America (Larsen 1980).

The tundra biome is very different from the boreal forest in its species composition and biophysical properties. The region is dominated by low stature vegetation like sedges, grasses, and some shrubs and is underlain by continuous permafrost. This contrasts the boreal forest which is dominated by evergreen forests and discontinuous permafrost. Historically, tundra regions have been replaced by forests which have reached to the Arctic Ocean as recently as 8000 years ago (MacDonald et al. 2000). Shrub distributions in the tundra have changed more rapidly than the treeline during the Holocene and are currently expanding northward as evidenced by repeat photography (Anderson and Brubaker 1993; Sturm et al. 2001; Stow et al. 2004; Sturm et al. 2005b). Owing to the impervious permafrost, low evaporation rates, and

glacial history, this region has a high concentration of lakes (Lehner and Döll 2004; Smith et al. 2007).

These unique landscapes combine to influence climate in powerful, and sometimes counter-intuitive, ways. This can make the region both interesting and difficult to study. Historically, modeling studies have performed poorly in the region because many were designed in temperate biomes with radically different properties (Bonan et al. 1992). Primary among these differences are the biophysical interactions between snow and vegetation and their impact on climate.

2.2 Biophysical Climate Connections

There are two primary ways that high latitude biomes interact with climate, through the cycling of carbon and other greenhouse gasses and through direct perturbation to the surface energy budget (Bonan et al. 1995). As components of the global carbon cycle, the boreal forest and tundra are currently carbon sinks (Goodale et al. 2002) but the balance is sensitive to temperature and could change to a source in a warmer climate (Goulden et al. 1998; Harden et al. 2000; Walter et al. 2006). The high latitudes also influence climate through the impact of snow cover on the surface radiation budget. The high albedo of snow (generally > 0.9) (Schaaf et al. 2002; Lyons et al. 2008) and its persistence on the ground enhances biophysical climate forcing (Randerson et al. 2006). Unlike tropical and temperate forests, which have a relatively small albedo difference between forested and deforested areas, the boreal forest has a large difference due to exposed snow (Betts 2000; Myhre et al. 2005). Evergreen needleleaf trees, the dominant plant functional type (PFT) in the region, block highly reflective snow in the winter and spring with a relatively dark forest canopy (Chapin et al. 1996; Betts and Ball 1997; Epstein et al.

2001). The absorbed solar energy is partitioned mostly to sensible heat flux because of the rough surface and evergreen needles which restrict evaporation (Pielke et al. 1998; Eugster et al. 2000).

2.2.1 Boreal Forest

A seminal paper by Bonan et al. (1992) replaced the boreal forest with bare ground in the National Center for Atmospheric Research Community Climate Model (CCM1) which resulted in significantly lower temperatures in the region as well as beyond. The largest change was a drop in temperature of 12° C in April at 60° N latitude but modeled temperature decreases of 1° C in January and October extended as far as 10°N latitude (zonally averaged). The modeled change in land cover also resulted in a southward movement of the July 13° C and July 18° C isotherms indicating a more complex causal relationship (Larsen 1980; Bonan et al. 1992). The spring season (March-April-May) had the largest temperature decrease when solar radiation was increasing and snow was still on the surface (Bonan et al. 1995; Snyder et al. 2004; Lyons et al. 2008). More realistic model experiments followed. The Holocene boreal forest extent as indicated by paleobotanical evidence was shown to be responsible for annual mean warming of 1.6° C in North America compared to 1.8°C for orbital forcing alone (Foley et al. 1994). In a fully coupled climate-vegetation model of future warming under a 2X CO_2 regime, high latitude vegetation feedbacks enhanced warming by 1.1° C in spring and 0.5° C in summer in land areas north of 45° N (Levis et al. 1999; Otto et al. 2011). Conversely, a projected 4° C warming in Europe was reduced by 1° C with the inclusion of vegetation feedback effects in a coupled climate-vegetation model due to increased evapotranspiration (Jeong et al. 2010).

After these modeling studies established the boreal forest as a climatologically important region, the Boreal Ecosystem-Atmosphere Study (BOREAS) was undertaken in 1994 and 1996

to further improve the understanding of heat, momentum, water, and carbon fluxes between the boreal ecosystem and the atmosphere (Sellers et al. 1995; Oncley et al. 1997; Sellers et al. 1997). The field data provided by the BOREAS project in addition to the previous meteorological data and general circulation model experiments pointed to additional factors other than albedo as important drivers of atmospheric heating. Although albedo is the primary driving factor in the spring season, surface roughness, evapotranspiration rates, and soil moisture are also important aspects of the land-atmosphere system which are more pronounced in the summer months (Chapin et al. 2000a). These factors are themselves determined largely by vegetation (Thomas and Rowntree 1992; Baldocchi et al. 2000). Further, the initial turbulent (sensible) heat flux from the surface to the Planetary Boundary Layer (PBL) is amplified by mesoscale turbulent eddies caused by heterogeneous land cover including lakes, wetlands, and meadows (Pielke and Vidale 1995; Pielke et al. 1998). In contrast, tundra provides very little atmospheric heating due to low stature grasses and shrubs, broadly homogeneous, low roughness, and higher albedo (Lynch et al. 1999b).

2.2.2 Tundra

There has been considerable study of the shifting snow melt timing because it has large potential for direct climate feedbacks on annual time scales. The seasonal cycle of snow cover controls the length of the growing season, the hydrologic cycle, surface temperatures, permafrost active layer thickness, and surface albedo (Chapin et al. 2000b).

An estimate by Dye (2002) used weekly satellite derived snow cover maps to determine trends in snow melt and snow onset date. They found a significant trend toward earlier snow melt of 3-5 days/decade and a lengthening of the snow free season by 3-6 days/decade from 1972

to 2000. The date of snow onset did not show a significant trend in this study, but others have shown weak trends toward later onset in North America and earlier onset in Eurasia (Frei et al. 1999; Brown 2000).

The strength of the snow cover-climate feedback is controlled by the amount of solar energy that can be reflected or absorbed by the surface. For example the warming trend from 1910-1940 was driven by warmer autumn temperatures which moved the date of snow onset later while the 1970-2000 period had warmer springs and a shifting towards earlier snow melt. The higher incoming solar energy in the spring amplified the snow effect by a factor of three (Euskirchen et al. 2007).

Changes to snow free season length are also amplified or dampened by interactions between the snow and vegetation. Surfaces with the highest seasonal variation in albedo like tundra will experience a larger radiative heating from earlier snowmelt than forests or woody shrublands which have a smaller seasonal variation (Sturm et al. 2005a; Euskirchen et al. 2007). The shift to earlier snow melt and longer snow free season also has impacts on vegetation. Higher spring and summer temperatures cause plants to follow the snow and begin their growing seasons earlier. Snow melt date is also related to soil freeze and thaw in the Arctic which is directly related to plant activity. The date of soil thaw has shifted earlier by 3.3 +/- 1.8 days/decade in tundra from 1988 to 2002 and increased the length of the growing season in North American tundra by 5.1 +/- 2.9 days/decade (Smith et al. 2004). This shift is observable in the seasonal variations in Northern Hemisphere CO_2 concentrations and directly in the greenness of Arctic plants as measured by Normalized Difference Vegetation Index (NDVI). The amplitude of the seasonal cycle of CO_2 concentration has increased 20% as measured in Hawaii and 40% as measured in Barrow Alaska and shifted 7 days earlier relative to the early 1960s

(Keeling et al. 1996). Claims about the "greening" of the Arctic generally are referring to increased NDVI values in the arctic tundra which vary by region. Much of Eurasia shows an increase due to longer growing season length while regions of boreal Alaska and Canada show a decrease due to climate change driven drought (Zhou et al. 2001). The broad trend of increasing greenness in high latitudes was validated by Lucht et al. (2002) who showed that the decreased temperatures after the Pinatubo eruption of 1991 depressed plant productivity even though precipitation and CO_2 concentrations were not as effected. Therefore the trend of earlier budburst and increased plant activity was caused almost entirely by changes in temperature rather than precipitation or direct CO_2 fertilization.

These albedo-vegetation feedbacks in the high latitudes are fairly well understood and have been extensively researched since the Bonan et al. (1992) paper pointed them out so dramatically. A less understood aspect of high latitude climate is the transfer of surface energy into the atmosphere and the influence of that atmospheric heating on circulation (Pielke and Vidale 1995). Since it has been shown that the extent of the boreal forest is largely prescribed by atmospheric circulation patterns, this forms a potential feedback loop wherein the boreal forest and tundra biomes regulate themselves. This relationship, if true, could radically change the predicted rates of northward boreal forest migration.

2.3 Influence on Circulation Patterns

Early studies considered the extents of boreal forests to be largely prescribed by climate circulation patterns, an idea originated at least in part, from Alexander von Humboldt (von Humbodt 1807; Larsen 1980). The northern and southern boundaries of the boreal forest were found to be coincident with the mean summer and winter positions of the Arctic Frontal Zone

respectively (Reed and Kunkel 1960; Bryson 1966) or with the July 13°C (northern) and July 18°C (southern) isotherms (Larsen 1980) or according to the number of months in which the air temperature is greater than 10°C (Woodward 1995) (Figure 2). Using maps of median summer arctic front location and forest-tundra ecotone in Eurasia, Krebs and Barry (1970) proposed that hemispherical scale temperatures and circulation patterns could be influenced by the position of the boreal forest (Figure 3). This hypothesis was later supported by the results of climate models as discussed in the previous section and also by the results of eddy co-variance flux measurements made in the field (Baldocchi et al. 1988). The incorporation of field data from BOREAS and other field campaigns highlighted the role of vegetation in energy partitioning and regulating surface-atmosphere fluxes (Sellers et al. 1995; Sellers et al. 1997; Baldocchi et al. 2000; Baldocchi et al. 2001). The impact of the resulting atmospheric heating over the boreal forest on general circulation is still a matter of debate in the literature (Liess et al. 2012).

It was hypothesized by Pielke and Vidale in 1995 that the atmospheric heating gradient between the boreal forest and tundra was responsible for the placement of the Arctic Summer Front which coincides with the northern treeline (Pielke and Vidale 1995). This bold claim was backed up by field observations during the 1994 BOREAS campaign and it relies on mesoscale eddies in the PBL generated from heterogeneities in the land cover. The eddies produce net radiation difference of 50 Wm^{-2} across the tundra-taiga ecotone (Pielke et al. 1998). Since their publication, several studies have attempted to recreate the results with varying success. Two studies that found particular fault with the hypothesis measured or modeled the boreal forest-tundra net radiation difference as smaller than the 50 Wm^{-2} thought necessary to establish a frontal zone (Beringer et al. 2001; Lynch et al. 2001). Using a limited area run of the ARCSyM model, Lynch et al. (2001) found a peak net radiation difference of 60 Wm^{-2} around

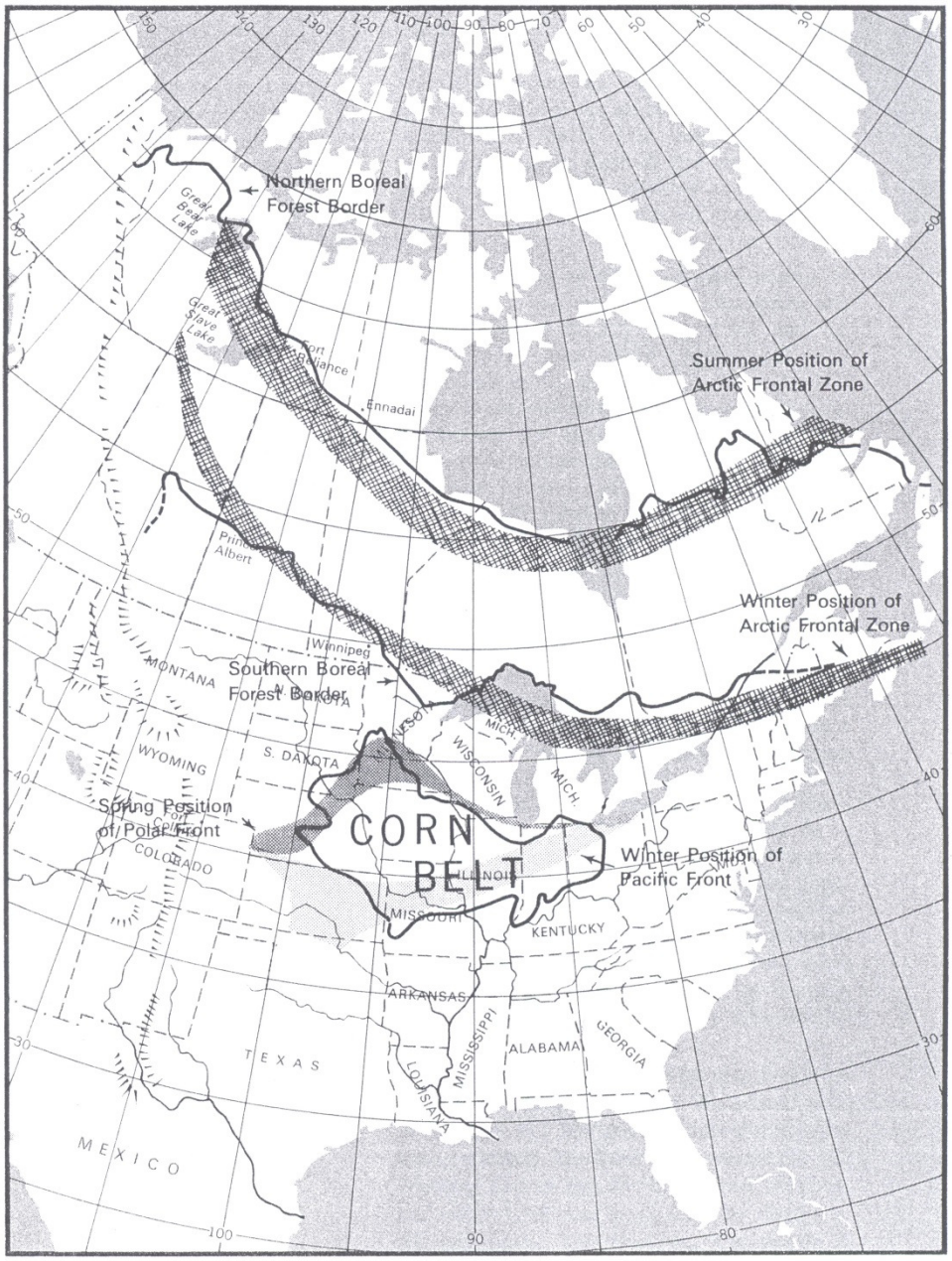

Figure 2.2. The summer and winter positions of the Arctic Frontal Zone (hashed areas) are shown overlaid on top of the northern and southern extents of the boreal forest (solid black lines) for North America (Bryson 1966).

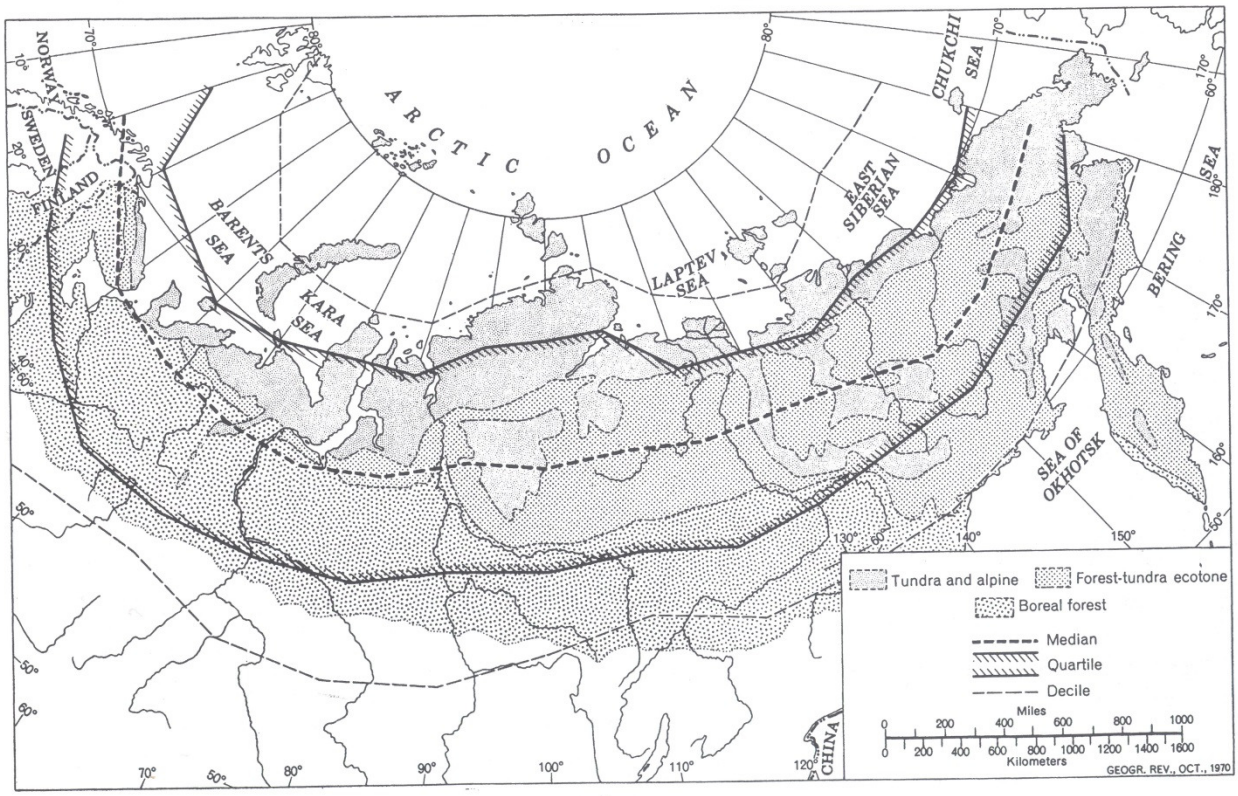

Figure 2.3. The median position of the Arctic Polar Front in Eurasia (dotted line) is shown overlaid on top of the extents of boreal forest and tundra biomes (shaded regions) (Krebs and Barry 1970).

noon but daily mean boreal forest-tundra difference was on the order of 10 Wm^{-2}. This smaller difference was not enough to generate a PBL height difference to drive geostrophic winds and influence regional weather patterns. This study however was conducted in Alaska where the large mountain ranges are the primary drivers of vegetation patterns (Viereck et al. 1986). The prescribed sensible heat flux difference of 12 Wm^{-2} occurred on the Seward Peninsula in Western Alaska which is not representative of the broader forest tundra ecotone in Canada and Eurasia (Lafleur et al. 1992; Lafleur and Rouse 1995). The other study was based on field observations of sensible heat flux and PBL height using eddy covariance towers and vertical radiosonde soundings (Beringer et al. 2001). Again, net radiation differences between forest and tundra sites were less than Pielke and Vidale's 50 Wm^{-2} estimate. Beringer et al. found a net radiation difference of 24.3 Wm^{-2} between tundra and forest sites and 29.6 Wm^{-2} between tundra and woodland sites. This study, however, was also conducted on the Seward Peninsula where the Arctic frontal zone is not as well established as elsewhere in the Arctic (Bryson 1966; Liess et al. 2012). The findings of these studies are then inconclusive with respect to the claims of Pielke and Vidale.

In an attempt to more closely test the direct sensitivity of regional climate to hypothetical boreal forest expansion, Liess et al. (2012) used the regional WRF atmospheric model version 3 with the NOAH-LSM (Land Surface Model) for land surface processes. In contrast to other model simulations, this study "focuses on a more realistic approach of modest boreal forest expansion and use of a regional model capable of resolving finer mesoscale and synoptic scale processes." (Liess et al. 2012). The results generally agreed with previous modeling experiments with regards to aboveground biomass, leaf area, surface albedo, net radiation, partitioning into sensible heat, and surface warming (Bonan et al. 1992; Bonan et al. 1995; Levis et al. 1999;

Snyder et al. 2004; Liess et al. 2012). The daily average net radiation difference between boreal forest and tundra was 19.9 Wm^{-2}, still below the 50 Wm^{-2} estimate of Pielke and Vidale (1995). Net radiation in western North America was generally lower (16.9 Wm^{-2}) than other circumpolar regions which corresponds well with the relatively low values found in western Alaska by other studies (Lynch et al. 1999a; Beringer et al. 2001). Despite the lower net radiation values, the simulated advance of the tundra-taiga ecotone caused a maximum increase of 19 m in the 1000-500-hPa thickness which corresponds well with the theoretical 20 m estimate from Pielke and Vidale (1995) and indicates higher sensitivity of the atmosphere to changes in surface net radiation. Although the modest 19 m increase in the 1000-500 hPa thickness was insufficient to generate its own front, it did influence the position of the Arctic frontal zone after boreal forest expansion. The control simulated Arctic frontal zone corresponded well with reanalysis data for the period 1979-1998 which placed the strongest frontal activity in Eastern Siberia and western Canada (Serreze et al. 2001). After boreal forest expansion, northward shifts in the Arctic frontal zone were observed in Eastern Siberia, central northern Canada, and the western Atlantic Ocean and a southward shift in central Russia. Since there were no changes in the model to CO^2 or sea ice, the northward shifts are "a direct effect of the boreal forest expansion" (Liess et al. 2012). This is a compelling finding that strengthens the case for boreal forest influence on synoptic climate.

It is worth pointing out here that Roger A. Pielke Sr., one of the two authors of Pielke and Vidale (1995), has more recently been accused of being a "climate change denier," a title that he refutes (*Climate Misinformer: Roger Pielke Sr*; Romm 2009). His public comments on the subject include claims that the IPCC is over-emphasizing the role of CO^2 and that heat transfer into and within the oceans is not well resolved in models. Both claims are contested by other

researchers who specialize in those areas and are topics outside of the scope of this study. Roger Pielke Sr.'s work on mesoscale atmospheric dynamics on the other hand is broadly accepted within the scientific community as he has published many highly cited papers in leading journals.

One reason for the Liess model's outperformance of other models in simulating the atmospheric dynamics above the boreal forest is the relatively fine horizontal spatial resolution of 30 km (Liess et al. 2012). This allowed the simulation of mesoscale processes that enhanced mechanical mixing above the PBL (Dalu et al. 2000). A major driver for these mesoscale eddies is heterogeneous land cover in the forested areas (Oncley et al. 1997; Steyaert et al. 1997; Chapin et al. 2000b). Abrupt changes in surface roughness at the forested edges of lakes, meadows, burn scars, etc. drive secondary circulation in addition to the sensible heat fluxes (Pielke et al. 1997). This secondary circulation carries heat further upwards into the atmosphere above the PBL. There has been some work involving mesoscale atmospheric modeling and the parameterization of these phenomena into coarse grained global or regional circulation models (Lynn et al. 1995; Zeng and Pielke 1995; Huang and Margulis 2009). These advances, however, have not been broadly incorporated and still require higher resolution maps of land cover than have been previously available (Gamon et al. 2004; Alsdorf et al. 2007). Instead, often single site based field measurements conducted in homogeneous stands of evergreen needleleaf forest are used as surface flux parameters to represent entire pixels on the scale of hundreds of kilometers (Baldocchi et al. 1988; Swenson and Lawrence 2012). No single land cover type represents the diversity of the boreal forest by itself.

These mesoscale processes, land cover heterogeneity and fluxes, are key to understanding how the treeline impacts atmospheric circulation. It is currently not certain whether the treeline

is stable or unstable with respect to climate change. Small perturbations to the treeline could cause a runaway feedback loop with increasing local temperatures driving further migration if the treeline is unstable. If it is stable, then those same small perturbations would tend to return to a normal state. Thus the fate of these biomes in a changing climate largely depends on the magnitude of these mesoscale processes.

2.4 Modern Drivers of Land Cover

The processes of fire disturbance and permafrost degradation are actively changing the nature of the boreal forest by redistributing plant functional types, lakes, and wetlands (Viereck 1973; Viereck 1983; Johnson 1992; Brown et al. 2002; Kasischke et al. 2002). These disturbance processes are subject to change along with climate and hold the potential for rapid change to the structure of the boreal forest (Payette et al. 2004; Jorgenson and Osterkamp 2005; Kasischke et al. 2010; Mann et al. 2012). Land cover and the processes that determine its distribution are the key to greater understanding of the high latitude environment.

Spatial heterogeneity in boreal forest vegetation is broadly driven by the fire regime. Regular fires in central Alaska create a pattern of early, middle, and late successional vegetation in burn scars with carbon and energy fluxes that change with age (Kasischke et al. 2002; Liu and Randerson 2007; Lyons et al. 2008). Since fires impact so much of the boreal forest so often, small changes to the disturbance regime could lead to rapid (decadal time scales) change at the continental scale.

Lakes and wetlands are important because they are common in the boreal forest and also influence mesoscale atmospheric eddy fluxes (Pielke and Vidale 1995). While the distribution of high latitude lakes is dependent on glacial history, permafrost, and topography (Smith et al.

2007), only permafrost can change on decadal time scales. Responses of high latitude lakes to melting permafrost has been observed in many cases but the nature of the change (increase or decrease in lake abundance) remains poorly understood (Osterkamp et al. 2000; Yoshikawa and Hinzman 2003; Smith et al. 2005).

2.4.1 Internal Vegetation Changes

Here we divide vegetation responses to climate change into internal changes and large-scale migrations. Internal vegetation changes are shifts in the composition of the two broad biomes of Arctic tundra and boreal forest. Changes to the structure of these biomes can be from disturbance, direct climate factors like CO^2 fertilization, drought, temperature, and direct human impact.

Fire is the primary factor controlling vegetation structure and dynamics in the boreal forest because it directly impacts a larger percentage of the region than any other disturbance. During the period from 1950 through 2004, 30% of the Alaskan interior burned (Lyons et al. 2008). More broadly, 87.4×10^4 km^2 of the boreal forest in North America burned over the period of 1959 – 1999 (Kasischke and Turetsky 2006). Wildfires in the boreal forest remove mature evergreen forests and replace them with grasslands and shrubs which eventually return to evergreen forest (Van Cleve and Viereck 1981; Dyrness et al. 1986). Thus the fires are stand replacing and have a fire return time of approximately 80-150 years (Larsen 1997; Lyons et al. 2008) but are expected to increase in frequency due to drought stress, longer fire season, and higher temperatures (Flannigan et al. 1998; Kasischke and Turetsky 2006; Kasischke et al. 2010).

Increased fire frequency will replace more mature forests with younger deciduous forests which have a higher albedo. The negative radiative forcing from increased albedo more than offsets the greenhouse gasses released during the fire (Randerson et al. 2006). Likewise, a decrease in fire frequency would cause a positive radiative forcing and a net warming effect. The relationship between fire and climate in high latitudes is a negative feedback, but the net climate effect of fires in the tropics is the opposite (Claussen et al. 2001). Active fire suppression and carbon sequestration through aforestation are both being considered for climate change mediation in the tropics but if those policies were extended into the high northern latitudes, they would have the opposite of the desired effect (Betts 2000). Floods and timber harvest are also disturbances that play a role in establishing boreal forest structure and operate much in the same was as fire but on different spatial and temporal scales.

In the Arctic tundra, increased woody shrub abundance has been observed and the many associated climate feedbacks are beginning to be explored (Sturm et al. 2001; Sturm et al. 2005a; Euskirchen et al. 2009). Shrubs have increased in area by 1.2% per decade, and increased in coverage from 14% to 20% of the Alaskan North Slope (Sturm et al. 2001). Shrubs are able to grow in regions that are too cold for trees because their dwarf stature decouples them from the atmosphere, thus insulating them and increasing winter temperatures immediately adjacent to the plant (Sturm et al. 2005b). Increasing winter temperatures are allowing shrubs to grow in regions previously covered by grasses and forbs while existing shrubs are becoming more woody and growing taller. Shrubs also require more nitrogen than annual grasses and their growth is therefore nitrogen limited. Increased shrub abundance also increases snow depth by generating snowdrifts. The snow insulates the soil in the winter which allows some microbes in the soil to produce more nitrogen, thereby allowing more shrubs to grow nearby (Sturm et al. 2005b)

The impact of shrubs on late winter and early spring albedo depends on the snow depth, shrub height, and compressibility (Sturm et al. 2005a). Taller and woodier, less compressible, shrubs will be able to project canopies above the snow and lower albedo while shorter, more compressible shrubs will be completely buried. Woodier shrubs over a larger area will therefore lower albedo. The radiative forcing from the observed shrub increase is 0.08 Wm^{-2} and would be 6.37 Wm-2 if all tundra were replaced by shrubs (Chapin et al. 2005). Along with lowering the albedo of the Arctic region in general, an increase in shrubs or trees in the tundra would decrease the importance of changes in snow cover and timing When compared to measured shrub increases and tree line shifts, the warming due to snowmelt advance is responsible for 95% of the observed atmospheric heating. That number falls to 28 and 5% when the tundra is replaced entirely with shrubs and forests respectively (Chapin et al. 2005). This finding also highlights the temporal scales involved in these different climate change effects. Changes to snow cover can occur on the daily or weekly scale, a gradual change in vegetation within the tundra or boreal forest could occur on the decadal scale, and the migration of trees significantly northward into the tundra would occur on the century scale.

2.4.2 Large-Scale Migration

Large-scale migration is a change in the relative areas of the boreal forest and Arctic tundra. Here the two biomes are considered to be homogeneous with a clear boundary between them. Some climate driven, large scale factors that determine the location of the tundra-taiga ecotone have already been discussed in this paper. At the forest stand and individual tree scale, there is a different set of ecophysiological factors that differ across space and time and all have different responses to climate change (Grace et al. 2002). There are five physiological

explanations of tree line formation: 1. Tree growth is limited due to stress on the plant from frost and other stressors, 2. Trees are not able to recover as fast as shrubs and grasses from disturbances such as damage from wind and herbivory, 3. Pollination, seed growth, seed dispersal, germination, and seedling establishment are limited and suppress recruitment at higher latitudes, 4. Carbon uptake and loss are out of balance making maintenance of tree biomass impossible, 5. Carbon utilization rate is decreased by low temperatures so that a plant cannot maintain biomass even with enough raw materials (Korner 1998). In reality, the location of any species along the tree line is explained by one or more of these hypotheses. The complex interactions of these factors make the response of the tree line nonlinear with respect to climate and therefore difficult to predict (Epstein et al. 2007). Predictive computer models have been developed and put to use on the problem with mixed results. BIOME4 is a global dynamic equilibrium vegetation model that contains five tundra PFTs, three extreme cold climate PFTs, two cold forest PFTs, and a cold parkland PFT [Kaplan and New, 2006]. As an equilibrium model, BIOME4 was first run with current climate values from reanalysis data and validated against current observed vegetation distributions. BIOME4 overestimated the current northern extent of tundra because it did not include soil types that are important limiters for tundra growth in the high Arctic. Cold forest extent was also exaggerated in western Alaska due to similar inability to model soil distribution (New et al. 2002; Epstein et al. 2004). When at equilibrium with a 2° C warmer climate, forests broadly increased in area at the expense of parkland and tundra. The change in forest cover under the robust mean climate scenario was an increase of 8710.3 km^2 (55.8%) coupled with a decrease of 4275.0 km^2 (-42.0%) in tundra area (Epstein et al. 2007).

Because BIOME4 is an equilibrium vegetation model and not mechanistic, it cannot tell us with any certainty, the timing of its predicted changes (Kittel et al. 2000). The model cannot, due to computing limitations, include the complexity of climate feedbacks that we know are important in accelerating or slowing the climate change (Epstein et al. 2007). Other models that operate on smaller spatial scales can, however, include more complex climate interactions and give us insight into the time lags associated with large-scale vegetation migration. TreeMig is a dynamic forest stand model that can determine population dynamics at the species, rather than PFT, level and includes seed production and dispersal, germination, growth, competition, and mortality (Lischke et al. 2006). TreeMig simulations, with similar climate values as the BIOME4 experiment, show the time required when migration mechanisms are taken into account. The forest expansion speed slows from 235 m/yr to 177 m/yr when migration mechanisms are included in the simulation (Epstein et al. 2007). The results from TreeMig indicate that the potential vegetation distributions simulated in the BIOME4 model, while possible, are not likely to happen for several centuries.

2.5 Summary

Study of the high northern latitudes requires a broad approach that considers the boreal forest and tundra biomes as dynamic components of the climate system. The region influences climate by regulating air temperature and circulation patterns throughout the northern hemisphere but it is also largely prescribed by those same patterns. This understanding is the result of studies from different sub-fields using different methods. Early studies of storm track and other data showed the first indications that the extent of the boreal forest was coincident with a suite of meteorological parameters like the Arctic frontal zone or 13° C isotherm. Climate

modeling experiments pointed out the importance of the extent and positioning of the boreal forest to global temperatures. Remote sensing studies have identified and measured changes within and between the boreal forest and tundra biomes. Eddy covariance flux measurements from field campaigns like BOREAS have focused on the effect of vegetation structure on energy partitioning and atmospheric heating. The next steps for research in this area involve building links between these fields to answer big questions about the state of high latitude climate as a whole.

One of these big questions is whether the boreal treeline is somewhat stable and resistant to change or is simply an expression of climatological conditions and would move along with them in the future. Previous work has pointed to a more complex relationship but it is only beginning to be properly understood. The implications of this treeline-climate relationship are profound as it would form either a positive or negative feedback loop with climate change. The width of the scientific disagreement on the subject is evidenced by two quotes from studies on the boreal forest and the Arctic frontal zone. One states that "it is an intriguing possibility that the boreal forest and climate are locked in a type of homeostatic relationship that might act to dampen the effects of climate change" (Liess et al. 2012). The other suggests "that transitions in vegetation that result from climate warming will result in a positive feedback to further warming in the Arctic" (Beringer et al. 2005). These opposing statements clearly indicate a field in need of further investigation.

2.6 References

(CEC), Comission for Environmental Cooperation. 1997. Ecological Regions of North America. edited by United States Environmental Protection Agency.

Alsdorf, D. E., E. Rodriguez, and D. P. Lettenmaier. 2007. "Measuring surface water from space." *Reviews of Geophysics* no. 45 (2):24. doi: Rg2002
10.1029/2006rg000197.

Anderson, PM, and LB Brubaker. 1993. "Holocene vegetation and climate histories of Alaska. ." In *Global Climates Since the Last Glacial Maximum*, edited by Kutzbach JE Wright HE, Ruddiman WF, Street-Perrott FA, Bartlein P, 386 - 400. Minneapolis: University of Minnesota Press.

Baldocchi, D. D., B. B. Hicks, and T. P. Meyers. 1988. "Measuring biosphere-atmosphere exchanges of biologically related gases with micrometeorological methods." *Ecology* no. 69 (5):1331-1340.

Baldocchi, D., E. Falge, L. H. Gu, R. Olson, D. Hollinger, S. Running, P. Anthoni, C. Bernhofer, K. Davis, R. Evans, J. Fuentes, A. Goldstein, G. Katul, B. Law, X. H. Lee, Y. Malhi, T. Meyers, W. Munger, W. Oechel, K. T. P. U, K. Pilegaard, H. P. Schmid, R. Valentini, S. Verma, T. Vesala, K. Wilson, and S. Wofsy. 2001. "FLUXNET: A new tool to study the temporal and spatial variability of ecosystem-scale carbon dioxide, water vapor, and energy flux densities." *Bulletin of the American Meteorological Society* no. 82 (11):2415-2434. doi: 10.1175/1520-0477(2001)082<2415:fantts>2.3.co;2.

Baldocchi, D., F. M. Kelliher, T. A. Black, and P. Jarvis. 2000. "Climate and vegetation controls on boreal zone energy exchange." *Global Change Biology* no. 6:69-83.

Beringer, J., F. S. Chapin, C. C. Thompson, and A. D. McGuire. 2005. "Surface energy exchanges along a tundra-forest transition and feedbacks to climate." *Agricultural and Forest Meteorology* no. 131 (3-4):143-161.

Beringer, J., N. J. Tapper, I. McHugh, F. S. Chapin, A. H. Lynch, M. C. Serreze, and A. Slater. 2001. "Impact of Arctic treeline on synoptic climate." *Geophysical Research Letters* no. 28 (22):4247-4250. doi: 10.1029/2001gl012914.

Betts, A. K., and J. H. Ball. 1997. "Albedo over the boreal forest." *Journal Of Geophysical Research-Atmospheres* no. 102 (D24):28901-28909.

Betts, R. A. 2000. "Offset of the potential carbon sink from boreal forestation by decreases in surface albedo." *Nature* no. 408 (6809):187-190.

Bonan, G. B., F. S. Chapin, and S. L. Thompson. 1995. "Boreal Forest and Tundra Ecosystems as Components of the Climate System." *Climatic Change* no. 29 (2):145-167.

Bonan, G. B., D. Pollard, and S. L. Thompson. 1992. "Effects of boreal forest vegetation on global climate." *Nature* no. 359 (6397):716-718.

Brown, J., O.J. Ferrians Jr., J.A. Heginbottom, and E.S. Melnikov. 2002. Circum-Arctic Map of Permafrost and Ground-Ice Conditions. Version 2. edited by National Snow and Ice Data Center. Boulder, Colorado USA.

Brown, R. D. 2000. "Northern hemisphere snow cover variability and change, 1915-97." *Journal of Climate* no. 13 (13):2339-2355.

Bryson, Reid A. 1966. "Air Masses, Streamlines and the Boreal Forest." *Geographical Bulletin* no. 8 (3):228-269.

Callaghan, T. V., R. M. M. Crawford, M. Eronen, A. Hofgaard, S. Payette, W. G. Rees, O. Skre, J. Sveinbjornsson, T. K. Vlassova, and B. R. Werkman. 2002. "The dynamics of the tundra-taiga boundary: An overview and suggested coordinated and integrated approach to research." *Ambio*:3-5.

CAVM_Team. 2003. Circumpolar Arctic Vegetation Map. U.S. Fish and Wildlife Service, Anchorage, Alaska.

Chapin, F. S., M. S. BretHarte, S. E. Hobbie, and H. L. Zhong. 1996. "Plant functional types as predictors of transient responses of arctic vegetation to global change." *Journal of Vegetation Science* no. 7 (3):347-358. doi: 10.2307/3236278.

Chapin, F. S., W. Eugster, J. P. McFadden, A. H. Lynch, and D. A. Walker. 2000a. "Summer differences among Arctic ecosystems in regional climate forcing." *Journal of Climate* no. 13 (12):2002-2010. doi: 10.1175/1520-0442(2000)013<2002:sdaaei>2.0.co;2.

Chapin, F. S., A. D. McGuire, J. Randerson, R. Pielke, D. Baldocchi, S. E. Hobbie, N. Roulet, W. Eugster, E. Kasischke, E. B. Rastetter, S. A. Zimov, and S. W. Running. 2000b. "Arctic and boreal ecosystems of western North America as components of the climate system." *Global Change Biology* no. 6:211-223.

Chapin, F. S., M. Sturm, M. C. Serreze, J. P. McFadden, J. R. Key, A. H. Lloyd, A. D. McGuire, T. S. Rupp, A. H. Lynch, J. P. Schimel, J. Beringer, W. L. Chapman, H. E. Epstein, E. S. Euskirchen, L. D. Hinzman, G. Jia, C. L. Ping, K. D. Tape, C. D. C. Thompson, D. A. Walker, and J. M. Welker. 2005. "Role of land-surface changes in Arctic summer warming." *Science* no. 310 (5748):657-660.

Christensen, J.H., B. Hewitson, A. Busuioc, A. Chen, X. Gao, I. Held, R. Jones, R.K. Kolli, W.-T. Kwon, R. Laprise, V. Magaña Rueda, L. Mearns, C.G. Menéndez, J. Räisänen, A. Rinke, Sarr A., and P. Whetton. 2007. "Regional Climate Projections." In *Climate Change 2007: The Physical Science Basis. Contribution of Working Group I to the Fourth Assessment Report of the Intergovernmental Panel on Climate Change*, edited by S. Solomon, D. Qin, M. Manning, Z. Chen, M. Marquis, K.B. Averyt, M. Tignor and

H.L. Miller, 847-940. Cambridge, United Kingdom and New York, NY, USA: Cambridge University Press.

Christensen, T. R., T. R. Johansson, H. J. Akerman, M. Mastepanov, N. Malmer, T. Friborg, P. Crill, and B. H. Svensson. 2004. "Thawing sub-arctic permafrost: Effects on vegetation and methane emissions." *Geophysical Research Letters* no. 31 (4). doi: L04501 Artn l04501.

Claussen, M., V. Brovkin, and A. Ganopolski. 2001. "Biogeophysical versus biogeochemical feedbacks of large-scale land cover change." *Geophysical Research Letters* no. 28 (6):1011-1014.

Climate Misinformer: Roger Pielke Sr. 2013. 2013]. Available from http://www.skepticalscience.com/skeptic_Roger_Pielke_Sr.htm.

Dalu, G. A., R. A. Pielke, P. L. Vidale, and M. Baldi. 2000. "Heat transport and weakening of atmospheric stability induced by mesoscale flows." *Journal of Geophysical Research-Atmospheres* no. 105 (D7):9349-9363. doi: 10.1029/1999jd901064.

Dye, D. G. 2002. "Variability and trends in the annual snow-cover cycle in Northern Hemisphere land areas, 1972-2000." *Hydrological Processes* no. 16 (15):3065-3077.

Dyrness, C. T., L. A. Viereck, and K. Van Cleve. 1986. "Fire in taiga communities of interior Alaska." In *Ecological series volume 57: forest ecosystems in the Alaskan taiga*, edited by K. Van Cleve, F. S. Chapin, P. W. Flanagan, L. A. Viereck and C. T. Dyrness, 74-86. New York: Springer Verlag.

Epstein, H. E., J. Beringer, W. A. Gould, A. H. Lloyd, C. D. Thompson, F. S. Chapin, G. J. Michaelson, C. L. Ping, T. S. Rupp, and D. A. Walker. 2004. "The nature of spatial transitions in the Arctic." *Journal of Biogeography* no. 31 (12):1917-1933.

Epstein, H. E., F. S. Chapin, M. D. Walker, and A. M. Starfield. 2001. "Analyzing the functional type concept in arctic plants using a dynamic vegetation model." *Oikos* no. 95 (2):239-252.

Epstein, H. E., Q. Yu, J. O. Kaplan, and H. Lischke. 2007. "Simulating future changes in Arctic and subarctic vegetation." *Computing in Science & Engineering* no. 9 (4):12-23.

Eugster, W., W. R. Rouse, R. A. Pielke, J. P. McFadden, D. D. Baldocchi, T. G. F. Kittel, F. S. Chapin, G. E. Liston, P. L. Vidale, E. Vaganov, and S. Chambers. 2000. "Land-atmosphere energy exchange in Arctic tundra and boreal forest: available data and feedbacks to climate." *Global Change Biology* no. 6:84-115. doi: 10.1046/j.1365-2486.2000.06015.x.

Euskirchen, E. S., A. D. McGuire, and F. S. Chapin. 2007. "Energy feedbacks of northern high-latitude ecosystems to the climate system due to reduced snow cover during 20th century warming." *Global Change Biology* no. 13 (11):2425-2438.

Euskirchen, E. S., A. D. McGuire, F. S. Chapin, S. Yi, and C. C. Thompson. 2009. "Changes in vegetation in northern Alaska under scenarios of climate change, 2003-2100: implications for climate feedbacks." *Ecological Applications* no. 19 (4):1022-1043. doi: 10.1890/08-0806.1.

Flannigan, M. D., Y. Bergeron, O. Engelmark, and B. M. Wotton. 1998. "Future wildfire in circumboreal forests in relation to global warming." *Journal of Vegetation Science* no. 9 (4):469-476.

Foley, J. A., J. E. Kutzbach, M. T. Coe, and S. Levis. 1994. "Feedbacks Between Climate and Boreal Forests During the Holocene Epoch." *Nature* no. 371 (6492):52-54. doi: 10.1038/371052a0.

Frei, A., D. A. Robinson, and M. G. Hughes. 1999. "North American snow extent: 1900-1994." *International Journal of Climatology* no. 19 (14):1517-1534.

Gamon, J. A., K. F. Huemmrich, D. R. Peddle, J. Chen, D. Fuentes, F. G. Hall, J. S. Kimball, S. Goetz, J. Gu, K. C. McDonald, J. R. Miller, M. Moghaddam, A. F. Rahman, J. L. Roujean, E. A. Smith, C. L. Walthall, P. Zarco-Tejada, B. Hu, R. Fernandes, and J. Cihlar. 2004. "Remote sensing in BOREAS: Lessons leamed." *Remote Sensing of Environment* no. 89 (2):139-162. doi: 10.1016/j.rse.2003.08.017.

Goodale, C. L., M. J. Apps, R. A. Birdsey, C. B. Field, L. S. Heath, R. A. Houghton, J. C. Jenkins, G. H. Kohlmaier, W. Kurz, S. R. Liu, G. J. Nabuurs, S. Nilsson, and A. Z. Shvidenko. 2002. "Forest carbon sinks in the Northern Hemisphere." *Ecological Applications* no. 12 (3):891-899.

Goulden, M.L., S.C. Wofsy, J.W. Harden, S.E. Trumbore, P.M. Crill, S.T. Gower, T. Fries, B.C. Daube, S.-M. Fan, D.J. Sutton, A. Bazzaz, and J.W. Munger. 1998. "Sensitivity of boreal forest carbon balance to warming." *Science* no. 279:214-217.

Grace, J., F. Berninger, and L. Nagy. 2002. "Impacts of Climate Change on the Tree Line." *Annals of Botany* (90):537-544.

Harden, J. W., S. E. Trumbore, B. J. Stocks, A. Hirsch, S. T. Gower, K. P. O'Neill, and E. S. Kasischke. 2000. "The role of fire in the boreal carbon budget." *Global Change Biology* no. 6:174-184.

Hare, F. K., and J. C. Ritchie. 1972. "Boreal Bioclimates." *Geographical Review* no. 62 (3):332-365.

Hinkel, K. M., W. R. Eisner, J. G. Bockheim, F. E. Nelson, K. M. Peterson, and X. Y. Dai. 2003. "Spatial extent, age, and carbon stocks in drained thaw lake basins on the Barrow Peninsula, Alaska." *Arctic Antarctic and Alpine Research* no. 35 (3):291-300.

Huang, Hsin-Yuan, and Steven A. Margulis. 2009. "On the impact of surface heterogeneity on a realistic convective boundary layer." *Water Resources Research* no. 45 (4):W04425. doi: 10.1029/2008wr007175.

Jeong, Su-Jong, Chang-Hoi Ho, Kwang-Yul Kim, Jinwon Kim, Jee-Hoon Jeong, and Tae-Won Park. 2010. "Potential impact of vegetation feedback on European heat waves in a 2 x CO (2) climate." *Climatic Change* no. 99 (3-4):625-635. doi: 10.1007/s10584-010-9808-7.

Johnson, E.A. 1992. *Fire and Vegetation Dynamics: Studies from the North American Boreal Forest*. Edited by H.J.B. Birks, *Cambridge Studies in Ecology*: Cambridge University Press.

Jorgenson, M. T., and T. E. Osterkamp. 2005. "Response of boreal ecosystems to varying modes of permafrost degradation." *Canadian Journal of Forest Research-Revue Canadienne De Recherche Forestiere* no. 35 (9):2100-2111. doi: 10.1139/x05-153.

Kasischke, E. S., and M. R. Turetsky. 2006. "Recent changes in the fire regime across the North American boreal region - Spatial and temporal patterns of burning across Canada and Alaska." *Geophysical Research Letters* no. 33 (9):L09703, doi:10.1029/2006GL025677. doi: L09703
Artn l09703.

Kasischke, E. S., D. Williams, and D. Barry. 2002. "Analysis of the patterns of large fires in the boreal forest region of Alaska." *International Journal of Wildland Fire* no. 11 (2):131-144.

Kasischke, Eric S., David L. Verbyla, T. Scott Rupp, A. David McGuire, Karen A. Murphy, Randi Jandt, Jennifer L. Barnes, Elizabeth E. Hoy, Paul A. Duffy, Monika Calef, and Merritt R. Turetsky. 2010. "Alaska's changing fire regime - implications for the vulnerability of its boreal forests." *Canadian Journal of Forest Research-Revue Canadienne De Recherche Forestiere* no. 40 (7):1313-1324. doi: 10.1139/x10-098.

Keeling, C. D., J. F. S. Chin, and T. P. Whorf. 1996. "Increased activity of northern vegetation inferred from atmospheric CO2 measurements." *Nature* no. 382 (6587):146-149.

Kittel, T. G. F., W. L. Steffen, and F. S. Chapin. 2000. "Global and regional modelling of Arctic-boreal vegetation distribution and its sensitivity to altered forcing." *Global Change Biology* no. 6:1-18. doi: 10.1046/j.1365-2486.2000.06011.x.

Korner, C. 1998. "A re-assessment of high elevation treline positions and their explanaition." *Oecologia* (115):445-459.

Krebs, J. S., and R. G. Barry. 1970. "Arctic Front and Tundra-Taiga Boundary in Eurasia." *Geographical Review* no. 60 (4):548-554. doi: 10.2307/213773.

Kuang, Z. M., and Y. L. Yung. 2000. "Observed albedo decrease related to the spring snow retreat." *Geophysical Research Letters* no. 27 (9):1299-1302.

Lafleur, P. M., and W. R. Rouse. 1995. "Energy Partitioning at Treeline Forest and Tundra Sites and its Sensitivity to Climate-Change." *Atmosphere-Ocean* no. 33 (1):121-133.

Lafleur, P. M., W. R. Rouse, and D. W. Carlson. 1992. "Energy-Balance Differences and Hydrologic Impacts Arcoss the Northern Treeline." *International Journal of Climatology* no. 12 (2):193-203. doi: 10.1002/joc.3370120208.

Landsberg, J.J., and S. T. Gower. 1997. *Applications of physiological ecology to forest management*. San Diego: Academic Press.

Larsen, C. P. S. 1997. "Spatial and temporal variations in boreal forest fire frequency in northern Alberta." *Journal Of Biogeography* no. 24 (5):663-673.

Larsen, J. A. 1980. *The boreal ecosystem*, *The boreal ecosystem.*: Academic Press, New York, London etc.

Lehner, B., and P. Döll. 2004. "Development and validation of a global database of lakes, reservoirs and wetlands." *Journal of Hydrology* no. 296 (1-4):1-22. doi: 10.1016/j.jhydrol.2004.03.028.

Levis, S., J. A. Foley, and D. Pollard. 1999. "Potential high-latitude vegetation feedbacks on CO2-induced climate change." *Geophysical Research Letters* no. 26 (6):747-750. doi: 10.1029/1999gl900107.

Liess, Stefan, Peter K. Snyder, and Keith J. Harding. 2012. "The effects of boreal forest expansion on the summer Arctic frontal zone." *Climate Dynamics* no. 38 (9-10):1805-1827. doi: 10.1007/s00382-011-1064-7.

Lischke, H., N. E. Zimmermann, J. Bolliger, S. Rickebusch, and T. J. Loffler. 2006. "TreeMig: A forest-landscape model for simulating spatio-temporal patterns from stand to landscape scale." *Ecological Modelling* no. 199 (4):409-420.

Liu, H., and J. T. Randerson. 2007. "Interannual variability of surface energy exchange depends on stand age in a boreal forest fire chronosequence." *Journal of Geophysical Research-Biogeosciences* no. In press.

Loranty, Michael M., Logan T. Berner, Scott J. Goetz, Yufang Jin, and James T. Randerson. 2013. "Vegetation controls on northern high latitude snow-albedo feedback: observations and CMIP5 model predictions." *Global Change Biology*:n/a-n/a. doi: 10.1111/gcb.12391.

Lucht, W., I. C. Prentice, R. B. Myneni, S. Sitch, P. Friedlingstein, W. Cramer, P. Bousquet, W. Buermann, and B. Smith. 2002. "Climatic control of the high-latitude vegetation greening trend and Pinatubo effect." *Science* no. 296:1687-1689.

Lynch, A. H., G. B. Bonan, F. S. Chapin, and W. Wu. 1999a. "Impact of tundra ecosystems on the surface energy budget and climate of Alaska." *Journal of Geophysical Research-Atmospheres* no. 104 (D6):6647-6660. doi: 10.1029/98jd02798.

Lynch, A. H., F. S. Chapin, L. D. Hinzman, W. Wu, E. Lilly, G. Vourlitis, and E. Kim. 1999b. "Surface energy balance on the arctic tundra: Measurements and models." *Journal of Climate* no. 12 (8):2585-2606. doi: 10.1175/1520-0442(1999)012<2585:sebota>2.0.co;2.

Lynch, A. H., A. G. Slater, and M. Serreze. 2001. "The Alaskan Arctic frontal zone: Forcing by orography, coastal contrast, and the boreal forest." *Journal of Climate* no. 14 (23):4351-4362. doi: 10.1175/1520-0442(2001)014<4351:taafzf>2.0.co;2.

Lynn, B. H., F. Abramopoulos, and R. Avissar. 1995. "Using Symilarity Theory to Parameteriza Mesoscale Heat Fluxes Generated by Subgrid-Scale Landscape Discontinuities in GCMs." *Journal of Climate* no. 8 (4):932-951. doi: 10.1175/1520-0442(1995)008<0932:usttpm>2.0.co;2.

Lyons, E. A., Y. F. Jin, and J. T. Randerson. 2008. "Changes in surface albedo after fire in boreal forest ecosystems of interior Alaska assessed using MODIS satellite observations." *Journal of Geophysical Research-Biogeosciences* no. 113 (G2). doi: 10.1029/2007jg000606.

MacDonald, G. M., A. A. Velichko, C. V. Kremenetski, O. K. Borisova, A. A. Goleva, A. A. Andreev, L. C. Cwynar, R. T. Riding, S. L. Forman, T. W. D. Edwards, R. Aravena, D. Hammarlund, J. M. Szeicz, and V. N. Gattaulin. 2000. "Holocene treeline history and climate change across northern Eurasia." *Quaternary Research* no. 53 (3):302-311. doi: 10.1006/qres.1999.2123.

Mann, Daniel H., T. Scott Rupp, Mark A. Olson, and Paul A. Duffy. 2012. "Is Alaska's Boreal Forest Now Crossing a Major Ecological Threshold?" *Arctic Antarctic and Alpine Research* no. 44 (3):319-331. doi: 10.1657/1938-4246-44.3.319.

McGlone, Matt S. 1996. "When History Matters: Scale, Time, Climate and Tree Diversity." *Global Ecology and Biogeography Letters* no. 5 (6):309-314. doi: 10.2307/2997586.

Myhre, A., M. M. Kvalevag, and C. Schaaf. 2005. "Radiative forcing due to anthropogenic vegetation change based on MODIS surface albedo data." *Geophysical Research Letters* no. 32, L21410 (10.1029/2005GL024004).

New, M., D. Lister, M. Hulme, and I. Makin. 2002. "A high-resolution data set of surface climate over global land areas." *Climate Research* no. 21 (1):1-25.

Nowacki, G., P. Spencer, T. Brock, M. Fleming, and T. Jorgenson. 2001. Ecoregions of Alaska and Neighboring Terroitory. Reston, VA: USGS.

Oncley, S. P., D. H. Lenschow, T. L. Campos, K. J. Davis, and J. Mann. 1997. "Regional-scale surface flux observations across the boreal forest during BOREAS." *Journal of Geophysical Research-Atmospheres* no. 102 (D24):29147-29154. doi: 10.1029/97jd00242.

Osterkamp, T. E., L. Viereck, Y. Shur, M. T. Jorgenson, C. Racine, A. Doyle, and R. D. Boone. 2000. "Observations of thermokarst and its impact on boreal forests in Alaska, USA." *Arctic Antarctic and Alpine Research* no. 32 (3):303-315.

Otto, J., T. Raddatz, and M. Claussen. 2011. "Strength of forest-albedo feedback in mid-Holocene climate simulations." *Climate of the Past* no. 7 (3):1027-1039. doi: 10.5194/cp-7-1027-2011.

Payette, S., A. Delwaide, M. Caccianiga, and M. Beauchemin. 2004. "Accelerated thawing of subarctic peatland permafrost over the last 50 years." *Geophysical Research Letters* no. 31 (18). doi: L18208
Artn l18208.

Pielke, R. A., R. Avissar, M. Raupach, A. J. Dolman, X. B. Zeng, and A. S. Denning. 1998. "Interactions between the atmosphere and terrestrial ecosystems: influence on weather and climate." *Global Change Biology* no. 4 (5):461-475. doi: 10.1046/j.1365-2486.1998.t01-1-00176.x.

Pielke, R. A., and P. L. Vidale. 1995. "The boreal forest and the polar front." *Journal of Geophysical Research-Atmospheres* no. 100 (D12):25755-25758. doi: 10.1029/95jd02418.

Pielke, R. A., X. B. Zeng, T. J. Lee, and G. A. Dalu. 1997. "Mesoscale fluxes over heterogeneous flat landscapes for use in larger scale models." *Journal of Hydrology* no. 190 (3-4):317-336. doi: 10.1016/s0022-1694(96)03132-0.

Pinker, R. T., and I. Laszlo. 1992. "Modeling Surface Solar Irradiance For Satellite Applications On A Global Scale." *Journal Of Applied Meteorology* no. 31 (2):194-211.

Randerson, J. T., H. Liu, M. G. Flanner, S. D. Chambers, Y. Jin, P. G. Hess, G. Pfister, M. C. Mack, K. K. Treseder, L. R. Welp, F. S. Chapin, J. W. Harden, M. L. Goulden, E. Lyons, J. C. Neff, E. A. G. Schuur, and C. S. Zender. 2006. "The impact of boreal forest fire on climate warming." *Science* no. 314 (5802):1130-1132.

Reed, R. J., and B. A. Kunkel. 1960. "The Arctic Circulation in Summer." *Journal of Meteorology* no. 17 (5):489-506. doi: 10.1175/1520-0469(1960)017<0489:tacis>2.0.co;2.

Romm, Joe. 2009. Like father, like son: Roger Pielke Sr. also doesn't understand the science of global warming — or just chooses to willfully misrepresent it. In *Think Progress, Climate*.

Schaaf, C. B., F. Gao, A. H. Strahler, W. Lucht, X. W. Li, T. Tsang, N. C. Strugnell, X. Y. Zhang, Y. F. Jin, J. P. Muller, P. Lewis, M. Barnsley, P. Hobson, M. Disney, G. Roberts, M. Dunderdale, C. Doll, R. P. d'Entremont, B. X. Hu, S. L. Liang, J. L. Privette, and D. Roy. 2002. "First operational BRDF, albedo nadir reflectance products from MODIS." *Remote Sensing of Environment* no. 83 (1-2):135-148.

Sellers, P., F. Hall, H. Margolis, B. Kelly, D. Baldocchi, G. Denhartog, J. Cihlar, M. G. Ryan, B. Goodison, P. Crill, K. J. Ranson, D. Lettenmaier, and D. E. Wickland. 1995. "The Boreal Ecosystem-Atmosphere Study (BOREAS) - An Overview and Early Results from the 1994 Field Year." *Bulletin of the American Meteorological Society* no. 76 (9):1549-1577. doi: 10.1175/1520-0477(1995)076<1549:tbesao>2.0.co;2.

Sellers, P. J., F. G. Hall, R. D. Kelly, A. Black, D. Baldocchi, J. Berry, M. Ryan, K. J. Ranson, P. M. Crill, D. P. Lettenmaier, H. Margolis, J. Cihlar, J. Newcomer, D. Fitzjarrald, P. G. Jarvis, S. T. Gower, D. Halliwell, D. Williams, B. Goodison, D. E. Wickland, and F. E. Guertin. 1997. "BOREAS in 1997: Experiment overview, scientific results, and future directions." *Journal of Geophysical Research-Atmospheres* no. 102 (D24):28731-28769. doi: 10.1029/97jd03300.

Serreze, M. C., A. H. Lynch, and M. P. Clark. 2001. "The Arctic frontal zone as seen in the NCEP-NCAR reanalysis." *Journal of Climate* no. 14 (7):1550-1567. doi: 10.1175/1520-0442(2001)014<1550:tafzas>2.0.co;2.

Sheng, Y. W., L. C. Smith, G. M. MacDonald, K. V. Kremenetski, K. E. Frey, A. A. Velichko, M. Lee, D. W. Beilman, and P. Dubinin. 2004. "A high-resolution GIS-based inventory of the west Siberian peat carbon pool." *Global Biogeochemical Cycles* no. 18 (3). doi: Gb3004 Artn gb3004.

Smith, L. C., Y. Sheng, G. M. MacDonald, and L. D. Hinzman. 2005. "Disappearing Arctic lakes." *Science* no. 308 (5727):1429-1429.

Smith, L. C., Y. W. Sheng, and G. M. MacDonald. 2007. "A first pan-Arctic assessment of the influence of glaciation, permafrost, topography and peatlands on northern hemisphere lake distribution." *Permafrost and Periglacial Processes* no. 18 (2):201-208.

Smith, N. V., S. S. Saatchi, and J. T. Randerson. 2004. "Trends in high northern latitude soil freeze and thaw cycles from 1988 to 2002." *Journal of Geophysical Research-Atmospheres* no. 109 (D12). doi: D12101
Artn d12101.

Snyder, P. K., C. Delire, and J. A. Foley. 2004. "Evaluating the influence of different vegetation biomes on the global climate." *Climate Dynamics* no. 23 (3-4):279-302.

Steyaert, L. T., F. G. Hall, and T. R. Loveland. 1997. "Land cover mapping, fire regeneration, and scaling studies in the Canadian boreal forest with 1 km AVHRR and Landsat TM data." *Journal of Geophysical Research-Atmospheres* no. 102 (D24):29581-29598. doi: 10.1029/97jd01220.

Stow, D. A., A. Hope, D. McGuire, D. Verbyla, J. Gamon, F. Huemmrich, S. Houston, C. Racine, M. Sturm, K. Tape, L. Hinzman, K. Yoshikawa, C. Tweedie, B. Noyle, C. Silapaswan, D. Douglas, B. Griffith, G. Jia, H. Epstein, D. Walker, S. Daeschner, A. Petersen, L. M. Zhou, and R. Myneni. 2004. "Remote sensing of vegetation and land-

cover change in Arctic Tundra Ecosystems." *Remote Sensing of Environment* no. 89 (3):281-308.

Sturm, M., T. Douglas, C. Racine, and G. E. Liston. 2005a. "Changing snow and shrub conditions affect albedo with global implications." *Journal of Geophysical Research-Biogeosciences* no. 110 (G1). doi: G01004
Artn g01004.

Sturm, M., C. Racine, and K. Tape. 2001. "Climate change - Increasing shrub abundance in the Arctic." *Nature* no. 411 (6837):546-547.

Sturm, M., J. Schimel, G. Michaelson, J. M. Welker, S. F. Oberbauer, G. E. Liston, J. Fahnestock, and V. E. Romanovsky. 2005b. "Winter biological processes could help convert arctic tundra to shrubland." *Bioscience* no. 55 (1):17-26.

Swenson, S. C., and D. M. Lawrence. 2012. "A new fractional snow-covered area parameterization for the Community Land Model and its effect on the surface energy balance." *Journal of Geophysical Research-Atmospheres* no. 117. doi: 10.1029/2012jd018178.

Thof, I., and R. H. Fraser. 2007. "Mapping northern land cover fractions using Landsat ETM." *Remote Sensing of Environment* no. 107 (3):496-509.

Thomas, G., and P. R. Rowntree. 1992. "The boreal forests and climate." *Quarterly Journal of the Royal Meteorological Society* no. 118 (505):469-497.

Van Cleve, K., and L.A. Viereck. 1981. "Forest succession in relation to nutrient cycling in the boreal forest of Alaska." In *Forest Succession: Concepts and Application*, edited by D. C. West, H. H. Shugart and D. B. Botkin, 185-211. Berlin: Springer.

Viereck, L. A. 1983. "The effects of fire in black spruce ecosystems of Alaska and northern Canada." In *The Role of Fire in Northern Circumpolar Ecosystems*, edited by R.W. Wein and D.A. MacLean, 201-220. Chichester: John Wiley and Sons.

Viereck, L. A., K. Van Cleve, and C. T. Dyrness. 1986. "Forest Ecosystem Distribution in the Taiga Environment." In *Forest Ecosystems in the Alaskan Taiga*, edited by K. Van Cleve, F. S. Chapin, P. W. Flanagan, L. A. Viereck and C. T. Dyrness, 22-43. New York: Springer-Verlag.

Viereck, L.A. 1973. "Wildfire in the taiga of Alaska." *Quaternary Research* no. 3:465-495.

von Humbodt, Alexander. 1807. *Ideen zu einer Geographie der Pflanzen. Hrsg. von Mauritz Dittrich. Mit einem Titelbildnis, und einer pflanzengeographischen Karte.* Leipzig: Akademische Verlagsgesellschaft Geest & Portig, 1960.

Walter, K. M., S. A. Zimov, J. P. Chanton, D. Verbyla, and F. S. Chapin. 2006. "Methane Bubbling from Siberian Thaw Lakes as a Positive Feedback to Climate Warming." *Nature* no. 443 (7107):71-75.

Woodward, F. I. 1995. *Ecophysiological controls of conifer distributions*. Edited by W. K. Smith and T. M. Hinckley, *Physiological Ecology; Ecophysiology of coniferous forests*.

Yoshikawa, K., and L. D. Hinzman. 2003. "Shrinking thermokarst ponds and groundwater dynamics in discontinuous permafrost near Council, Alaska." *Permafrost and Periglacial Processes* no. 14 (2):151-160.

Zeng, X. B., and R. A. Pielke. 1995. "Landscape-Induced Atmospheric Flow and its Parameterization in Large-Scale Numerical Models." *Journal of Climate* no. 8 (5):1156-1177. doi: 10.1175/1520-0442(1995)008<1156:liafai>2.0.co;2.

Zhou, L. M., C. J. Tucker, R. K. Kaufmann, D. Slayback, N. V. Shabanov, and R. B. Myneni. 2001. "Variations in northern vegetation activity inferred from satellite data of vegetation index during 1981 to 1999." *Journal of Geophysical Research-Atmospheres* no. 106 (D17):20069-20083.

Chapter 3

Land Cover Change and Heterogeneity in the Boreal Forest Measured with Landsat

Abstract

The boreal forest has an active fire regime that puts it at risk for rapid change in the face of climate change. Shifts in the fire regime could change the extent and the spatial pattern of land cover types in the region. This study quantifies the observed changes to land cover in central Canada using Landsat data from three time steps and compares landscape heterogeneity across space and time. A historical fire database was used to isolate the effect of fire on this observed change. The study region was very dynamic with 23% to 35% of the land area experiencing some change over the past two decades. 42% of that observed change was caused, either directly or indirectly, by fire. Land cover patches within recently burned forests were found to be broadly larger, more regularly shaped, and more densely packed than patches in unburned areas. This study brings in new high resolution imagery to add to the legacy of the BOREAS datasets.

3.1 Introduction

The boreal forest is a dynamic biome with an active fire regime that regularly disturbs stands of evergreen forest and kicks off a well-studied successional trajectory that includes transition through multiple land cover types (Lutz 1953; Viereck 1983; Larsen 1997; Johnstone and Chapin 2006). Immediately following fire, grasses and other low stature plants establish rapidly while the standing dead spruce boles can remain standing for several years. Eventually the temperature limited decomposition breaks down the dead spruce roots enough that the boles fall. A mid-successional phase dominated by deciduous species takes over the forest canopy for several decades. Depending on various factors including fire burn severity, soil drainage, and permafrost state, the forest stand may remain deciduous dominated or return to an evergreen needleleaf dominant climax forest after approximately 80 – 150 years (Viereck 1983; Lyons et al. 2008). Because of the large number of fires and the area they cover each year, they are important for setting the distribution and pattern of vegetation land cover in the boreal forest. Furthermore, the fire regime is subject to change with climate and is expected to become more intense in the future (Chapin et al. 2000; Kasischke et al. 2010). More fires would tend to shift the makeup of the boreal forest to younger, more deciduous dominant stands. Also, more intense fires, as are predicted to accompany climate change, are more likely to result in permanently deciduous dominant forests (Barrett et al. 2011; Hollingsworth et al. 2013). The rate and direction of land cover change in the boreal forest will determine if it expands northward into the tundra or is replaced by deciduous forests from within.

Beyond the first order area of land cover classes, we can also measure the patterns of the landscape and how those patches are shaped and oriented in space. Spatial heterogeneity can be defined broadly as “the spatially structured variability of a property of interest, which may be a

categorical or quantitative, explanatory or dependent variable" (Wagner and Fortin 2005). Originally purely a spatial metric it was defined as the variance in the rate of an ecological process over space (Smith 1972). This definition expanded to include "the complexity and/or variability of a system in space and/or time" (Li and Reynolds 1995) and ultimately should be defined independently for each situation depending on the specific circumstances (Kolasa and Rollo 1991). Heterogeneity can be caused by any process that occurs across neighboring geographical units.

This study quantifies land cover change over time and the influence of fire on land cover change and heterogeneity at the fine scale (30m spatial resolution) using Landsat satellite data over two decades. In the study area, 42.3% of the land cover changes occurred within recently burned fire scars (within 5 to 22 years). Burned areas had roughly three times more land cover change than unburned regions. Burned areas also had land cover patches that were larger, more densely packed, and more regularly shaped than regions that had not been burned within the last 50 years. This result at the fine scale is an important step to understanding changes happening in the broader boreal forest. Furthermore, the results from this study, although limited in spatial extent, will form the basis of the continental scale boreal forest heterogeneity mapping in Chapter 4.

3.1.1 Study Area

The region near Thompson, Manitoba was chosen because it is representative of the broader Canadian Shield boreal forest and is situated near the transition zone to tundra (Sellers et al. 1995). The region was also intensely studied as the Northern Study Area (NSA) of the

BOREAS study and therefore has several study sites which will help in land cover classification and provide ground truth (Figure 3.1)(Sellers et al. 1997; Steyaert et al. 1997). The study area is

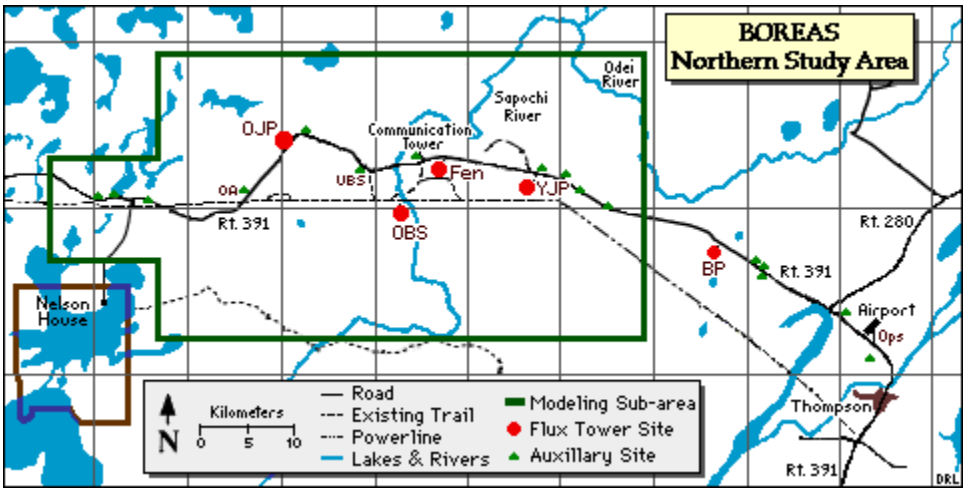

Figure 3.1. Map of the BOREAS Northern Study Area

a rectangular region of roughly 1.3 x10^6 hectares (ha) selected to minimize cloud contamination in the Landsat images (Figure 3.2).

3.2 Data and Methods

This study involved processing and preparing three Landsat scenes from two different sensors, classifying them into land cover types, and analyzing the land cover across space and time. Other data used include forest fire data and local site descriptions from BOREAS studies.

3.2.1 Data

The remote sensing data for this study came from two Landsat sensors, Thematic Mapper (TM) and Enhanced Thematic Mapper Plus (ETM+). Originally the goal was to have one TM image from the mid-1990s to match up with the BOREAS field data, one from the ETM+ SLC-on period (1999-2003), and one recent image from the Operational Land Imager (OLI) aboard Landsat 7. Unfortunately, there were no cloud free summertime OLI images available which left the Landsat 5 TM archive from which the most recent image was from September, 2009. Thus the three scenes used in this study were acquired by TM on 12 June, 1992, ETM+ on 17 September, 2001, and TM on 15 September, 2009. These three scenes were compiled by the Global Land Survey (GLS) (Gutman et al. 2008). They were selected for the best seasonal comparability available given cloud cover and data availability constraints (Arvidson et al. 2001; Goward et al. 2006; Tatem et al. 2006). All three scenes are from path 33 and row 21 according to the WRS2 reference system. Although the scenes were broadly cloud free, there was limited cloud contamination in the southwest corner of the study area in the 2009 scene (Figure 3.3).

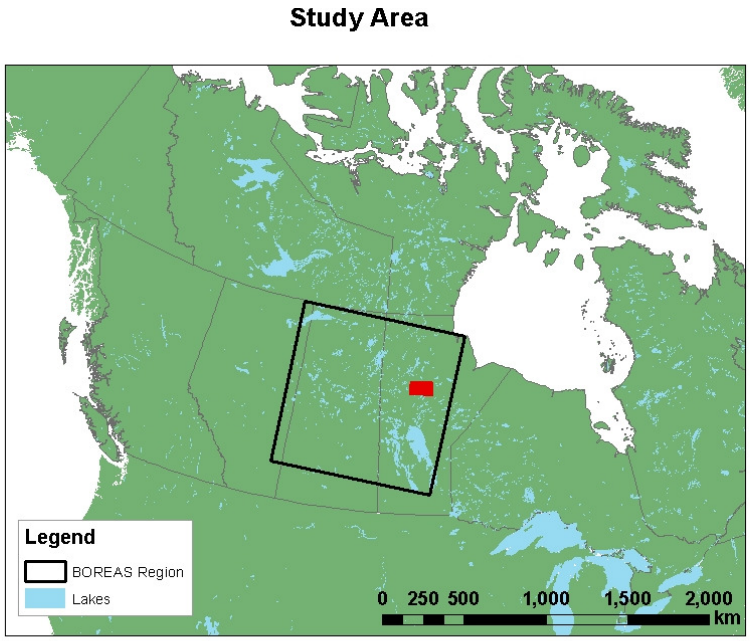

Figure 3.2. Study Area in central Manitoba, Canada

Because the land cover classification was performed at three time steps, the Landsat scenes had to be properly calibrated. All three Landsat scenes were pre-processed to convert them from digital number (DN) to top-of-atmosphere (TOA) reflectance (Chander et al. 2009). The built in calibration functions in ENVI were used along with metadata for each image. The spatial accuracy of the images was assumed to be sub-pixel and was therefore not altered (USGS 2010).

To quantify the role of fire in land cover changes in the study area, a GIS database of fire scars from the department of Natural Resources Canada (NRC) was used. The National Fire Database (NFDB) includes fires near the study area from as far back as 1928 but the documentation of older fires is inconsistent until the mid-twentieth century. To exclude erroneous historical fires, all fires prior to 1950 were excluded from analysis.

3.2.2 Classification

After several attempts using different methods, a classification scheme using training data guided by the BOREAS field sites and expert input provided the best classifications. The first approach was to use a single set of training data to correspond with the 1992 image and then use spectral endmembers to carry that information forward to the 2001 and 2009 images. Spectral and radiometric differences between the TM and ETM+ scenes proved too great even after calibration and seasonal differences between the 1992 image (acquired in June) and the others (both acquired in September) compounded the problem. Some of the BOREAS field sites proved to be indistinguishable in the Landsat images, particularly the fen site, meaning that these

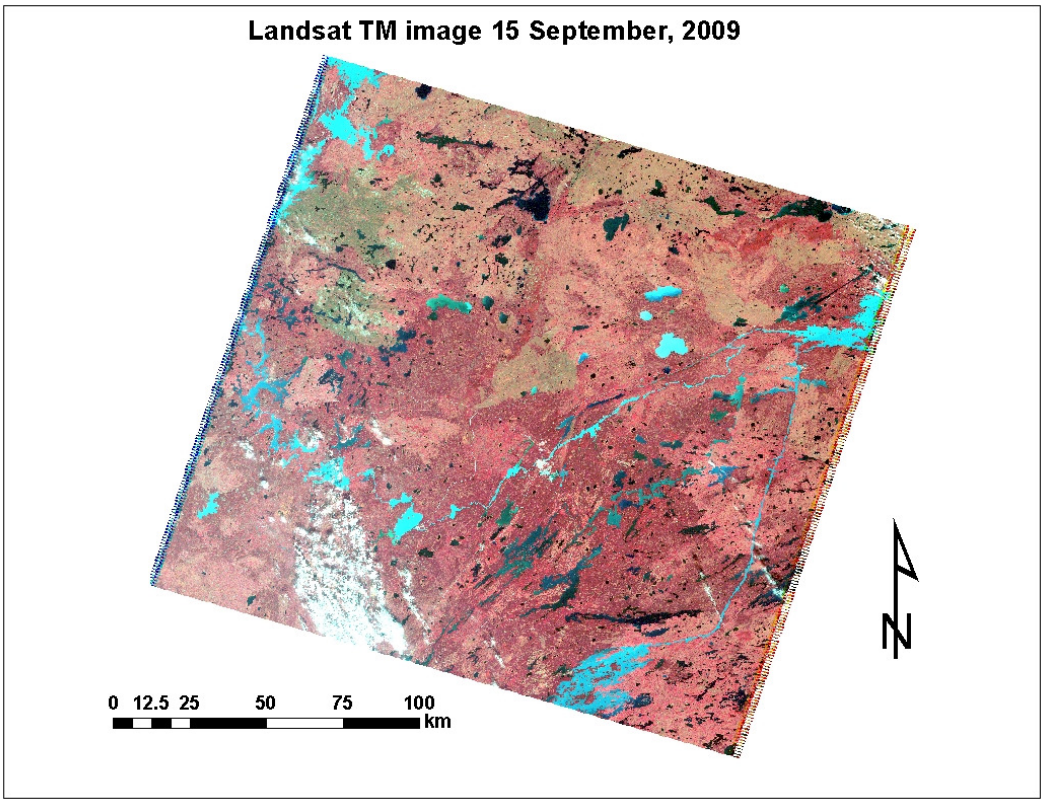

Figure 3.3. False color Landsat TM image (bands 4, 3, 2)

land cover types had to be aggregated. Ultimately, five land cover classes were selected which best represented the variety of the region and allowed consistent classification. The classes used in this study were dense forest, mixed forest, barren/cleared, fire blackened, and open water.

Three training datasets, one for each time step, were generated by hand using areas of stable land cover where available. The training datasets were fed into a minimum distance classifier in ENVI which generated a classified image for each time step (Figure 3.4). The minimum distance classification method was chosen because it generated the most cohesive land cover patches with the least noise. Maximum likelihood, in comparison, had many more small patches of one or two pixels. A straightforward change detection analysis generated change matrices for 1992-2009, 1992-2001, and 2001-2009.

3.2.3 Heterogeneity

A suite of heterogeneity metrics were calculated using Fragstats spatial analysis software (McGarigal 2012). The following were calculated for the entire landscape: patch density, mean patch area, mean patch shape, mean fractal dimension, mean perimeter-area ratio, contagion, cohesion, effective mesh size, Shannon's diversity, and Simpson's diversity.

For isolating the influence of fire, three metrics were calculated for four different burned and unburned classes: areas that burned during the change detection period, 1992-2009, areas that burned within 5 years from the start of the change detection period, 1987-1992, areas that burned anytime between 1950 and 1992, and areas that did not burn at all between 1950 and 1992. For each of these areas, Fragstats calculated the mean patch area, patch shape index, and patch density.

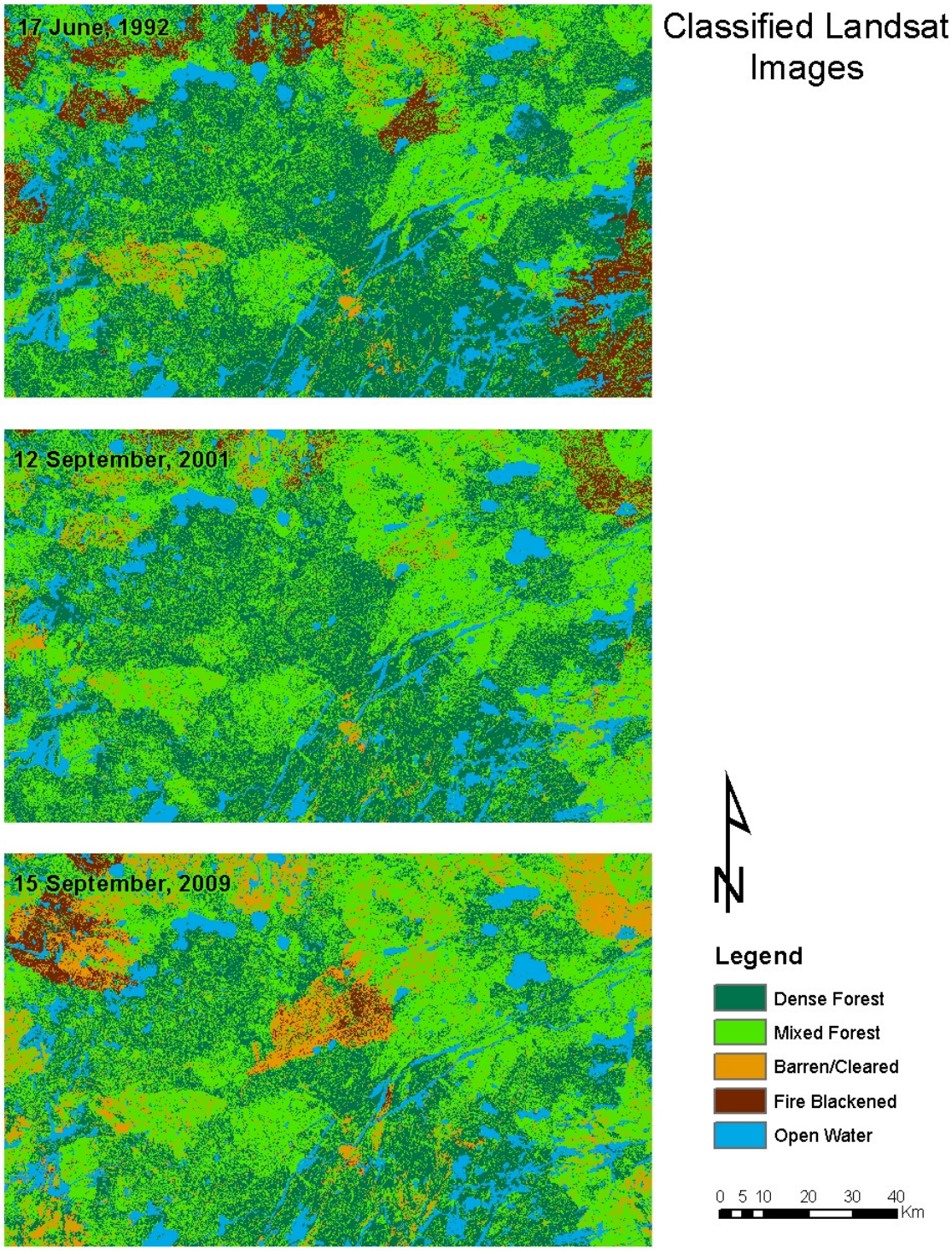

Figure 3.4. Results of minimum distance classification of Landsat images at three time steps.

3.3 Results

The boreal forest in this study area was more dynamic than originally expected. In addition to the direct land cover changes from fires, the successional changes occurred rapidly enough that they were clear even in this relatively short time scale study. There were significant differences in the pattern of land cover patches within and without burn scars but any trend over time was lost in noise between time steps. A qualitative visual analysis of the three classified images indicates that land cover change detection in the boreal forest is possible at this scale. In addition to the large fires visible in Figure 3.4, there was some anthropogenic forest clearing near the town of Thompson, Manitoba in the lower right corner of the study area. These clearing areas are distinguishable from fires because they do not go through a fire blackened land cover stage and they are smaller and more elongated in shape.

3.3.1 Change Detection

The entire study area experienced change in each land cover class and at each time step. The changes are summarized in Table 3.1 which is a change matrix with original land cover type across the top and the ultimate land cover type down the columns in hectares (ha) and percent (%). The bold numbers represent pixels that did not change across that particular time step. In total 35% of the study area went through some kind of change between 1992 and 2009. Between 1992 - 2001 and 2001 – 2009 there was 27% and 24% change respectively. While there is certainly some error in the classification, the higher change for the longer time step indicates that there is also real change signal as well. The most stable land cover class was open water which had over 90% of the pixels remain the same across all time steps. This is not surprising as lakes in this region change more slowly than the time scale of this study could capture. The least

stable land cover class was fire blackened; only 1.9% of the fire blackened area from 1992 was still fire blackened in 2009. Between 1992 – 2001 and 2001 – 2009 there was still 10.8% and 4.1% fire blackened respectively which indicates that the charcoal left from a fire washes away and is overgrown by primary successional plants quickly (less than 9 years).

There is further evidence in the change detection matrix to support the established trajectory for post-fire succession in this region (Lutz 1953; Viereck 1983; Larsen 1997). In the terms of these land cover classes, succession would start with fire blackened and move to barren/cleared, mixed forest, and finally to dense forest (right to left and bottom to top in Table 3.1). Values broadly increase going up from the bold values in the middle of Table 3.1. For instance in the 1992 – 2009 table, the fire blackened class changes 36% to barren/cleared and 58% to mixed forest. There is also a strong push from barren/cleared to mixed forest (52%, 62%, and 25% for 1992 – 2009, 1992 – 2001, and 2001 – 2009 respectively). Forests are therefore establishing quickly in disturbed lands but the relatively low values for transitions from mixed forest to dense forest (9%, 15%, and 6% for 1992 – 2009, 1992 – 2001, and 2001 – 2009 respectively) indicate that the rapid growth slows as the forests approach maturity.

Table 3.1a.	Dense Forest		Mixed Forest		Barren/Cleared		Fire Blackened		Water		Row Total
1992-2009	Area (ha)	Area %	Area (ha)	Area %	Area (ha)	Area %	Area (ha)	Area %	Area (ha)	Area %	Area (ha)
Dense Forest	**343778**	**64.1**	41458	9.0	1524	2.9	3333	3.2	8455	6.4	398548
Mixed Forest	117674	22.0	**348368**	**75.6**	27485	52.4	60115	58.0	2066	1.6	555708
Barren/Cleared	46922	8.8	58951	12.8	**22313**	**42.6**	38181	36.8	1885	1.4	168253
Fire Blackened	21681	4.0	11903	2.6	921	1.8	**1919**	**1.9**	758	0.6	37183
Water	5970	1.1	203	0.0	160	0.3	127	0.1	**119285**	**90.1**	125745
Class Total	536026	100.0	460883	100.0	52403	100.0	103675	100.0	132450	100.0	1285437
Class Changes	192247	35.9	112515	24.4	30090	57.4	101756	98.1	13164	9.9	449772
Image Difference	-137478	-25.6	94825	20.6	115850	221.1	-66492	-64.1	-6705	-5.1	0

Table 3.1b.	Dense Forest		Mixed Forest		Barren/Cleared		Fire Blackened		Water		Row Total
1992-2001	Area (ha)	Area %	Area (ha)	Area %	Area (ha)	Area %	Area (ha)	Area %	Area (ha)	Area %	Area (ha)
Dense Forest	**409173**	**76.3**	67170	14.6	1204	2.3	3217	3.1	7215	5.4	487978
Mixed Forest	99878	18.6	**378998**	**82.2**	32877	62.7	67423	65.0	2488	1.9	581664
Barren/Cleared	6054	1.1	9914	2.2	**17723**	**33.8**	21762	21.0	623	0.5	56076
Fire Blackened	14785	2.8	4690	1.0	497	0.9	**11180**	**10.8**	558	0.4	31710
Water	6136	1.1	112	0.0	102	0.2	93	0.1	**121565**	**91.8**	128008
Class Total	536026	100.0	460883	100.0	52403	100.0	103675	100.0	132450	100.0	1285437
Class Changes	126853	23.7	81885	17.8	34680	66.2	92495	89.2	10884	8.2	346798
Image Difference	-48048	-9.0	120781	26.2	3673	7.0	-71965	-69.4	-4441	-3.4	0

Table 3.1c.	Dense Forest		Mixed Forest		Barren/Cleared		Fire Blackened		Water		Row Total
2001-2009	Area (ha)	Area %	Area (ha)	Area %	Area (ha)	Area %	Area (ha)	Area %	Area (ha)	Area %	Area (ha)
Dense Forest	**359142**	**73.6**	32259	5.5	1050	1.9	875	2.8	5222	4.1	39855
Mixed Forest	76292	15.6	**456614**	**78.5**	14545	25.9	8013	25.3	245	0.2	55571
Barren/Cleared	23778	4.9	82462	14.2	**39801**	**71.0**	21275	67.1	937	0.7	16825
Fire Blackened	25077	5.1	9750	1.7	523	0.9	**1295**	**4.1**	538	0.4	3718
Water	3689	0.8	579	0.1	158	0.3	253	0.8	**121067**	**94.6**	12575
Class Total	487978	100.0	581664	100.0	56076	100.0	31710	100.0	128008	100.0	1285437
Class Changes	128836	26.4	125050	21.5	16275	29.0	30416	95.9	6941	5.4	307518
Image Difference	-89430	-18.3	-25956	-4.5	112176	200.0	5473	17.3	-2263	-1.8	0

3.3.2 Influence of Fire

Of the approximately 450,000 ha of the study area that experience change between 1992 and 2009, 190,000 ha was in the scars of recent fires. That is 42% of the total change even though the recent fires (1987 to 2009) only make up 20% of the total study area. This makes the recently burned areas more dynamic than areas that have not burned. 76% of areas that burned between 1987 and 2009 experienced a land cover change. These changes were mostly the direct effect of fire burning one land cover type and replacing it with another. The indirect influence of fires in areas that have not burned for decades was also significant as 50% of areas burned between 1950 and 1992 experienced change compared to 25% for areas that have not burned since 1950. These values are greater than any other mechanisms causing land cover change in this part of the boreal forest.

The pattern of land cover within burn scars was broadly larger, more densely packed, and more regularly shaped than in unburned landscapes. The mean patch area, shape index, and patch density for different burned and unburned regions within the study area are shown in Figure 3.5. Mean patch size (Figure 3.5a) was considerably larger for the two most disturbed classes (burned 1992-2009 and burned 1987-1992). Any temporal trend in these two classes was questionable given the inter-decadal variability. Burned and unburned mean patch size were very similar with less variability except that the unburned class slightly decreased in size. Area weighted mean shape index is superior to the un-weighted shape index because very small patches of one or two pixels have very regular shapes (rectangles) and are very numerous. By weighting these small patches less and larger patches more, the effect was reduced and the shape signal in the data was more pronounced. The unburned since 1950 class had the most irregularly

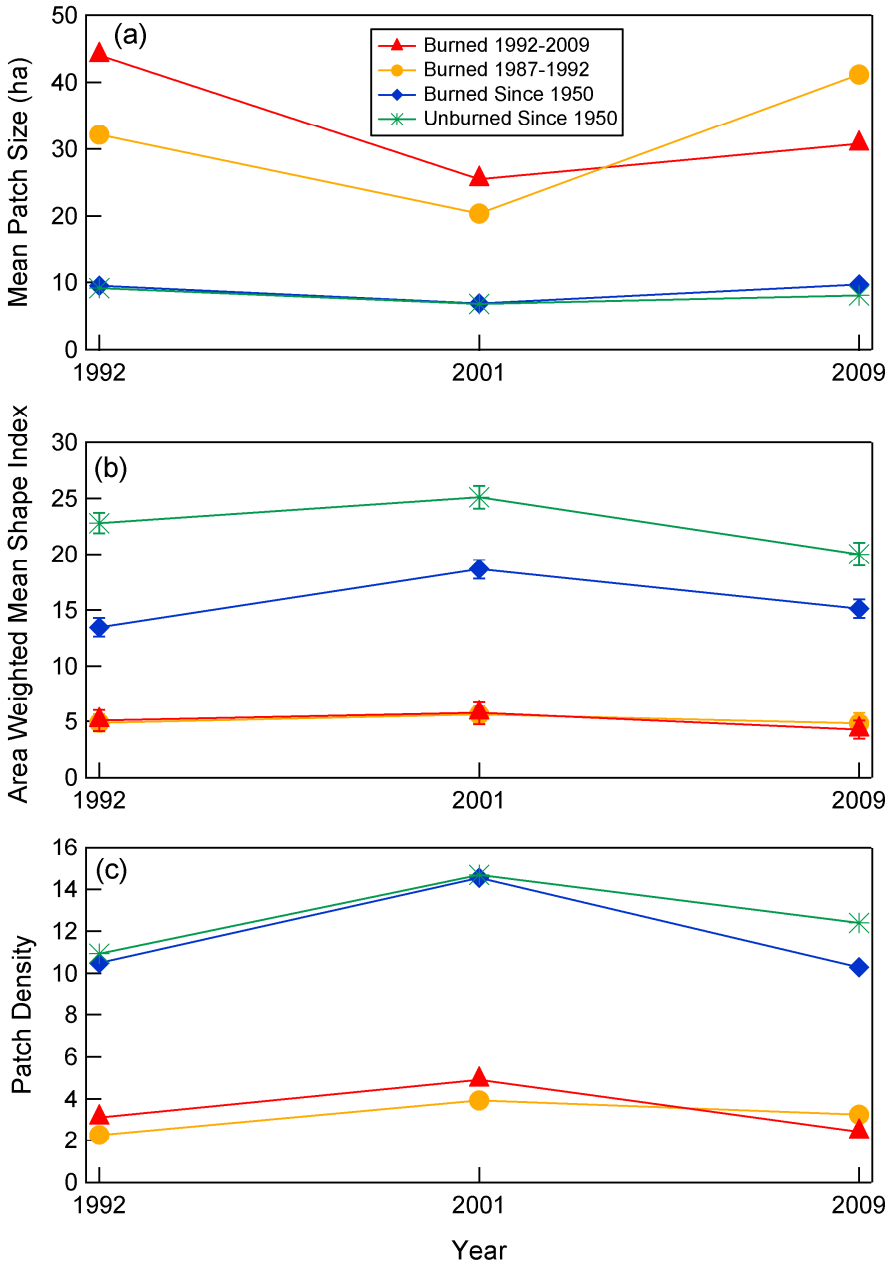

Figure 3.5. Patch area, shape, and density metrics for various burned and unburned sub-regions of the study area. Standard deviation error bars are shown for Area Weighted Mean Shape Index (b) only.

shaped patches (area weighted mean shape index 22.65) (Figure 3.5b), areas burned between 1950 and 1992 were in the middle, and the two recent fire classes had the most regular patches despite being the largest. Recent fire activity, then, resulted in larger, more regularly shaped land cover patches while unburned, presumably mature, forests had small, irregular patches.

The existence of many small patches in unburned forests also helps explain Figure 3.5c which shows a much higher density of patches in unburned forest, 12.67 patches per hectare, than in recent burns, 3.32 patches per hectare. There was still no strong trend in any of the patch metrics over time which would not be expected anyways because the influence of fire has already been controlled for in the case of Figure 3.5.

3.4 Discussion

The multitemporal approach of this study sheds new light on the role of fire in the boreal forest in terms of land cover change. The relative speed of establishment for intermediate forest stages like mixed forest highlights the indirect influence of fire even decades after the fire itself. There are many avenues to continue this research at different scales and with different sensors.

3.4.1 Boreal Forest Land Cover Dynamics

The rate of change of land cover in the boreal forest is one of the factors that put it at risk for rapid degradation in the face of climate change. While forests are already slow to migrate to keep up with their shifting climatic zones, if they are exposed to a changed disturbance regime, they may never get the chance. It is important, therefore, to monitor the rates of change of land cover types within the boreal forest to identify this problem early. This study starts laying the

groundwork for broader land cover monitoring that looks, rather than at the treeline, at the body of the boreal forest biome. A common problem when using satellite remote sensing to observe biome shifts is the relatively short instrument record (Danby and Hik 2007). In this case, there was ample time to observe many different changes happening simultaneously in the landscape. This is promising for future work in the field.

The boreal forest fire regime is broadly predicted to become more intense in the future (Kasischke et al. 2010) and it has been shown that the post-fire successional trajectory can be altered in areas of severe burning in Alaska (Barrett et al. 2011). The rapid establishment of saplings and young forests in severe burn scars could be responsible for the rapid and extensive land cover shifts from fire blackened and barren/cleared to mixed forest observed in this study. Whether or not this is part of a broader trend will require more data at a continental extent.

Fire, as an ecological mechanism, works differently in different forest biomes and boreal forests are some of the best adapted to fire in the world. By analyzing forests in Yellowstone National Park, Romme (1982) found increased heterogeneity and patchiness in fire scars which runs contrary, at least in part, to the results of this study. The difference largely responsible for this inconsistency is the time scale at work in both regions. Fires in Romme's study were from 200 to 300 years previous which cannot compare to the relatively young stands in the boreal forest which are rarely over 150 years old (Viereck 1983). Therefore in the boreal forest, even mature forest stands are patterned by the most recent fire when they are ignited again, so the ecosystem may never reach a truly mature, or stable, state.

3.4.2 Error Sources and Next Steps

Several limitations in this study can be easily overcome in the future. First, data availability for the OLI will undoubtedly improve over the coming years which would add new, more up-to-date data to the analysis. Furthermore, Multi-Spectral Scanner (MSS) data could be incorporated but would require heavy processing and likely add uncertainty due to the coarser spatial and radiometric resolution of the MSS sensor. Better field data would likely improve the classification and allow independent accuracy assessment at each time step. Erroneous classifications including cloud and shadow contamination contributed considerably to the noise in the inter-decadal heterogeneity metrics, downing any potential signal. A more conservative classification scheme with a fully utilized "unclassified" class could greatly reduce that noise.

The broader future of this work is at the same scale but at a much broader extent. Thanks to the availability of Landsat data and the accessibility of cloud computing resources, it is possible to perform this kind of analysis at the continental to global scale. The classification steps from the first part of this study that formed the basis for the broader spatial analysis has been undertaken in a global forest cover mapping project by Hansen et al. (2013). Future forest dynamics studies will be able to rely on their seamless global dataset.

The amount of change that was detected given the relatively short time scale in this study is promising because it indicates that the generally short time scales observed by sensors like MODIS can still be used for mapping forest dynamics. Mapping changes in the boreal treeline has been hampered by the availability of historical images for comparison. The disturbance driven changes studied here do not require time scales that are beyond the reach of modern remote sensing datasets.

3.5 Conclusions

This study analyzed the landscape heterogeneity and land cover change in a region within the boreal forest using Landsat data and fire scar maps. Between 1992 and 2009, up to 35% of the landscape underwent some land cover change and that change was predominantly caused, either directly or indirectly, by fire. Changes broadly followed the established patterns of post fire succession that has been documented before. Simultaneous land cover changes occurred causing a chaotic and dynamic landscape without any strong temporal trends. Because almost the entire area of the boreal forest is impacted by fire over a relatively short time period, there are few, if any, pure, undisturbed, climax forests that could act as a background or control region. This is a fundamentally different way of thinking about forests than those in temperate or tropical regions. Rather than searching for an undisturbed forest stand to represent the broader boreal forest as a field site or to parameterize surface fluxes in a model, the entire changing landscape must be taken into account. The boreal forest is in a constant state of flux making it particularly susceptible to climate change.

The landscape heterogeneity and pattern is clearly affected by fire history as forest patches in recent burns tend to be larger, more regularly shaped, and densely packed than in unburned stands. Those recently burned areas are rapidly colonized by early and mid-successional plants like grasses and mixed forest stands but the creation of dense “mature” forest stands is much slower. Given the potential for the boreal forest to change rapidly from the inside-out, it is important to monitor the fire regime and resulting land cover changes.

3.6 References

Arvidson, T., J. Gasch, and S. N. Goward. 2001. "Landsat 7's long-term acquisition plan - an innovative approach to building a global imagery archive." *Remote Sensing of Environment* no. 78 (1-2):13-26.

Barrett, K., A. D. McGuire, E. E. Hoy, and E. S. Kasischke. 2011. "Potential shifts in dominant forest cover in interior Alaska driven by variations in fire severity." *Ecological Applications* no. 21 (7):2380-2396.

Chander, Gyanesh, Brian L. Markham, and Dennis L. Helder. 2009. "Summary of current radiometric calibration coefficients for Landsat MSS, TM, ETM+, and EO-1 ALI sensors." *Remote Sensing of Environment* no. 113 (5):893-903. doi: http://dx.doi.org/10.1016/j.rse.2009.01.007.

Chapin, F. S., A. D. McGuire, J. Randerson, R. Pielke, D. Baldocchi, S. E. Hobbie, N. Roulet, W. Eugster, E. Kasischke, E. B. Rastetter, S. A. Zimov, and S. W. Running. 2000. "Arctic and boreal ecosystems of western North America as components of the climate system." *Global Change Biology* no. 6:211-223. doi: 10.1046/j.1365-2486.2000.06022.x.

Danby, R. K., and D. S. Hik. 2007. "Evidence of recent treeline dynamics in southwest Yukon from aerial photographs." *Arctic* no. 60 (4):411-420.

Goward, S., T. Arvidson, D. Williams, J. Faundeen, J. Irons, and S. Franks. 2006. "Historical record of Landsat global coverage: Mission operations, NSLRSDA, and international cooperator stations." *Photogrammetric Engineering and Remote Sensing* no. 72 (10):1155-1169.

Gutman, G., R. Byrnes, J. Masek, S. Covington, C. Justice, S. Franks, and R. Headley. 2008. "Towards monitoring land-cover and land-use changes at a global scale: The Global Land Survey 2005." *Photogrammetric Engineering and Remote Sensing* no. 74 (1):6-10.

Hansen, MC, PV Potapov, R Moore, M Hancher, SA Turubanova, A Tyukavina, D Thau, SV Stehman, SJ Goetz, and TR Loveland. 2013. "High-resolution global maps of 21st-century forest cover change." *Science* no. 342 (6160):850-853.

Hollingsworth, Teresa N, Jill F Johnstone, Emily L Bernhardt, and F Stuart Chapin III. 2013. "Fire severity filters regeneration traits to shape community assembly in Alaska's boreal forest." *PloS one* no. 8 (2):e56033.

Johnstone, J. F., and F. S. Chapin. 2006. "Fire interval effects on successional trajectory in boreal forests of northwest Canada." *Ecosystems* no. 9 (2):268-277.

Kasischke, Eric S., David L. Verbyla, T. Scott Rupp, A. David McGuire, Karen A. Murphy, Randi Jandt, Jennifer L. Barnes, Elizabeth E. Hoy, Paul A. Duffy, Monika Calef, and Merritt R. Turetsky. 2010. "Alaska's changing fire regime - implications for the

vulnerability of its boreal forests." *Canadian Journal of Forest Research-Revue Canadienne De Recherche Forestiere* no. 40 (7):1313-1324. doi: 10.1139/x10-098.

Kolasa, Jurek, and C David Rollo. 1991. "Introduction: the heterogeneity of heterogeneity: a glossary." In *Ecological heterogeneity*, 1-23. Springer.

Larsen, C. P. S. 1997. "Spatial and temporal variations in boreal forest fire frequency in northern Alberta." *Journal Of Biogeography* no. 24 (5):663-673.

Li, H, and JF Reynolds. 1995. "On definition and quantification of heterogeneity." *Oikos*:280-284.

Lutz, H. J. 1953. The effects of forest fires on the vegetation of interior Alaska. Juneau: Alaska Forest Research Center, U.S. Department of Agriculture.

Lyons, E. A., Y. F. Jin, and J. T. Randerson. 2008. "Changes in surface albedo after fire in boreal forest ecosystems of interior Alaska assessed using MODIS satellite observations." *Journal of Geophysical Research-Biogeosciences* no. 113 (G2). doi: 10.1029/2007jg000606.

McGarigal, K., SA Cushman, and E Ene. 2014. *FRAGSTATS v4: Spatial Pattern Analysis Program for Categorical and Continuous Maps* 20122014]. Available from http://www.umass.edu/landeco/research/fragstats/fragstats.html.

Romme, William H. 1982. "Fire and landscape diversity in subalpine forests of Yellowstone National Park." *Ecological Monographs* no. 52 (2):199-221.

Sellers, P., F. Hall, H. Margolis, B. Kelly, D. Baldocchi, G. Denhartog, J. Cihlar, M. G. Ryan, B. Goodison, P. Crill, K. J. Ranson, D. Lettenmaier, and D. E. Wickland. 1995. "The Boreal Ecosystem-Atmosphere Study (BOREAS) - An Overview and Early Results from the 1994 Field Year." *Bulletin of the American Meteorological Society* no. 76 (9):1549-1577. doi: 10.1175/1520-0477(1995)076<1549:tbesao>2.0.co;2.

Sellers, P. J., F. G. Hall, R. D. Kelly, A. Black, D. Baldocchi, J. Berry, M. Ryan, K. J. Ranson, P. M. Crill, D. P. Lettenmaier, H. Margolis, J. Cihlar, J. Newcomer, D. Fitzjarrald, P. G. Jarvis, S. T. Gower, D. Halliwell, D. Williams, B. Goodison, D. E. Wickland, and F. E. Guertin. 1997. "BOREAS in 1997: Experiment overview, scientific results, and future directions." *Journal of Geophysical Research-Atmospheres* no. 102 (D24):28731-28769. doi: 10.1029/97jd03300.

Smith, Frederick E. 1972. "Spatial heterogeneity, stability, and diversity in ecosystems." *Trans. Conn. Acad. Arts Sci* no. 44 (30):335.

Steyaert, L. T., F. G. Hall, and T. R. Loveland. 1997. "Land cover mapping, fire regeneration, and scaling studies in the Canadian boreal forest with 1 km AVHRR and Landsat TM data." *Journal of Geophysical Research-Atmospheres* no. 102 (D24):29581-29598. doi: 10.1029/97jd01220.

Tatem, A. J., A. Nayar, and S. I. Hay. 2006. "Scene selection and the use of NASA's global orthorectified Landsat dataset for land cover and land use change monitoring." *International Journal of Remote Sensing* no. 27 (14):3073-3078.

USGS. *The Website of the Land Processes Distributed Active Archive Center (LP DAAC).* USGS/EROS 2010. Available from http://ldcm.nasa.gov/.

Viereck, L. A. 1983. "The effects of fire in black spruce ecosystems of Alaska and northern Canada." In *The Role of Fire in Northern Circumpolar Ecosystems*, edited by R.W. Wein and D.A. MacLean, 201-220. Chichester: John Wiley and Sons.

Wagner, Helene H., and Marie-Josée Fortin. 2005. "SPATIAL ANALYSIS OF LANDSCAPES: CONCEPTS AND STATISTICS." *Ecology* no. 86 (8):1975-1987. doi: 10.1890/04-0914.

Chapter 4

Mapping Boreal Forest Heterogeneity in North America

Abstract

Measuring the spatial patterns of the boreal forest is essential for understanding the role of the region in the global climate system. These patterns also give insight into the processes that have shaped the forest we see today and how the forest might change in the future. This study takes high resolution forest cover data and summarizes the fine scale spatial patterns at a coarser resolution. The results can then be used to analyze the distributions of spatial patterns themselves and also be fed into climate models to aid in representing mesoscale processes. Observed patterns in the maps included broadly smaller land cover patches in the boreal forest than the tundra to the north and the temperate forests to the south, decreased contagion within the boreal forest, and class specific percentage of like adjacencies values that indicated a moderately clustered landscape. The boreal forest had a significantly higher fractal dimension (1.384 ±0.024) than the neighboring regions due to the highly complex landscape. Because the patch cohesion values never reached the percolation threshold in the boreal forest, no single forest cover class was ever dominant in the boreal forest. Patch cohesion of the 0-25% cover class did reach the percolation threshold near the boreal treeline and was successfully used as a new way of mapping that border. The datasets produced here will enable many future studies in the region and perhaps form the basis of a new method for delineating the extent of the boreal forest, tundra, and the taiga transitional zone.

4.1 Introduction

It is a common misconception that the boreal forest is a uniform carpet of trees stretching around the top of the globe. In fact, the boreal forest is an extremely heterogeneous and dynamic landscape. This has become even clearer through the use of remote sensing, which finally gives us a high resolution view of the entire boreal forest on the continental scale (Steyaert et al. 1997; Gutman et al. 2008). The complexity of the boreal forest biome, however, is still often over simplified and poorly parameterized in global climate models (Loranty et al. 2013). Advances in remote sensing and data analysis technology now give us the ability to map the heterogeneity and spatial complexity of the entire North American boreal forest. This study presents such a map and some analysis and observations of patterns in the data. We found that the boreal forest was dominated by many small land cover patches with high diversity of forest cover types. This map has and will continue to provide its own insight into the spatial structure of the boreal forest but will also provide important spatial heterogeneity metrics to improve land-atmosphere interactions in climate models.

4.1.1 The Boreal Forest Ecosystem

The boreal forests of North America range from 68° N latitude in the Brooks Range of Alaska and stretches southeast to 58° N latitude at the west coast of the Hudson Bay (Larsen 1980). The southern extent of the boreal forest is less well defined than the northern ecotone as it gradually transitions into broadleaf deciduous forests, parkland, grassland, and agriculture. The boreal forest, and high latitudes in general, are characterized by low temperatures and cold tolerant plant species. Plant species diversity is broadly lower than temperate and tropical forests because of the history of glacial and interglacial cycles which have reduced opportunities for

specialization (McGlone 1996). The Alaskan and Canadian boreal forest is broadly composed of mixed stands of evergreen conifer species including black spruce (*Picea mariana*), white spruce (*Picea glauca*), and Jack pine (*Pinus banksiana*) and deciduous broadleaf species including quaking aspen (*Populus tremuloides*) and paper birch (*Betula papyrifera*) (Dyrness et al. 1986; Landsberg and Gower 1997). The tundra biome is very different from the boreal forest in its species composition and biophysical properties. The region is dominated by low stature vegetation like sedges, grasses, and some shrubs and is underlain by continuous permafrost. This contrasts with the boreal forest which is dominated by evergreen forests and discontinuous permafrost. Historically, tundra regions have been occupied by forests which had reached to the Arctic Ocean as recently as 8000 years ago (MacDonald et al. 2000). Shrub distributions in the tundra have changed more rapidly than the treeline during the Holocene and are currently expanding northward as evidenced by repeat photography (Anderson and Brubaker 1993; Sturm et al. 2001; Stow et al. 2004; Sturm et al. 2005). Owing to the impervious permafrost, low evaporation rates, and glacial history, this region also has a high concentration of lakes (Lehner and Döll 2004; Smith et al. 2007).

4.1.2 Defining Spatial Heterogeneity

There is a growing acceptance of the role of spatial processes in ecological studies and other traditionally non-spatial disciplines. Geography has crept into these areas of study as it has become clear to researchers that the heterogeneity that they had previously been attempting to exclude from analysis was rich with its own information (Wagner and Fortin 2005). Furthermore, the proliferation of Geographic Information Systems (GIS) technology has made this kind of work more accessible to researchers (Mayer and Greenberg 2005). Studying

heterogeneity and patchiness, however, presents some challenges for statistical analysis due to autocorrelation (Legendre 1993; Legendre et al. 2002). In order to take advantage of the information in spatial heterogeneity it is important to understand its causes and effects and to have some tools or metrics with which to express it.

Spatial heterogeneity can be defined broadly as "the spatially structured variability of a property of interest, which may be a categorical or quantitative, explanatory or dependent variable" (Wagner and Fortin 2005). Originally purely a spatial metric it was defined as the variance in the rate of an ecological process over space (Smith 1972). This definition expanded to include "the complexity and/or variability of a system in space and/or time" (Li and Reynolds 1995) and ultimately should be defined independently for each situation depending on the specific circumstances (Kolasa and Rollo 1991). Heterogeneity can be caused by any process that occurs across neighboring geographical units. Identifying this underlying process is made difficult by the existence of other confounding processes and by changes in the process itself across space and time (Levin 1992).

4.1.3 Spatial Heterogeneity in Land Cover

Land cover maps show the type of land cover that exists at a certain location, at a certain time. This is useful from a reference mapping perspective and for suitability analysis it but doesn't give much quantitative information about the landscape on its own. The real quantitative information in land cover maps is in the spatial patterns formed by the different land cover patches (Baskent and Jordan 1995; O'Neill et al. 1999). The heterogeneity in the distribution of land cover classes can provide insight into the underlying processes that shape the landscape (Schumaker 1996; Harper et al. 2002; Zhang et al. 2006; Barrett et al. 2011) and also potentially

determine how that landscape interacts with the atmosphere and the broader climate system (Pielke and Vidale 1995; Zeng and Pielke 1995; Oleson and Bonan 2000). Observed land cover patches are the result of both ecological processes produced by the species in the ecosystem (endogenic processes like seed dispersal) and also environmental processes that are imposed on the ecosystem from outside (exogenous processes like disturbance and climate) (Wagner and Fortin 2005). Without information about these external spatial forces, the two cannot be distinguished and in some cases they are fundamentally interrelated (Fahrig 2002). Because different land cover types have different biophysical properties, they can influence fluxes of water, carbon, and energy between the land surface and the atmosphere (Baldocchi et al. 1988; Oleson and Bonan 2000). The spatial distribution of those land cover types can also influence surface-atmosphere fluxes through the generation of mesoscale eddies (Zeng and Pielke 1995; Dalu et al. 2000; Beringer et al. 2001; Huang and Margulis 2009).

Land cover type is a categorical variable because an area is categorized as one type or another based on some classification method (Shortridge 2004). Land cover maps, therefore, show the location and characteristics of distinct patches of homogeneous land cover. The patches can be described quantitatively in terms of their composition and configuration (Gustafson 1998). The composition of land cover patches is described in terms of number, frequency, fraction of total coverage, etc. The configuration of land cover patches describes their spatial arrangement in terms of size, shape, patch density, connectivity, fractal dimension, etc. These various metrics can be used in multiple disciplines to illuminate the ecological, environmental, and even economic processes that shape the landscape.

Measuring and cataloging land cover heterogeneity data has been identified as a research priority for the United States (Riitters et al. 2000) and the field of landscape ecology is rich with

examples of the application of heterogeneity metrics in environments around the world. For instance, land cover diversity indices were found to be positively correlated with actual diversity on the ground in terms of number of species per grid cell for test sites in Belgium (Honnay et al. 2003), Eastern Europe (Kowarik 2008), and Britain (Roy et al. 1999). One creative example compared land cover diversity and land values in Wyoming and found that diverse landscapes provided more "environmental amenities" and therefore, had higher land values (Bastian et al. 2002). Wildfire in temperate forest was shown to increase landscape diversity and spatial variability in clearings to a greater extent than logging (Kushla and Ripple 1998). By measuring land cover change in Ohio over the 20th century, the spatial heterogeneity of land cover was shown to drive agricultural land use change as much as the differences in productivity between soil types (Pan et al. 1999). These examples and others show the broad applicability in land cover heterogeneity studies. However, gridded mapping of land cover heterogeneity at the continental scale has not been undertaken before now primarily due to the unavailability of high resolution land cover data and the computational expense of the analysis.

4.1.4 The Impact of Changing Scale

All of the spatial heterogeneity indices discussed here are sensitive to scale. By plotting seventeen different landscape metrics relative to grain size and extent Wu (2004) found different responses for landscapes in boreal forest, Minden NV, and Phoenix AZ. The general direction of the index response to grain size and extent were the same across all three landscapes but there were differences in the shape and slope of the curves. Benson and MacKenzie (1995) calculated several landscape indices at the native resolutions of the High Resolution Vvisible multispectral sensor (HRV) aboard the French satellite *Systéme Pour l'Observation de la Terre* (SPOT),

Landsat Thematic Mapper (TM), the Advanced Very High Resolution Radiometer (AVHRR), and some simulated images to fill the scale gaps between them. The indices were based on classified open water pixels (lakes) in Wisconsin. They found that as grain size increased number of lakes decreased, water fraction decreased, mean lake size increased, and mean lake perimeter increased (Benson and MacKenzie 1995). Grain size and extent, as fundamental elements of scale in GIS, must always be taken into account when calculating and interpreting any landscape pattern metrics.

The variance of an area or image will depend on the particular grain or resolution of the observations and the extent. If extent its held constant and the grain increased (resolution decreased), the variance will generally decrease as more of the heterogeneity is averaged out inside of each observation or pixel (Wiens 1989). Conversely variance broadly increases with decreasing grain (increasing resolution) to a saturation point that depends on the size of the objects being observed (Shortridge 2004). This concept has been studied extensively in the context of mapping accuracy for homogeneous regions like lakes or agricultural fields (Crapper 1980; Ozdogan and Woodcock 2006; Lyons et al. 2013). For natural and simulated images analyzed at increasing spatial resolution, the local variance of images peaks at grain sizes that are a factor of 0.5-0.75 of the size of the objects in the image (Woodcock and Strahler 1987). Using a log/log plot based on object perimeter, Shortridge (2004) found a log-linear relationship between variance in area estimate and grain or resolution that can then be used to define a maximum grain (minimum resolution) for an acceptable level of variance or to define a minimum detectable object size for a given grain and variance.

In addition to variance, population statistics are also sensitive to gain and extent. Ecological statistics on species occurrence and diversity are scale dependent (depend on both

extent and grain). Rare species occurrence in an observational unit will decrease with increasing grain size if the occurrence requires a certain fractional cover to be counted. If, however, species occurrence only requires one individual within the observational unit, then the larger grain will generally exhibit greater diversity metrics (Wiens 1989; Turner and Tjørve 2005). In remote sensing, mapping cohesive land cover units like forest stands, burn scars, agricultural fields, and lakes, population statistics are influenced by scale as well. Borders between land cover types are difficult to map and measure because of their fractal nature. The length of a complex fractal land cover border like a shoreline will be different depending on the grain size (Mandelbrot 1982). If object sizes obey a power law distribution with respect to size within the population there will be many smaller objects and fewer large ones. Thus, removing small objects according to a minimum size threshold removes a large portion of the total number of objects without drastically changing the total area (Birkett and Mason 1995; Lehner and Döll 2004). In ecology, species occurrence can be counted according to fractional cover or individuals present as described above. This is because ecology based on field surveys generally aggregates up from individuals to observational units like plots, transects, or grains (Levin 1989). Remote sensing, in comparison, has no information of finer grain than the single pixel. Land cover classification from remote sensing data is generally either a fuzzy classification which includes an estimate of the fractional sub-pixel area of each land cover type or based on statistical analysis of spectral information yielding a hypothetical ≥50% sub-pixel area of one majority cover type (Foody 2002; Sawaya et al. 2003). Landscape structure parameters like variance, patch area, number of patches, patch perimeter, and fractal dimension are all based on classification of pixels and are all sensitive to grain and extent. As grain size approaches the patch size, the patches may disappear entirely or blend together with their neighbors. Thus landscapes may appear to have a

smaller patch number, a lower fraction of the total landscape classified as that land cover type, larger mean patch areas, and longer mean patch perimeters when observed at grain sizes that approach the size of the patches themselves (Benson and MacKenzie 1995).

4.1.5 Boreal Forest Heterogeneity

This study takes high resolution forest cover data and summarizes the fine scale spatial patterns at a coarser resolution. The results can then be used to analyze the distributions of spatial patterns themselves and also be fed into coarse resolution climate models to aid in representing mesoscale processes. The datasets produced here will enable many future studies in the region and perhaps form the basis of a new method for delineating the extent of the boreal forest, tundra, and the taiga transitional zone.

4.2 Data and Methods

Landscape and class specific heterogeneity metrics were calculated for forest cover data across boreal North America. The forest cover data was processed using the spatial statistics package Fragstats. The forest cover data had a resolution of 30 m x 30 m and the metrics were calculated for overlapping extents of 30 km x 30 km which is equivalent to 1000 x 1000 pixels. This extent was determined to be large enough to produce statistically significant results according to the resolution of the forest cover dataset and the sizes of the land cover patches in the boreal forest. The results were gridded into multiband rasters with a resolution of 10 km x10 km.

4.2.1 Data

The primary data used in this analysis was the Global Forest Change 2000-2013 Dataset produced at the University of Maryland (Hansen et al. 2013). This global dataset maps forest cover as a percent and how it has changed since 2000. The data has a resolution of 30m as it was generated from Landsat Enhanced Thematic Mapper (ETM+) and Operational Land Imager (OLI) data. This dataset was a significant improvement over previous maps of forest cover that were either high resolution with only regional extent or global extent but with coarse resolution (Hansen et al. 2010; DiMiceli 2011). While this dataset has some difficulty distinguishing plantations from forests in tropical regions, it has been shown to be accurate in temperate and high latitude forests (Tropek et al. 2014).

The Global Forest Change 2000-2013 Dataset was produced entirely in Google Earth Engine using Landsat images that are available through the cloud computing service. The raw Landsat data were resampled, converted to top of atmosphere (TOA) reflectance, cloud/shadow/water masked, and normalized for pre-processing. Training datasets were generated from a variety of very high resolution remote sensing products such as Quickbird using manual image interpolation. The training data and pre-processed Landsat data were fed into a decision tree to classify forest cover and change. The data processing used one million CPU-core hours on 10000 computers and could not have been completed without the use of massive cloud computing services like Google Earth Engine (Hansen et al. 2013). The resulting data is freely available for download in 10 deg x 10 deg blocks (http://earthenginepartners.appspot.com/science-2013-global-forest/download_v1.1.html) and is also available in Google Earth Engine for further analysis. There are seven map products

available: the tree canopy cover for year 2000, global forest cover loss 2000-2013, global forest cover gain 2000-2013, year of gross forest cover loss event, a data mask, circa year 2000 Landsat 7 cloud-free image composite, and a circa 2013 Landsat cloud-free image composite.

I downloaded the tree canopy cover for year 2000 (treecover2000) and data mask (datamask) files for the 10 deg x 10 deg grid boxes covering the boreal region of North America (Figure 4.1). These data were then pre-processed for use in calculating heterogeneity metrics. First, each 10 deg x 10 deg file was reclassified and then reprojected to the Canada Albers Equal Area Conic Projection with a central meridian of 96° W, standard parallels of 50° and 70° N, and the latitude of origin at 40° N. The highest priority for choosing this projection was that it be equal area so that patches could be compared across the entire dataset. Minor distortion is acceptable and this projection covers North America with minimal distortion. The resolution of the output dataset was set to 30 m x 30 m which matched the resolution of the Landsat source data from which the Hansen treecover2000 data produced. The single resampling step was performed using the nearest neighbor method to avoid altering data values and because the resolution changes were small. The data were then reclassified into four bins at 25% intervals as recommended by Hansen et al. (2013) (Appendix A). In addition to the four forest cover classes, one "water" class and one "no data" class were added.. Once each 10 deg x 10 deg raster was pre-processed, they could be run through Fragstats to calculate heterogeneity metrics (McGarigal 2012). Because Fragstats is limited in the size of raster that can be processed and the neighboring sub-sections required overlap to remove edge effects in the final results, the processed 10 deg by 10 deg rasters were mosaicked and subset to 250 km x 500 km rasters (Appendix B). Fragstats results files were gridded and compiled into multiband rasters using an IDL script (Appendix C).

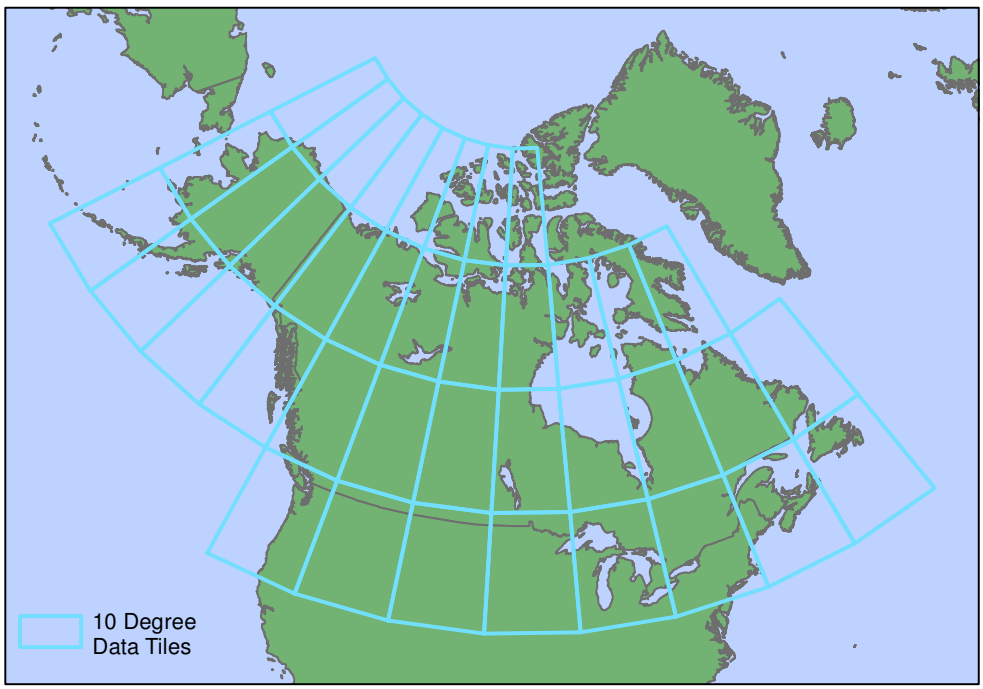

Figure 4.1. Data tiles downloaded from the Hansen et al. (2013) Global Forest Cover dataset.

Also used in some analysis was the predecessor to the Global Forest Change Dataset, MODIS Vegetation Continuous Fields (VCF) which is MODIS data product MOD44B (DiMiceli 2011). This data product is available at 250 m x 250 m, 500 m x 500 m, and 1 km x 1 km resolution for the global land surface and has similar attributes to the Global Forest Change Dataset. It represents forest cover as a percent stored as an integer. The MOD44B VCF dataset has been used extensively around the globe and in the boreal region specifically (Olthof and Pouliot ; Montesano et al. 2009).

Fragstats calculated 32 landscape wide metrics and 33 land cover class specific metrics. Since the class specific metrics produce raster results for each land cover, there are five class specific results rasters with 33 bands each ("no data" is ignored) and one landscape results raster with 32 bands. The bands with their metrics and Fragstats IDs are listed in Table 1.

To single out the boreal forest for analysis, I used two broadly accepted datasets which both represent the northern extent of trees in North America. The first was the Circumpolar Arctic Vegetation Map (CAVM), produced by the U.S. Fish and Wildlife Service, which mapped vegetation north of the boreal forest (CAVM_Team 2003). This map's southern extent marks the boreal treeline. The second dataset was the Ecoregions of North America map produced by the Commission for Environmental Cooperation (CEC), a joint project conducted by the environmental agencies of Canada, the U.S. and Mexico ((CEC) 1997). Of the 50 level II ecoregions in North America, the eight regions were selected to represent the boreal forest in this study were: Alaska Boreal Interior, Taiga Cordillera, Taiga Plain, Taiga Shield, Hudson Plain, Softwood Shield, Boreal Plain, and Boreal Cordillera (Figure 4.2) (Nowacki et al. 2001). All of

Table 4.1a Metrics Calculated for Whole Landscape

Abbreviation	Type	Metric	Statistic
NP	Configuration	Number of Patches	
PD	Configuration	Patch Density	
LPI	Configuration	Largest Patch Index	
ED	Configuration	Edge Density	
LSI	Configuration	Landscape Shape Index	
AREA_MN	Configuration	Patch Area Distribution	Mean
AREA_AM	Configuration	Patch Area Distribution	Area Weighted Mean
AREA_MD	Configuration	Patch Area Distribution	Median
AREA_SD	Configuration	Patch Area Distribution	Standard Deviation
SHAPE_MN	Configuration	Shape Index Distribution	Mean
SHAPE_AM	Configuration	Shape Index Distribution	Area Weighted Mean
SHAPE_MD	Configuration	Shape Index Distribution	Median
SHAPE_SD	Configuration	Shape Index Distribution	Standard Deviation
FRAC_MN	Configuration	Fractal Index Distribution	Mean
FRAC_AM	Configuration	Fractal Index Distribution	Area Weighted Mean
FRAC_MD	Configuration	Fractal Index Distribution	Median
FRAC_SD	Configuration	Fractal Index Distribution	Standard Deviation
PARA_MN	Configuration	Perimeter-Area Ratio Distribution	Mean
PARA_AM	Configuration	Perimeter-Area Ratio Distribution	Area Weighted Mean
PARA_MD	Configuration	Perimeter-Area Ratio Distribution	Median
PARA_SD	Configuration	Perimeter-Area Ratio Distribution	Standard Deviation
CONTIG_MN	Configuration	Contiguity Index Distribution	Mean
CONTIG_AM	Configuration	Contiguity Index Distribution	Area Weighted Mean
CONTIG_MD	Configuration	Contiguity Index Distribution	Median
CONTIG_SD	Configuration	Contiguity Index Distribution	Standard Deviation
PAFRAC	Configuration	Perimeter-Area Fractal Dimension	
CONTAG	Configuration	Contagion	
PLADJ	Configuration	Percentage of Like Adjacencies	
COHESION	Configuration	Patch Cohesion Index	
PR	Configuration	Patch Richness	
PRD	Configuration	Patch Richness Density	
SHDI	Composition	Shannon's Diversity Index	
SIDI	Composition	Simpson's Diversity Index	

Table 4.1b

Abbreviation	Metric	Statistic
CA	Total (Class) Area	
PLAND	Percentage of Landscape	
NP	Number of Patches	
PD	Patch Density	
LPI	Largest Patch Index	
TE	Total Edge	
ED	Edge Density	
LSI	Landscape Shape Index	
AREA_MN	Patch Area Distribution	Mean
AREA_AM	Patch Area Distribution	Area Weighted Mean
AREA_MD	Patch Area Distribution	Median
AREA_SD	Patch Area Distribution	Standard Deviation
SHAPE_MN	Shape Index Distribution	Mean
SHAPE_AM	Shape Index Distribution	Area Weighted Mean
SHAPE_MD	Shape Index Distribution	Median
SHAPE_SD	Shape Index Distribution	Standard Deviation
FRAC_MN	Fractal Index Distribution	Mean
FRAC_AM	Fractal Index Distribution	Area Weighted Mean
FRAC_MD	Fractal Index Distribution	Median
FRAC_SD	Fractal Index Distribution	Standard Deviation
PARA_MN	Perimeter-Area Ratio Distribution	Mean
PARA_AM	Perimeter-Area Ratio Distribution	Area Weighted Mean
PARA_MD	Perimeter-Area Ratio Distribution	Median
PARA_SD	Perimeter-Area Ratio Distribution	Standard Deviation
CONTIG_MN	Contiguity Index Distribution	Mean
CONTIG_AM	Contiguity Index Distribution	Area Weighted Mean
CONTIG_MD	Contiguity Index Distribution	Median
CONTIG_SD	Contiguity Index Distribution	Standard Deviation
PAFRAC	Perimeter-Area Fractal Dimension	
CLUMPY	Clumpiness Index	
PLADJ	Percentage of Like Adjacencies	
COHESION	Patch Cohesion Index	

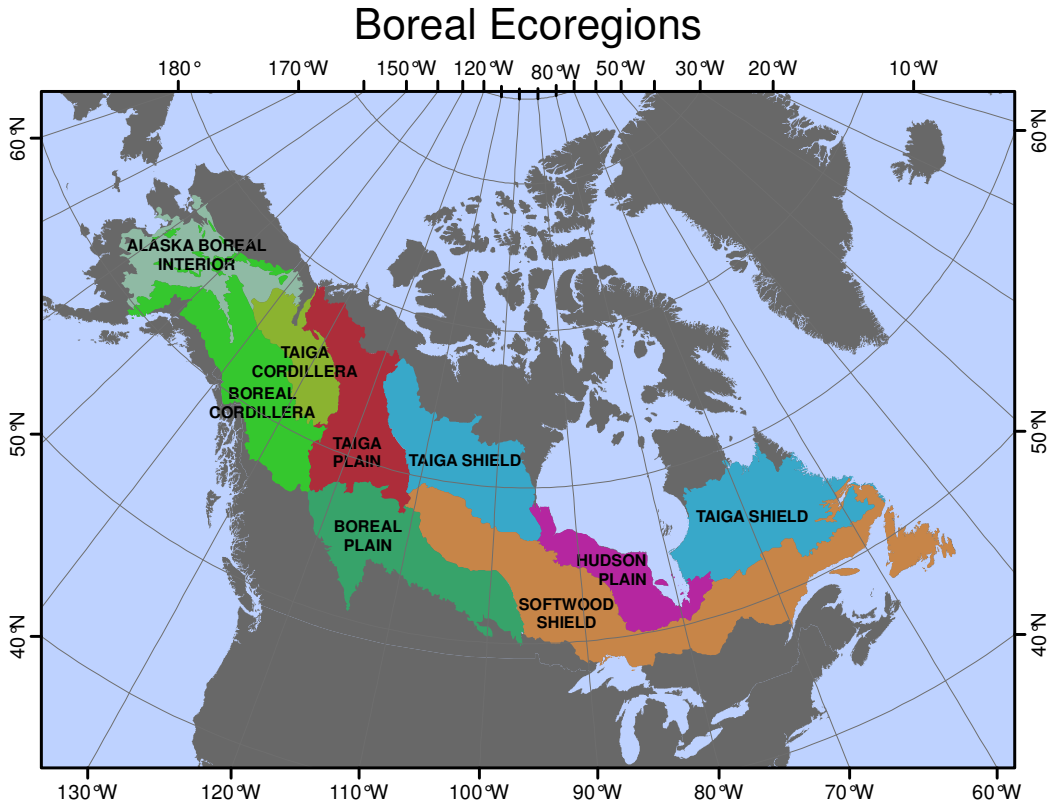

Figure 4.2. Boreal ecoregions defined by the CEC Map of North American Ecoregions.

the boreal forest ecoregions were dissolved to form one North American boreal forest polygon. Because the boreal treeline polyline from the CAVM only identified the northern extent of the boreal forest, it was combined with the southern extent from the North American Ecoregions map. These ecoregions and the two estimates of the boreal treeline represent the extent of the boreal forest for this study.

4.2.2 Land Cover Heterogeneity Metrics

There are several metrics for calculating spatial heterogeneity that are used in this study. Some are specifically designed for certain uses like forestry or mining and some are generic statistical models that can be more broadly applied (O'Neill and Milne 1988; Gustafson 1998; O'Neill et al. 1999; Balaguer-Beser et al. 2013). Some common metrics come packaged with GIS software (Mayer and Greenberg 2005; McGarigal 2012). In any case they are closely linked with the scale of measurement (Wu 2004). This section discusses several metrics for quantifying spatial heterogeneity focusing on pixel based methods that apply to remote sensing land cover.

4.2.2.1 Composition

As mentioned before, metrics for categorical data, like land cover type, can be divided into composition metrics which are non-spatial and configuration metrics which are spatial (Gustafson 1998). Some more common composition metrics include number of categories, proportions of total area, and diversity. The number of categories is simply counted by the user after classification or specified as a parameter of the classification itself (Khorram 1999; Foody 2002). Proportion of area covered is also easily calculated using GIS or image processing software.

The last composition characteristic is diversity which is more complicated and can be represented many ways. Originally designed for ecological studies, diversity represents both the richness and evenness of species distributions. In terms of population, richness is the total number of different species present and evenness is the distribution of the total population between species (Gustafson 1998). In terms of categorical maps, richness and evenness are the same as the number of classes and proportions are explicitly defined at the beginning. Shannon's index is popular in ecological literature and, in land cover mapping terms, represents the uncertainty in the prediction of the cover type for one unit of area (Shannon and Weaver 1949).

$$SHDI = -\sum_{i=1}^{m}(P_i \ln P_i$$

Where P_i is the proportion of the landscape occupied by land cover patch type i. Also common in ecological literature is the Simpson index which represents the probability that two random locations will have the same land cover type (Simpson 1949).

$$SIDI = 1 - \sum_{i=1}^{m} {P_i}^2$$

Computationally, the Simpson index is the same as an area (abundance) weighted mean of the land cover types. When compared over the same landscapes, the Shannon index has greater sensitivity to rare cover types and the Simpson index is more sensitive in landscapes that are dominated by a single cover type (Nagendra 2002). The behavior of these metrics is important to understand as they are commonly used for designing and managing conservation projects to maximize diversity (Roy et al. 1991; Rey-Benayas and Pope 1995). While these composition metrics are non-spatial, they can be made spatial by calculating any one of them in a moving window at different locations across a larger study area (Ritters and Wickham 1995). For

explicitly spatial metrics of heterogeneity and landscape pattern one must use configuration metrics.

4.2.2.2 Configuration

Spatial configuration metrics express the patterns of land cover type in the landscape. They can describe the spatial properties of individual patches or the patterns created by many patches in a neighborhood (Gustafson 1998). Patch based metrics are fairly straightforward and often performed in the first exploratory analysis. Simple patch based metrics include size, density, and perimeter. These metrics are calculated for each patch and then generally expressed in statistical terms (mean, median, number, frequency) for the entire study area. For instance the global scale lake mapping study undertaken by Lehner and Döll (2004) expressed total number of lakes, mean lake sizes, and histograms of lake size for different regions and found a power law distribution of lake sizes. Because of this power law distribution in lakes and other land cover patches, mean size and other similar statistics are poor descriptors. One method that works well for populations in a power law distribution is Largest Patch Index (LPI). LPI is the area of the largest patch of a specific land cover class relative to the total landscape area. The formula is as follows:

$$LPI = \frac{\max_{j=1}(a_{ij})}{A}(100)$$

where a_{ij} is the area of patch ij and A is the total landscape area (McGarigal 2012). Shape can be more complicated and is generally expressed as some ratio of area and perimeter (Osserman 1978; Baskent and Jordan 1995). Perimeter Area Ratio (PARA) is calculated for each patch using the following simple formula:

$$PARA = \frac{p_{ij}}{a_{ij}}$$

where p_{ij} is the patch perimeter and a_{ij} is the patch area. This metric is not standardized to a simple Euclidean shape like a circle or a square, so it varies with the size of the patch. One common method of standardizing this ratio is the shape index (SHAPE) which uses a square standard shape (McGarigal 2012). It is calculated as follows:

$$\text{SHAPE} = \frac{.25\, p_{ij}}{\sqrt{a_{ij}}}$$

For a square, the SHAPE value will be one and any shape that is more complicated will have a higher number. Because it is standardized to a simple shape, the size problem of the perimeter-area ratio is corrected. For raster analysis, this square reference shape can is preferred over a circle as it more closely matches the shape of a single pixel. For vector analysis, a circle may also be used. For representing the aggregate shape of an entire landscape, the shape index can be modified to take all patches in the landscape into account. Landscape shape index is calculated using the total of the perimeters, edges, from all patches in the landscape (E^*) and the total landscape area (A):

$$LSI = \frac{.25\, E^*}{\sqrt{A}}$$

Also used for representing shape is the fractal dimension (*D*) which for objects in two dimensions varies between one and two (Mandelbrot 1982). Simple shapes have a fractal dimension closer to one and as they become more complicated and their boundaries become longer and more irregular, the value approaches two. One formula for fractal dimension can be calculated directly from perimeter and area (Lovejoy 1982). The fractal dimension equals two

divided by the slope of a regression line of the logarithm of patch area and the logarithm of patch perimeter. It is calculated as follows:

$$D = \frac{2}{\frac{\left[N\sum_{i=1}^{m}\sum_{j=1}^{n}(\ln p_{ij} * \ln a_{ij})\right] - \left[\left(\sum_{i=1}^{m}\sum_{j=1}^{n}\ln p_{ij}\right) - \left(\sum_{i=1}^{m}\sum_{j=1}^{n}\ln a_{ij}\right)\right]}{\left(N\sum_{i=1}^{m}\sum_{j=1}^{n}\ln {p_{ij}}^{2}\right) - \left(\sum_{i=1}^{m}\sum_{j=1}^{n}\ln p_{ij}\right)^{2}}}$$

The advantages of shape index and fractal dimension are their ease of calculation because they only involve area and perimeter. It is possible, however, for multiple shapes to have the same area and perimeter so these two metrics do not completely capture all the variability in shape (LaGro Jr 1991). Factor analyses of shape index and fractal dimension shape metrics have found them to represent complimentary heterogeneity factors (Riitters et al. 1995). Fractal dimension represented the complexity of perimeters while shape index was more an indicator of average patch compaction. One example of shape indices in remote sensing of land cover is the mapping of oriented thaw lakes in the Arctic. Mean size, mean shape, and mean orientation were calculated for a subset of lakes in northern Alaska and northwest Canada which indicated that the lakes were generally elongated and oriented in the same direction (Carson and Hussey 1962; Cote and Burn 2002; Frohn et al. 2005).

One particularly useful patch based metric is patch cohesion (Schumaker 1996) which relies on percolation theory (O'Neill et al. 1999). Patch cohesion measures of the connectedness of a landscape which is important from an ecological standpoint because of the migrations of plants and animals. Patch cohesion is higher for landscapes with clumped land cover patches and higher for increased fraction of the landscape that that land cover type occupies. The values increase from zero to an asymptote which indicates that the land cover type is no longer many patches, but one large interconnected patch (Gustafson 1998). Patch cohesion is calculated as follows:

$$\mathrm{PC} = \left(1 - \frac{\sum p}{\sum(p\sqrt{a})}\right)\left(1 - \frac{1}{\sqrt{N}}\right)^{-1}$$

Where p is the patch perimeter, a is the patch area, and N is the number of pixels in the in the study area. Patch cohesion is also often scaled to percentage by multiplying by 100. According to this percolation theory, a random distribution of land cover patches will reach the percolation threshold, total interconnectedness, at a critical proportion (p_c) of 0.5928 (Stauffer and Aharony 1994). Conservation biologists uses percolation theory and p_c to predict the number of steps or boundaries that a migrating animal must cross in order to reach another patch of the same land cover and design conservation areas accordingly (O'Neill et al. 1999). Also because the landscape becomes one continuous patch at p_c, the largest patch size would then be size of the study area multiplied by the proportion p_c.

Pixel based neighborhood metrics include contagion and lacunarity which measure the clustering of pixels and the texture of a raster. Contagion (*C*) is calculated based on the number of land cover classes and the probability of different land cover type pixels being next to each other (O'Neill and Milne 1988; O'Neill et al. 1999). Contagion is calculated as follows:

$$C = 1 + \frac{1}{2\ln(n)}\sum_{i=1}^{n}\sum_{j=1}^{n} p_{ij}\ln(p_{ij})$$

Where n is the number of land cover classes and p_{ij} is the probability of land cover type *i* being adjacent to land cover type *j*. The appeal of the contagion index is that it represents the "clumpiness" of categorical raster data very effectively but it only returns a single index value of an entire study area (Gustafson 1998). Lacunarity uses a moving window to represent the texture of a raster. In addition to two dimensional maps, lacunarity can also be used in one dimensional time series and three dimensional space (Plotnick et al. 1996). PC and C are different methods

for calculating and representing the same factor of categorical data heterogeneity and are therefore highly correlated (Riitters et al. 1995; Gustafson 1998). Their main difference is the form of data that they work on. PC is a metric based fundamentally on vectorized patch data so each patch has an area and perimeter and is one solid unit. Cohesion is fundamentally pixel or raster based so the patches are broken up into pixels that are used as the fundamental unit for analysis. Of course, GIS data can be converted from raster to vector and vice-versa but the pixel size must be specified by the user in order to go from vector to raster and the sensitivity of both of these metrics to resolution and scale makes that a difficult and perilous decision to make.

4.2.3 Selecting the Scale of Analysis

Prior to conducting the analysis using Fragstats, it was necessary to select the appropriate scale and extent for the analysis. As discussed before many spatial metrics are sensitive to both resolution and extent (Benson and MacKenzie 1995; Riitters et al. 1995; Wu et al. 2002; Wu 2004). The resolution, as is the case in many remote sensing studies, was prescribed by the sensor that collected the data to be analyzed. In this case the forest cover data was based on Landsat images and therefore had a nominal resolution of 30m (the data was reprojected from the original Landsat sensor data at 30m to Web Mercator with a resolution of 1 arc-second at the equator within Google Earth Engine and then reprojected back to a 30 m equal area conic projection for the spatial heterogeneity analysis). Given this resolution, I had to select an extent at which to calculate the metrics such that there was enough area large enough to satisfy the sample size requirements of the heterogeneity analysis and also small enough to allow broad spatial trends to be visible at the continental scale. This scale analysis was performed in the

Northern Study Area (NSA), a region near Thompson, Manitoba, in central Canada, that was the site of many previous studies associated with the BOREAS research program (Figure 4.3) (Sellers et al. 1995; Gamon et al. 2004). The study area is a rectangular region of roughly 1.3 $x10^6$ hectares (ha) selected to minimize cloud contamination in the Landsat images.

The first test of to define a minimum extent for analysis involved analyzing the semivariogram for the landscape at different resolutions. The semivariogram was calculated for the BOREAS NSA region using both the 30 m Global Forest Change and MODIS VCF (resampled and reprojected to 130m resolution) (Figure 4.4). Each dataset was reclassified as above to four 25% forest cover classes and a water class. A semivariogram shows the extent of the influence of spatial autocorrelation in a gridded dataset. Pixels closer to each other, smaller spatial lag, are more likely to have similar values and therefore, a lower semivariance. This is the case here as the two graphs have low semivariance values which rapidly increase to a limit with higher lags. The lag at which the semivariance stops increasing is called the range and represents the distance at which pixel values are no longer related to each other due to spatial autocorrelation. The extent must be larger than the range for that landscape and resolution. The range of the 30 m Global Forest Change dataset was roughly 375 pixels or 11.25 km. This same distance converted to 130m MODIS VCF pixels is roughly 87 pixels. These values indicate that a 10 km grid cell would be the smallest extent possible while avoiding spatial autocorrelation problems. Whether this is a large enough extent to robustly calculate heterogeneity metrics will depend on each metric's response to extent changes.

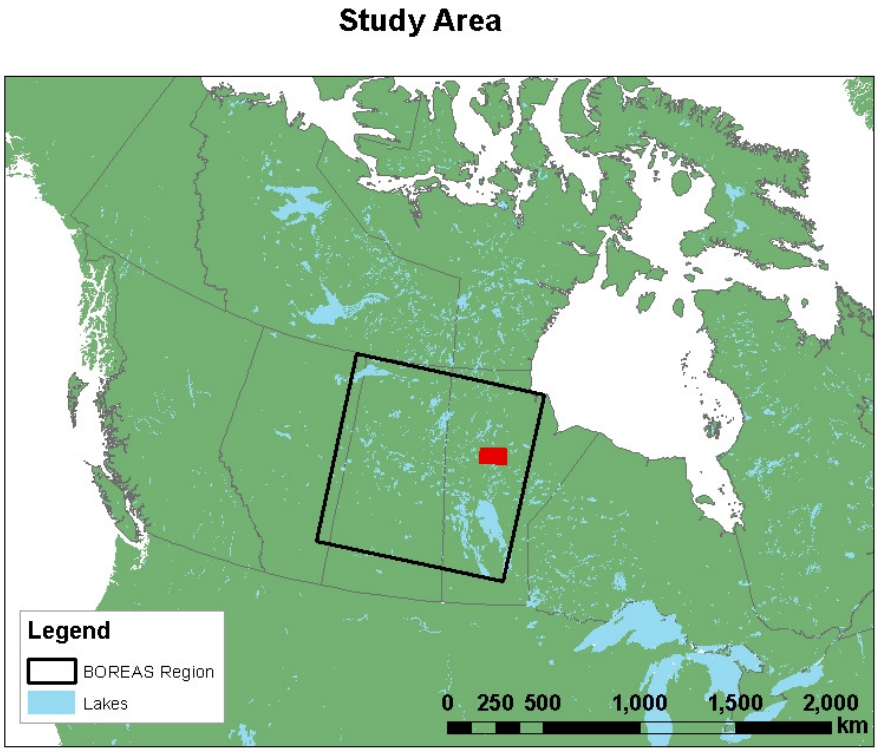

Figure 4.3. The BOREAS study region and the Northern Study Area (NSA) where the scale analysis took place

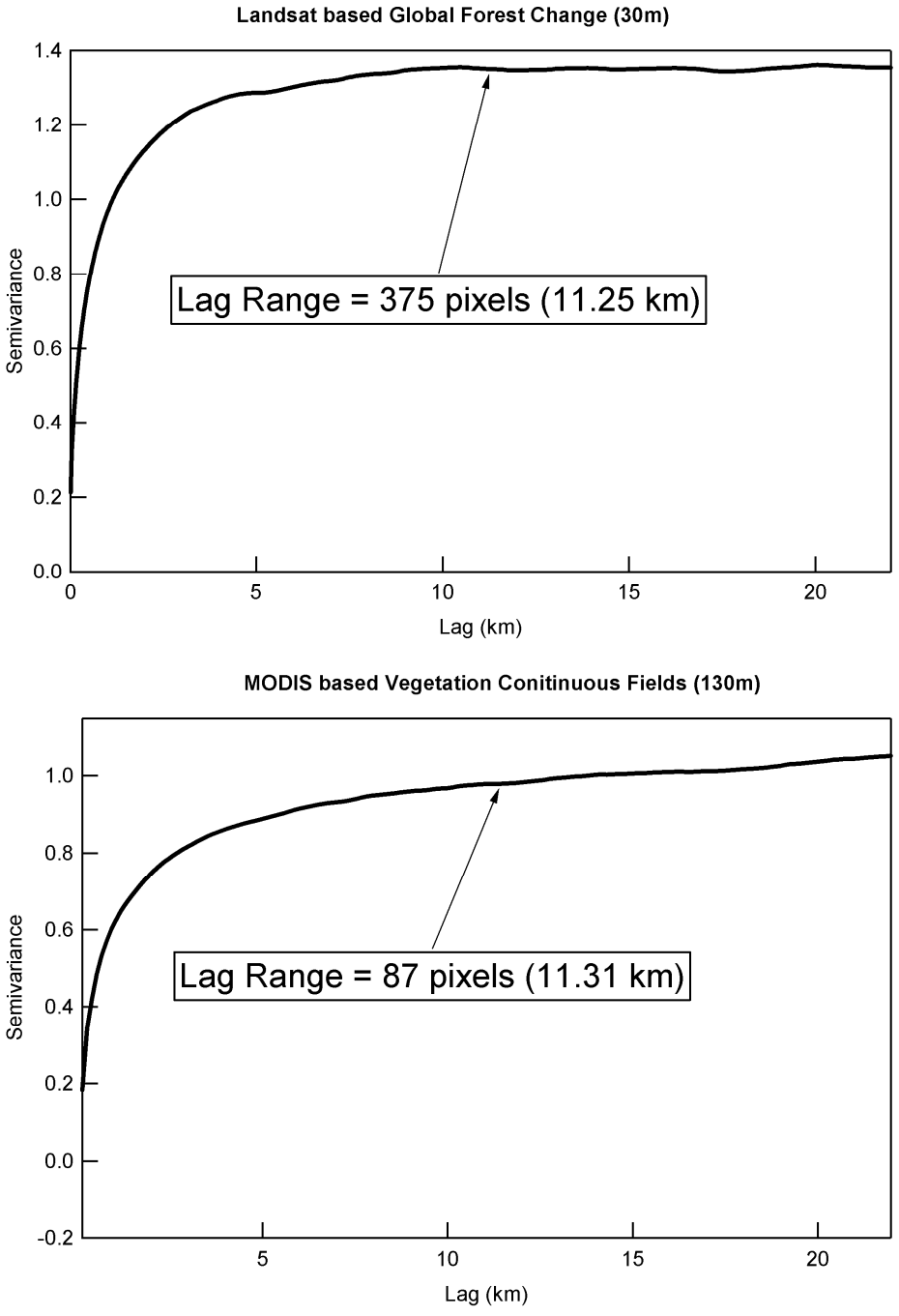

Figure 4.4. Semivariograms for the Global Forest Cover dataset and Modis Vegetation Continuous fields. The lag ranges indicated both correspond to roughly 11 km.

The scaling relationships for different landscape metrics were calculated for four different regions by Wu et al. (2002) including the same BOREAS NSA region that was used above. They divided landscape metrics into three types: Type I are metrics that show predictable changes with scale, Type II are metrics that show staircase-like responses, and Type III are metrics showing erratic or unpredictable responses. Each metric was classified according to its response to change in both resolution and extent. Here we are only interested in the changes with respect to extent because the pixel size was set at the 30 m resolution of the dataset. Because the scale relationships can depend strongly on the landscape patterns, it is particularly important that this study included the boreal landscape explicitly.

The Type I metrics, with respect to extent, include Number of Patches, Shannon's Diversity Index, Patch Richness Density, and Landscape Shape Index (Wu et al. 2002). The values of these metrics are directly related to the extent used to measure them. This is particularly clear with the Number of Patches metric because a larger extent will inevitably include more patches. Because of the relatively simple nature of their relationship with scale, these metrics can easily be estimated for any extent and therefore do not require any specific extent in order to be calculated accurately. Type II and Type III metrics, with respect to extent, include Patch Richness, Patch Size Standard Deviation, Area-Weighted Mean Shape Index, Area-Weighted Mean Patch Fractal Dimension, Patch Density, Edge Density, Landscape Fractal Dimension, Mean Patch Size, Largest Patch Index, Contagion, Mean Patch Shape Index, and Mean Patch Fractal Dimension. These metrics, on the other hand, would result in unpredictable values with changing scale.

The Type II and Type III metrics make unpredictable changes with respect to extent because different land features are partially or completely excluded from the calculation. When enough features, or patches, are included in the metric calculation, the result begins to behave more predictably with changing extent. Based on the scalograms produced by Wu et al. (2002 and 2004) an extent of 1000 x 1000 Global Forest Change (30 m x 30 m) pixels (30 km x30 km) includes enough patches that the patch based Type II and Type III metrics can be calculated with confidence.

In order to maximize the spatial variability that can be mapped, both the 10 km and 30 km extents were used. A 30 km x 30 km moving window was used at 10 km spatial steps. The result is a 10 km x 10 km raster where each grid cell represents a metric value for the 30 km x 30 km grid box that surrounds it.

4.3 Results

The raster results obtained from gridding the Fragstats metrics showed significant variation and spatial patterns in forest heterogeneity across the North American continent. Observed patterns included broadly smaller land cover patches in the boreal forest than the tundra to the north and the temperate forests to the south, decreased contagion within the boreal forest, and class specific percentage of like adjacencies values that indicated a moderately clustered landscape. Patch cohesion of the 0-25% cover class reached the percolation threshold near the boreal treeline.

Within the boreal forest, the Taiga Cordillera region generally performed differently than the others because it was dominated by mountains which were largely unforested. The boreal forest had a mean fractal dimension of 1.384 ±0.024 which was statistically different from both the tundra and the temperate forest regions to the south. Patch cohesion values within the boreal forest never reached the percolation threshold in any forest cover class indicating that no forest cover class was dominant.

By using the percolation threshold to classify 0-25% forest cover class patch cohesion values, a new boreal treeline was created that was based on the southern extent of tundra dominated landscape rather than the northern extent of individual trees. This new treeline map can be generated easily from remotely sensed data and is standard and repeatable.

4.3.1 Heterogeneity Metrics Results

There were too many metrics to include figures for all of the raster results that were calculated so the most interesting metrics are compiled here. Most metrics were calculated for both the broader landscape and for each individual class. The metrics Contagion, Patch Richness, Patch Richness Density, Shannon's Diversity Index, and Simpson's Diversity Index are all independent of land cover class and therefore were not calculated for each class. Conversely, the metrics Total (Class) Area, Percentage of Landscape, and Clumpiness Index require a specific class to be calculated and therefore were only calculated for the individual classes and not the broader landscape.

4.3.1.1 Area Coverage and Patch Area Metrics

The first order analysis of land cover was simply the relative areas of the different forest cover classes (Figure 4.5). Several lakes in Canada are larger than single 10 km grid cells and therefore result in 100% water values. Elsewhere, water is found in highest concentration on the Canadian Shield. The four forest cover classes are broadly laid out in latitudinal bands from sparse in the north to dense in the south. The 0-25% class reappears to the south of the boreal forest as the northern extent of the Great Plains and in several mountainous patches within the boreal forest. The Taiga Cordillera Ecozone in the Yukon and Northwest Territories of Canada contains the Selwyn and Mackenzie Mountains. The Boreal Cordillera Ecozone also contains much of the Alaska Mountain Range and parts of the Tanana Uplands. As a result, these regions have higher concentrations of sparse forest cover classes which make them stand out against the other boreal forest ecoregions. The 75-100% forest cover class generally occupies the southern half of the boreal forest as defined here. This highlights the difference between the boreal forest and taiga. Taiga is most closely represented here as the 25-50% forest cover class and it broadly covers the northern half of the boreal forest.

Number of patches and patch density convey the same information in their distribution as patch density is normalized by landscape area and all grid cells in this analysis have the same area. Patch Density was broadly higher in the boreal forest than in the tundra for the general landscape (Figure 4.6). The 0-25% forest cover class and the 75-100% forest cover classes showed clear latitudinal bands within the boreal forest with denser forests having higher values in the south and sparse forests having higher values in the north. Patch density for all landscape and the middle density forest cover classes had a very clear boundary with the northern treeline

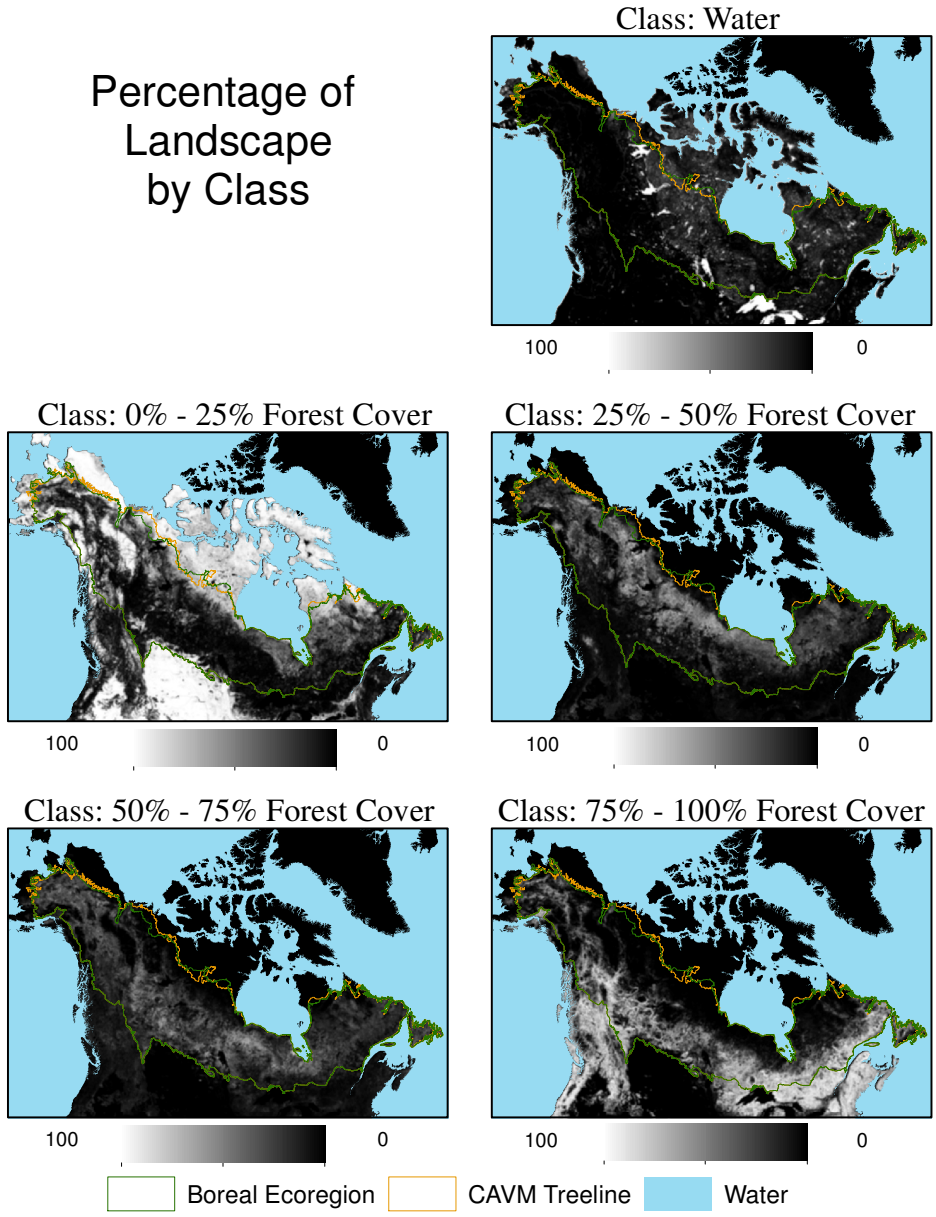

Figure 4.5. Percentage of landscape area by class for each land cover class. All rasters were scaled to 100%.

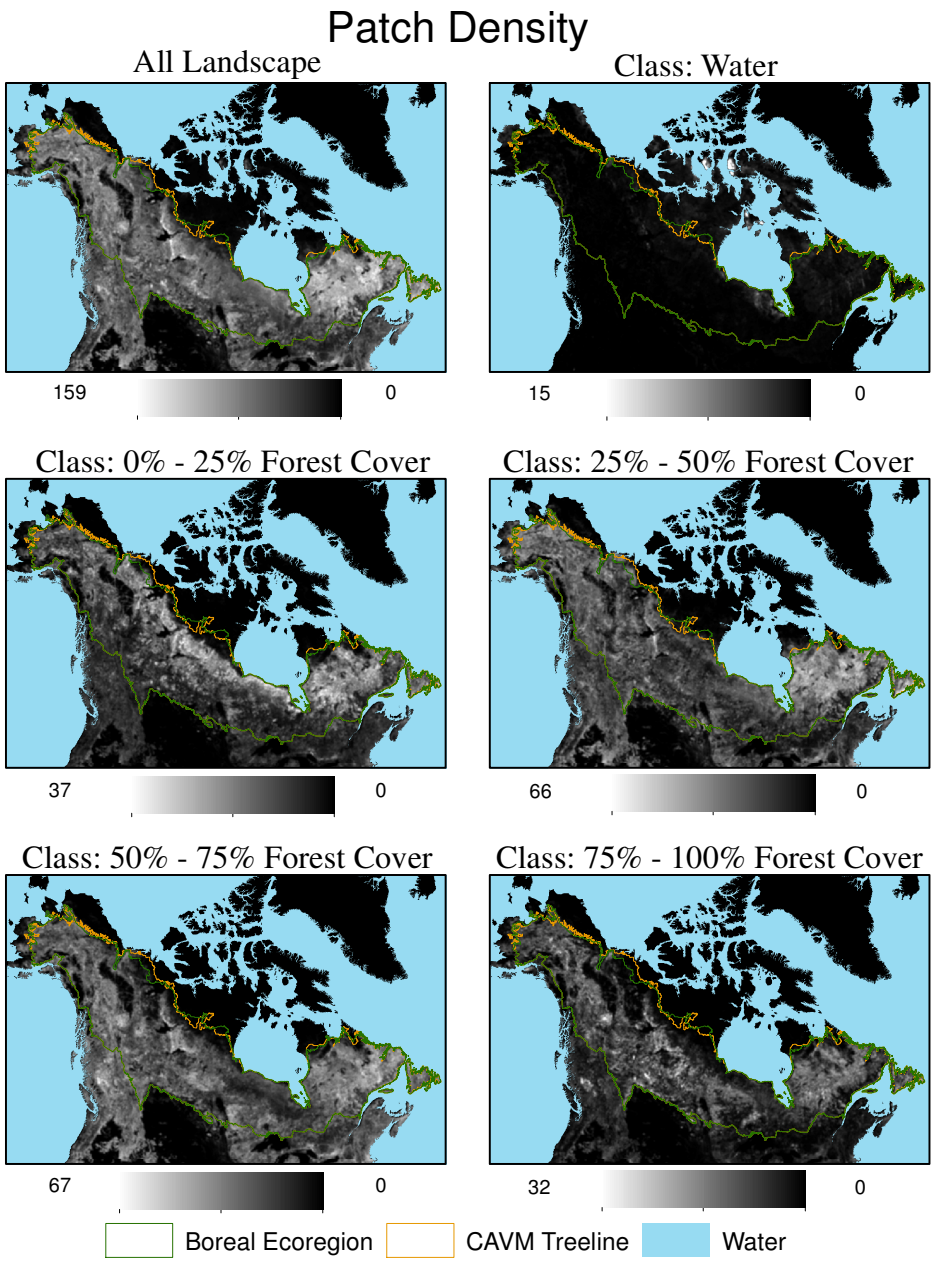

Figure 4.6. Patch density is the number of patches of the land cover type within the landscape area. It is closely related to mean patch area as the landscape size is identical for all grids.

but there was little to no differentiation between the southern boreal forest and the temperate forests of the Pacific Northwest. Because class specific patch density is related to both patch size and class abundance, these patterns could be caused by relative changes in forest cover type or changes in patch size across space.

Patch size showed very different spatial patterns depending on the land cover class but values were broadly low in the boreal forest region (Figure 4.7). High patch area values ringed the edges of the boreal forest and highlighted the mountainous regions within. The tundra regions north of the tree line and the grasslands of the Great Plains were visible in the 0-25% forest cover class map with high mean patch area values. This pattern was also observed in the 75-100% forest cover class which had higher patch area values in the mixed wood shield region of southeast Canada, south of the Softwood Shield ecoregion. The contributions from both of these class specific patterns were identifiable together in the all landscape map. There appeared to be no one land cover class that dominated with large patch areas in the boreal forest. Water and 0-25% forest cover classes had larger mean patch sizes because of the large lakes and mountainous regions within the broader boreal forest. Their mean patch sizes were: 3801 ha for water and 1049 ha for 0-25% cover. The mean patch areas for the more densely forested classes were much smaller: 0.24 ha for 25-50% cover, 0.24 ha for 50-75% cover, and 3.24 ha for 75-100% cover (Table 2).

Similar to mean patch area is the largest patch index which is the ratio of the area of the largest patch to the area of the landscape, expressed as a percentage (McGarigal 2012). Because it is a normalized metric, it is easier to see some of the spatial patterns in this rather than mean patch area (Figure 4.8). There was a clear region of high largest patch index values in the

Table 4.2a		Water			
Metric Name	Statistic	Min	Max	Mean	Stdev
Total (Class) Area		0	90180.09	10484.09	22712.6
Percentage of Landscape		0	100	11.63047	25.19533
Number of Patches		0	59305	488.6709	1388.404
Patch Density		0	65.7629	0.541979	1.539698
Largest Patch Index		0	100	9.510318	24.91875
Total Edge		0	15903810	367038.9	732898.4
Edge Density		0	176.3561	4.070636	8.127378
Landscape Shape Index		0	250.7132	10.33134	15.82404
Patch Area Distribution	Mean	0	90180.09	3800.74	17213.63
Patch Area Distribution	Area Weighted Mean	0	90180.09	8084.059	22326.98
Patch Area Distribution	Median	0	90180.09	3697.431	17198.8
Patch Area Distribution	Standard Deviation	0	45089.28	505.4172	2920.238
Shape Index Distribution	Mean	0	4.2785	0.639747	0.59775
Shape Index Distribution	Area Weighted Mean	0	32.045	1.532955	2.049735
Shape Index Distribution	Median	0	4.2785	0.56368	0.527221
Shape Index Distribution	Standard Deviation	0	3.9271	0.181631	0.225956
Fractal Index Distribution	Mean	0	1.1903	0.557235	0.514656
Fractal Index Distribution	Area Weighted Mean	0	1.3744	0.597917	0.553843
Fractal Index Distribution	Median	0	1.1903	0.550679	0.508638
Fractal Index Distribution	Standard Deviation	0	0.1271	0.019154	0.020601
Perimeter-Area Ratio Distribution	Mean	0	1333.333	442.8969	463.8578
Perimeter-Area Ratio Distribution	Area Weighted Mean	0	1333.333	103.573	185.1131
Perimeter-Area Ratio Distribution	Median	0	1333.333	463.0643	500.0091
Perimeter-Area Ratio Distribution	Standard Deviation	0	666.0002	183.8194	193.8414
Contiguity Index Distribution	Mean	0	0.9987	0.201903	0.248294
Contiguity Index Distribution	Area Weighted Mean	0	0.9987	0.455128	0.438766
Contiguity Index Distribution	Median	0	0.9987	0.178501	0.247184
Contiguity Index Distribution	Standard Deviation	0	0.4993	0.125243	0.133472
Perimeter-Area Fractal Dimension		0	1.5805	0.638012	0.634172
Clumpiness Index		-1	1	0.444696	0.438997
Percentage of Like Adjacencies		0	99.9001	46.24624	44.29199
Patch Cohesion Index		0	100	49.81181	46.98574

Table 4.2b		0-25			
Metric Name	Statistic	Min	Max	Mean	Stdev
Total (Class) Area		0	90180.09	20879.91	31033.97
Percentage of Landscape		0	100	23.17622	34.44346
Number of Patches		0	33551	2677.197	4999.727
Patch Density		0	37.2044	2.969776	5.544857
Largest Patch Index		0	100	18.83102	33.70566
Total Edge		0	15906210	1616701	2518296
Edge Density		0	176.3827	17.93834	27.9377
Landscape Shape Index		0	201.3832	27.66199	41.285
Patch Area Distribution	Mean	0	90180.09	1049.339	8030.099
Patch Area Distribution	Area Weighted Mean	0	90180.09	15933.9	30000
Patch Area Distribution	Median	0	90180.09	750.7379	7823.222
Patch Area Distribution	Standard Deviation	0	45088.61	1504.943	5007.486
Shape Index Distribution	Mean	0	4.6328	0.570115	0.572938
Shape Index Distribution	Area Weighted Mean	0	132.6036	5.860781	10.31753
Shape Index Distribution	Median	0	4.6328	0.504571	0.506282
Shape Index Distribution	Standard Deviation	0	3.904	0.289567	0.389652
Fractal Index Distribution	Mean	0	1.2233	0.512629	0.511943
Fractal Index Distribution	Area Weighted Mean	0	1.4664	0.604849	0.607351
Fractal Index Distribution	Median	0	1.2233	0.503998	0.503342
Fractal Index Distribution	Standard Deviation	0	0.1395	0.018207	0.019267
Perimeter-Area Ratio Distribution	Mean	0	1333.333	516.4254	527.9842
Perimeter-Area Ratio Distribution	Area Weighted Mean	0	1333.333	105.7935	189.5461
Perimeter-Area Ratio Distribution	Median	0	1333.333	577.4744	600.5787
Perimeter-Area Ratio Distribution	Standard Deviation	0	665.9947	161.0302	169.0551
Contiguity Index Distribution	Mean	0	0.9987	0.118462	0.143612
Contiguity Index Distribution	Area Weighted Mean	0	0.9987	0.415732	0.433389
Contiguity Index Distribution	Median	0	0.9987	0.093152	0.126978
Contiguity Index Distribution	Standard Deviation	0	0.4993	0.103899	0.110256
Perimeter-Area Fractal Dimension		0	2	0.648103	0.665523
Clumpiness Index		-1	1	0.363747	0.382995
Percentage of Like Adjacencies		0	99.9001	42.17832	43.70236
Patch Cohesion Index		0	100	47.46624	48.08309

Table 4.2c		25-50			
Metric Name	Statistic	Min	Max	Mean	Stdev
Total (Class) Area		0	71137.8	3750.461	8714.098
Percentage of Landscape		0	78.8842	4.16019	9.663609
Number of Patches		0	59781	5956.982	9552.495
Patch Density		0	66.2907	6.610177	10.5993
Largest Patch Index		0	77.1609	0.709971	4.115319
Total Edge		0	17954550	1879420	3448386
Edge Density		0	199.0966	20.85082	38.24709
Landscape Shape Index		0	261.0084	48.97432	67.16482
Patch Area Distribution	Mean	0	20.4109	0.244683	0.644307
Patch Area Distribution	Area Weighted Mean	0	68063.8	345.9338	2764.503
Patch Area Distribution	Median	0	0.81	0.050552	0.063093
Patch Area Distribution	Standard Deviation	0	1052.311	6.464754	38.63704
Shape Index Distribution	Mean	0	1.6667	0.471352	0.532821
Shape Index Distribution	Area Weighted Mean	0	123.1387	2.090874	7.512461
Shape Index Distribution	Median	0	1.6667	0.439977	0.496411
Shape Index Distribution	Standard Deviation	0	1.6367	0.115673	0.197078
Fractal Index Distribution	Mean	0	1.1135	0.448155	0.505653
Fractal Index Distribution	Area Weighted Mean	0	1.4583	0.483939	0.549231
Fractal Index Distribution	Median	0	1.1135	0.441251	0.497858
Fractal Index Distribution	Standard Deviation	0	0.0681	0.013459	0.016677
Perimeter-Area Ratio Distribution	Mean	0	1333.333	491.9617	556.4417
Perimeter-Area Ratio Distribution	Area Weighted Mean	0	1333.333	336.9669	411.3555
Perimeter-Area Ratio Distribution	Median	0	1333.333	546.1964	624.1116
Perimeter-Area Ratio Distribution	Standard Deviation	0	388.8889	112.9102	130.8244
Contiguity Index Distribution	Mean	0	0.5	0.071151	0.086354
Contiguity Index Distribution	Area Weighted Mean	0	0.9114	0.175347	0.231535
Contiguity Index Distribution	Median	0	0.5	0.05491	0.072453
Contiguity Index Distribution	Standard Deviation	0	0.25	0.069304	0.08073
Perimeter-Area Fractal Dimension		0	2	0.586022	0.66734
Clumpiness Index		-1	1	0.167327	0.216935
Percentage of Like Adjacencies		0	91.6585	18.74292	24.19265
Patch Cohesion Index		0	99.9697	27.05955	34.68111

Table 4.2d		50-75			
Metric Name	Statistic	Min	Max	Mean	Stdev
Total (Class) Area		0	69677.55	3877.72	7818.436
Percentage of Landscape		0	77.2649	4.301239	8.67042
Number of Patches		0	60481	6282.856	10341.83
Patch Density		0	67.0669	6.971589	11.47481
Largest Patch Index		0	65.0532	0.397194	2.39691
Total Edge		0	18107940	2056216	3586859
Edge Density		0	200.7975	22.81113	39.78229
Landscape Shape Index		0	264.9855	49.53741	71.22686
Patch Area Distribution	Mean	0	14.4158	0.237984	0.513891
Patch Area Distribution	Area Weighted Mean	0	56802.27	147.181	1445.124
Patch Area Distribution	Median	0	1.755	0.054984	0.069351
Patch Area Distribution	Standard Deviation	0	904.4623	3.898228	23.35771
Shape Index Distribution	Mean	0	1.5111	0.474368	0.540115
Shape Index Distribution	Area Weighted Mean	0	116.508	1.583844	4.813401
Shape Index Distribution	Median	0	1.5	0.436491	0.496004
Shape Index Distribution	Standard Deviation	0	1.5845	0.124338	0.192668
Fractal Index Distribution	Mean	0	1.0901	0.445641	0.506415
Fractal Index Distribution	Area Weighted Mean	0	1.4536	0.482522	0.55065
Fractal Index Distribution	Median	0	1.0901	0.438439	0.498228
Fractal Index Distribution	Standard Deviation	0	0.0765	0.01457	0.018149
Perimeter-Area Ratio Distribution	Mean	0	1333.333	480.5129	547.6416
Perimeter-Area Ratio Distribution	Area Weighted Mean	0	1333.333	317.5454	390.4932
Perimeter-Area Ratio Distribution	Median	0	1333.333	524.1677	605.2952
Perimeter-Area Ratio Distribution	Standard Deviation	0	455.5556	116.0623	136.1612
Contiguity Index Distribution	Mean	0	0.5833	0.076437	0.093396
Contiguity Index Distribution	Area Weighted Mean	0	0.9106	0.186449	0.240673
Contiguity Index Distribution	Median	0	0.5972	0.060376	0.07856
Contiguity Index Distribution	Standard Deviation	0	0.3167	0.07161	0.084454
Perimeter-Area Fractal Dimension		0	2	0.582845	0.672853
Clumpiness Index		-1	1	0.177877	0.232445
Percentage of Like Adjacencies		0	91.6501	19.86414	25.16885
Patch Cohesion Index		0	99.9618	28.72631	36.3798

Table 4.2e		75-100			
Metric Name	Statistic	Min	Max	Mean	Stdev
Total (Class) Area		0	87457.86	8922.848	18889.84
Percentage of Landscape		0	96.9813	9.900421	20.95494
Number of Patches		0	29002	1827.192	3437.317
Patch Density		0	32.1601	2.027113	3.812406
Largest Patch Index		0	96.9018	5.317217	15.14332
Total Edge		0	14297520	1324121	2385520
Edge Density		0	158.5441	14.69192	26.46437
Landscape Shape Index		0	185.7835	23.9249	36.01745
Patch Area Distribution	Mean	0	1236.606	3.244801	13.17129
Patch Area Distribution	Area Weighted Mean	0	87314.46	3706.221	12033.71
Patch Area Distribution	Median	0	413.325	0.062553	1.34836
Patch Area Distribution	Standard Deviation	0	8813.96	98.56728	328.9858
Shape Index Distribution	Mean	0	3.2466	0.479803	0.551285
Shape Index Distribution	Area Weighted Mean	0	85.7838	4.865287	10.38386
Shape Index Distribution	Median	0	3.2466	0.432811	0.495795
Shape Index Distribution	Standard Deviation	0	1.5547	0.19582	0.301131
Fractal Index Distribution	Mean	0	1.1699	0.442019	0.50628
Fractal Index Distribution	Area Weighted Mean	0	1.43	0.511231	0.590927
Fractal Index Distribution	Median	0	1.1699	0.434653	0.497831
Fractal Index Distribution	Standard Deviation	0	0.0869	0.014763	0.018792
Perimeter-Area Ratio Distribution	Mean	0	1333.333	469.1038	541.1162
Perimeter-Area Ratio Distribution	Area Weighted Mean	0	1333.333	203.6398	341.4994
Perimeter-Area Ratio Distribution	Median	0	1333.333	524.1306	610.3161
Perimeter-Area Ratio Distribution	Standard Deviation	0	647.5991	124.2253	150.8604
Contiguity Index Distribution	Mean	0	0.96	0.081021	0.10439
Contiguity Index Distribution	Area Weighted Mean	0	0.9898	0.271592	0.365558
Contiguity Index Distribution	Median	0	0.96	0.05896	0.082117
Contiguity Index Distribution	Standard Deviation	0	0.4833	0.079057	0.097143
Perimeter-Area Fractal Dimension		0	2	0.560917	0.660642
Clumpiness Index		-1	1	0.25599	0.350707
Percentage of Like Adjacencies		0	99.0739	28.0837	37.14026
Patch Cohesion Index		0	99.9946	33.55337	43.29393

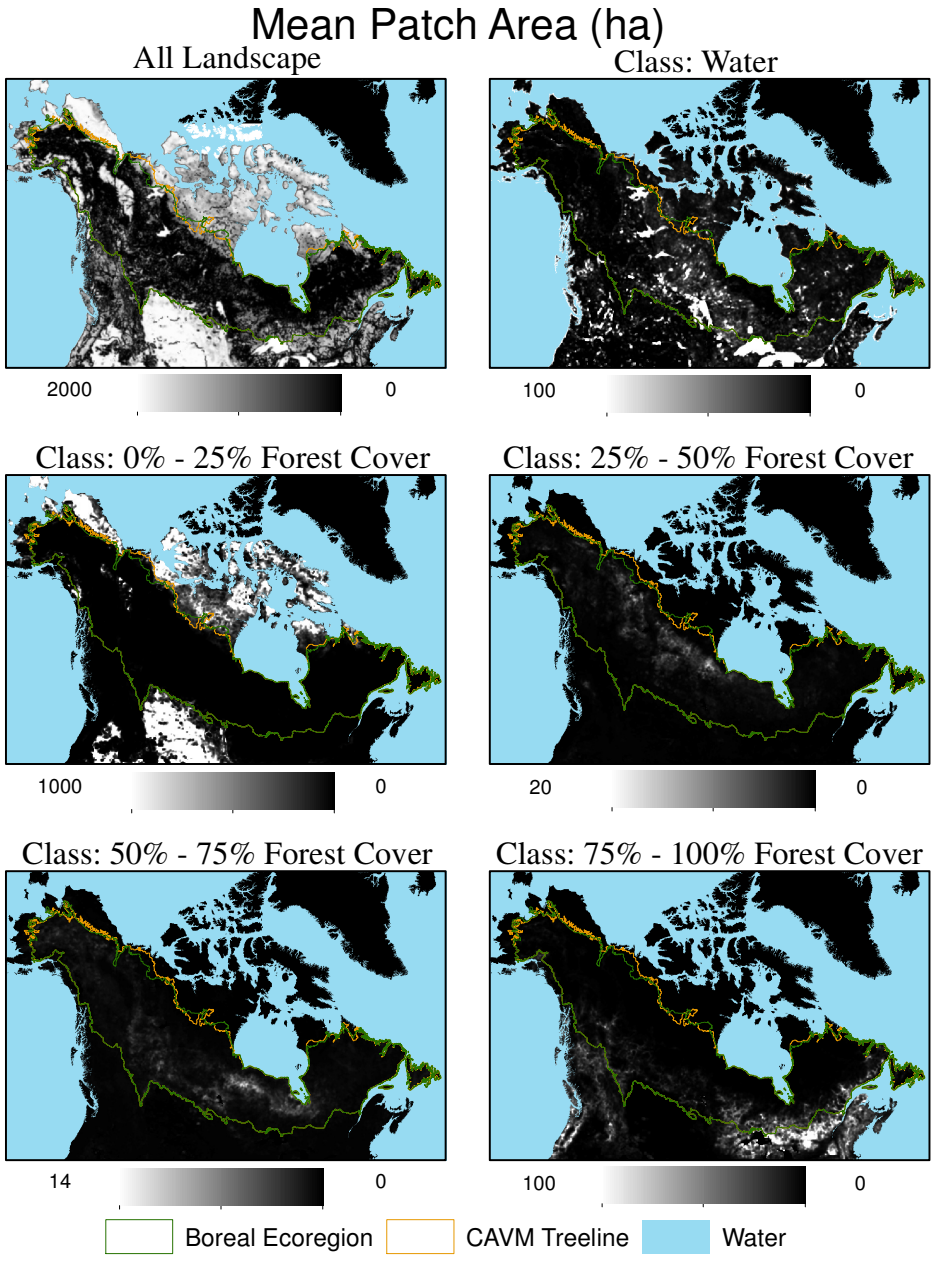

Figure 4.7. Mean Patch Area in hectares. Take particular notice of the very low data limits in the 25-50% and 50-75% forest cover classes. The boreal forest is not dominated by large patches of any particular forest cover class.

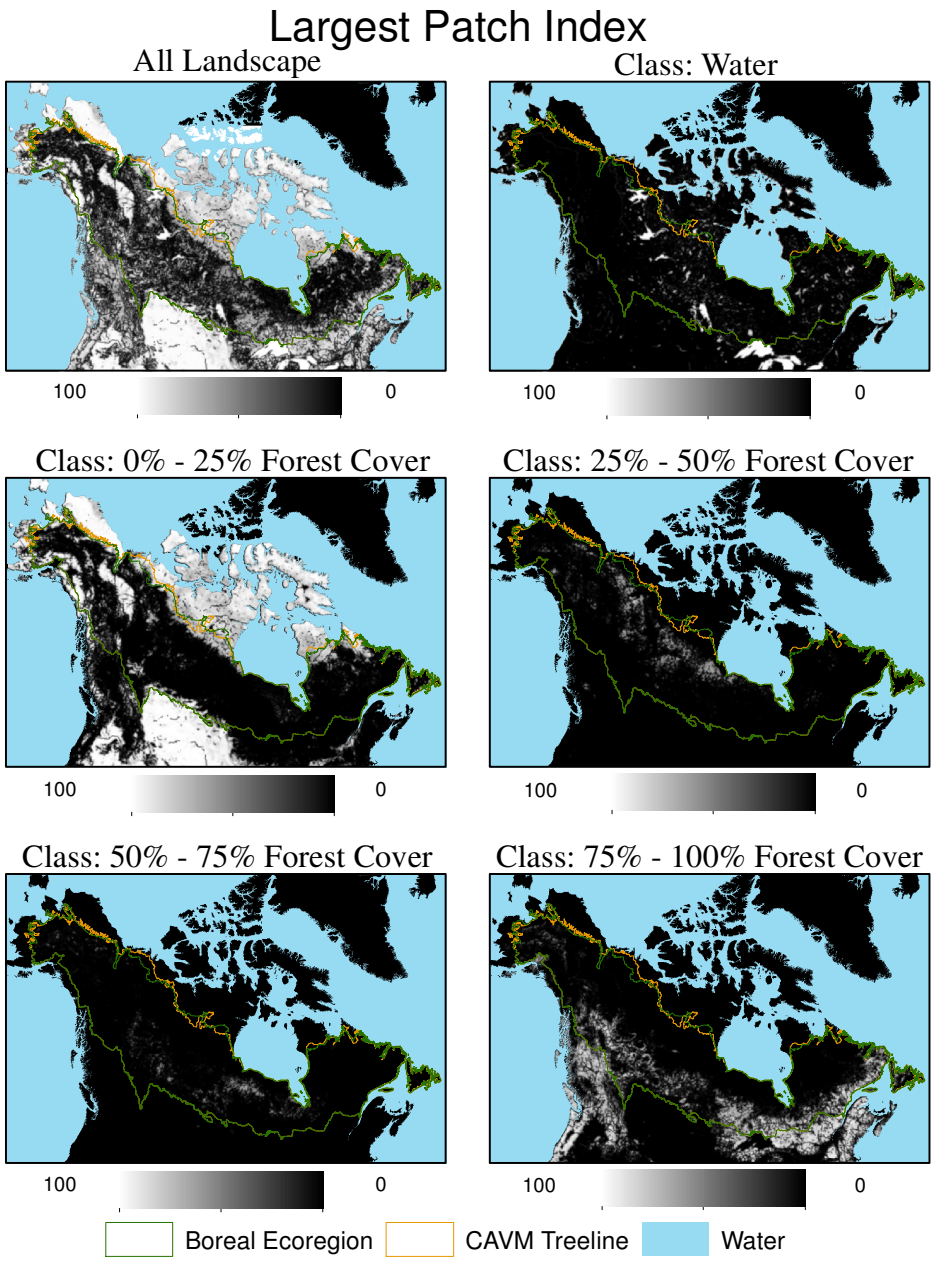

Figure 4.8. Largest patch index is the area of the largest patch in the landscape normalized by the area of the landscape and scaled to 100%. The boreal forest has small patches especially for intermediate forest cover classes.

forested Pacific Northwest for the 75-100% cover class that was not as clear for mean patch area. To visualize these patterns in one map, see Figure 4.9 which combines the all landscape largest patch index with the 50-75% and 0-25% forest cover classes in an RGB composite, false color image. The magenta areas of Figure 4.9 indicate high largest patch index values and high coverage of the 0-25% cover class. This region included tundra, barren mountainous regions, and grasslands to the south. The two red regions in Southwestern and Southeastern Canada had high largest patch index values and low coverage of 0-25% and 50-75% cover classes. The % coverage of these two classes was low in these regions because they were dominated by the densest 75-100% cover class (Figure 4.5). The green areas indicate high coverage of the 50-75% cover class and low largest patch index values. This was the heart of the boreal forest region with small forest cover patches and a relatively high percent coverage of mixed forests. Rather than large patches of the dominant forest cover type, the boreal forest region had many small patches making it unique among other forested regions to the southwest and southeast (red areas). Also visible in Figure 4.9 was a patch of blue between the green boreal forest and magenta tundra. This region had low largest patch index values and high % coverage of the 0-25% cover class identifying it as the transitional zone between the boreal forest and tundra called the taiga. Here the open forest cover class is beginning to dominate in terms of % area but there are still many small patches of other forest cover types making it distinctly different from pure tundra. These combinations of patch area and % coverage metrics form the basis of a new definition of the boreal forest based on spatial structure rather than other traditional methods.

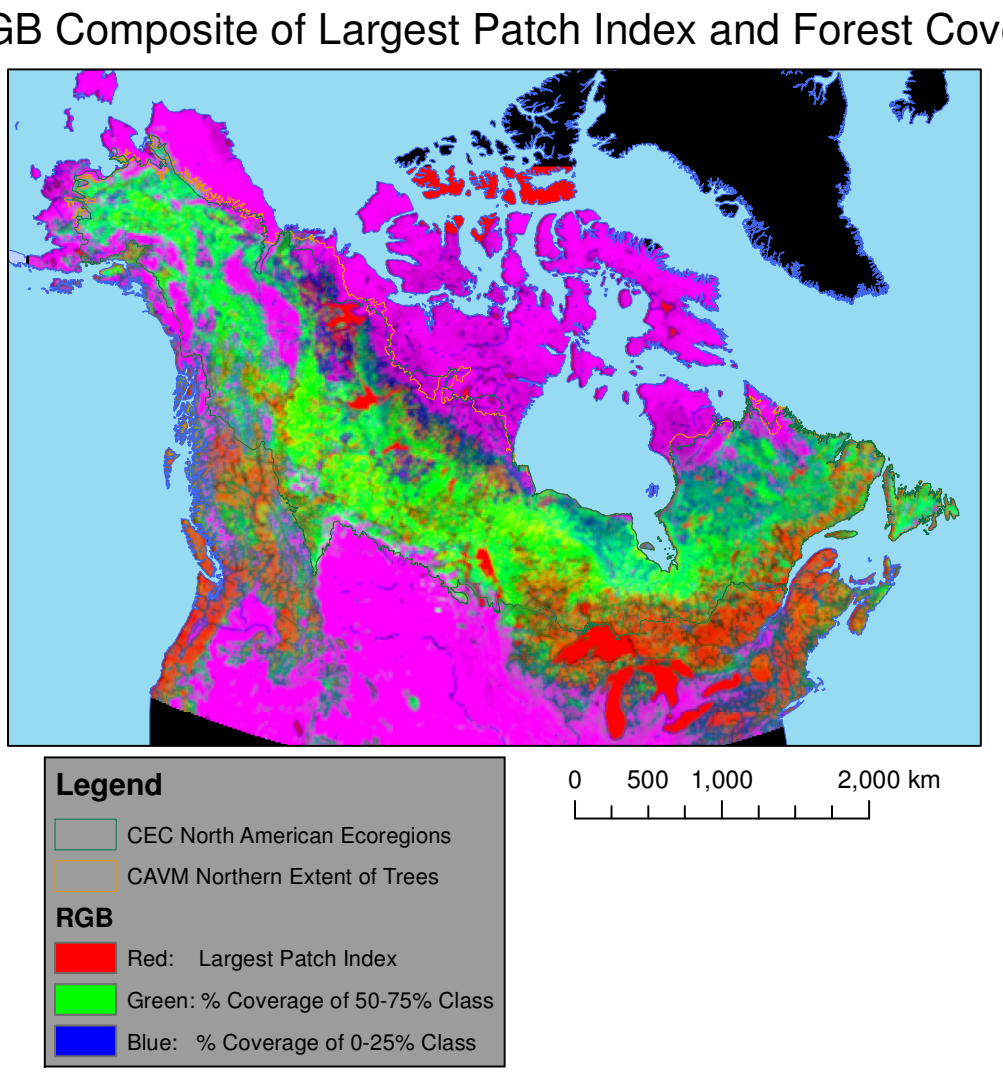

Figure 4.9. This RGB composite image highlights the small patches in the boreal forest. Largest patch index is red, percent coverage of the intermediate 50-75% cover class is green, and percent coverage of the sparsest 0-25% cover class is in blue. The red regions are temperate forests that have broadly larger patches and more dense forest cover class than the boreal forest and therefore appear red.

4.3.1.2 Shape Metrics

The simplest way to represent the shape complexity of a landscape is a ratio of the perimeter and area of each patch (Figure 4.10). Although mathematically straightforward, this index is sensitive to patch area because it is not standardized (McGarigal 2012). The perimeter-area ratio can be standardized in two ways, by adjusting for a square standard in the formula for each patch or by calculating the area weighted mean rather than simple mean of all patches in the landscape. The first method as calculated in Fragstats results in the shape index and it is slightly different from the traditional shape index mentioned in section 3.2.4.2 because it uses a square standard rather than a circle. This is more applicable in raster analysis like this because the smallest shape is a square pixel rather than a circle. Mean shape index is shown in Figure 4.11 and the higher values in the tundra region show that the larger individual patch areas in this region are no longer suppressing the index values. Shape index is very robust and is "perhaps the most straightforward measure of shape complexity" (McGarigal 2012).

The other method of standardizing the perimeter-area ratio is by weighting the ratio of each patch according to its area and then calculating the mean. This turns out to be mathematically similar to the landscape shape index so even though they are calculated differently, they arrive at a similar distribution (Figure 4.12). The biggest difference between Figures 3.11 and 3.12 was in the tundra where mean shape index had high values and the area weighted perimeter-area ratio had low values. This region was almost completely dominated by the 0-25% cover class which meant that there was essentially one patch that covered most of the area in each landscape grid cell and less total length of borders between classes. Because of the

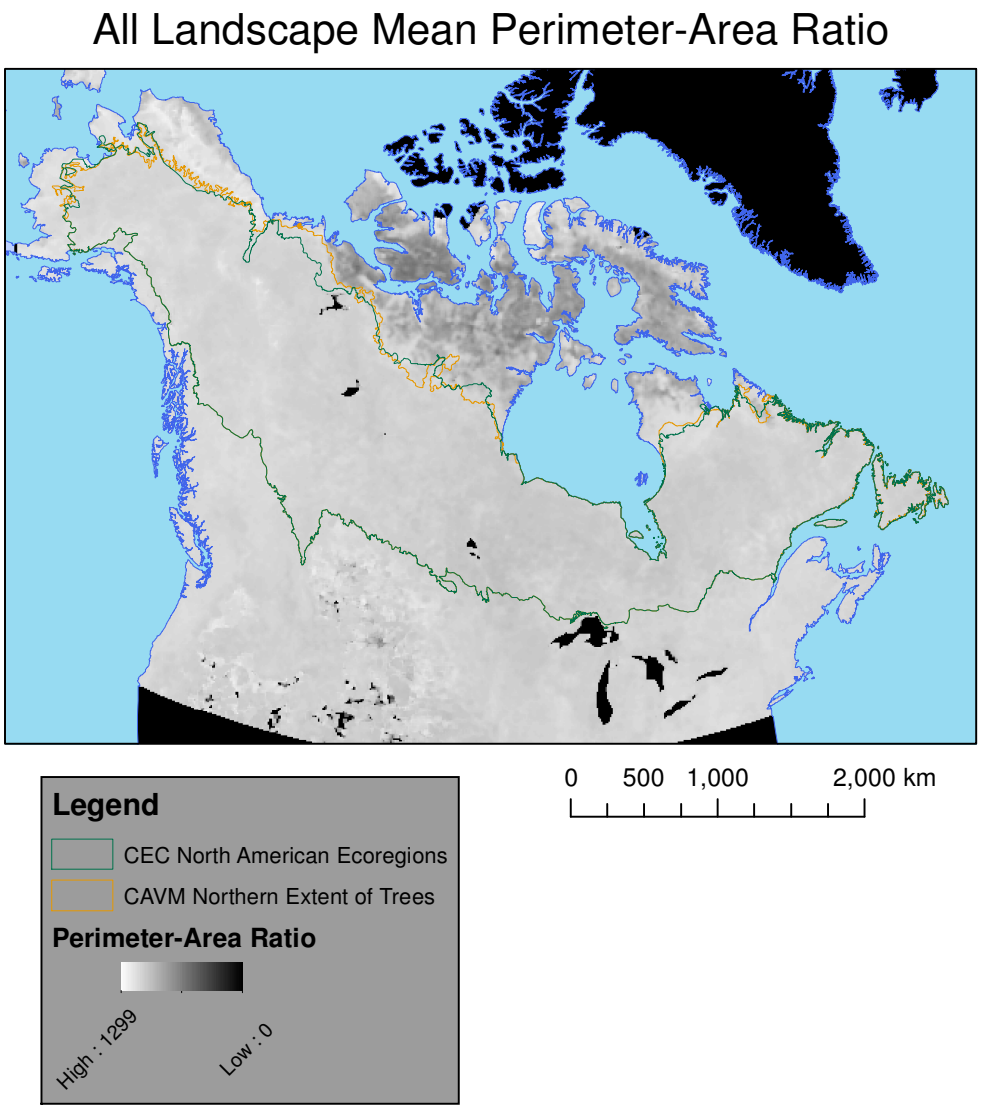

Figure 4.10. Perimeter-area ration is the simplest shape metric to calculate.

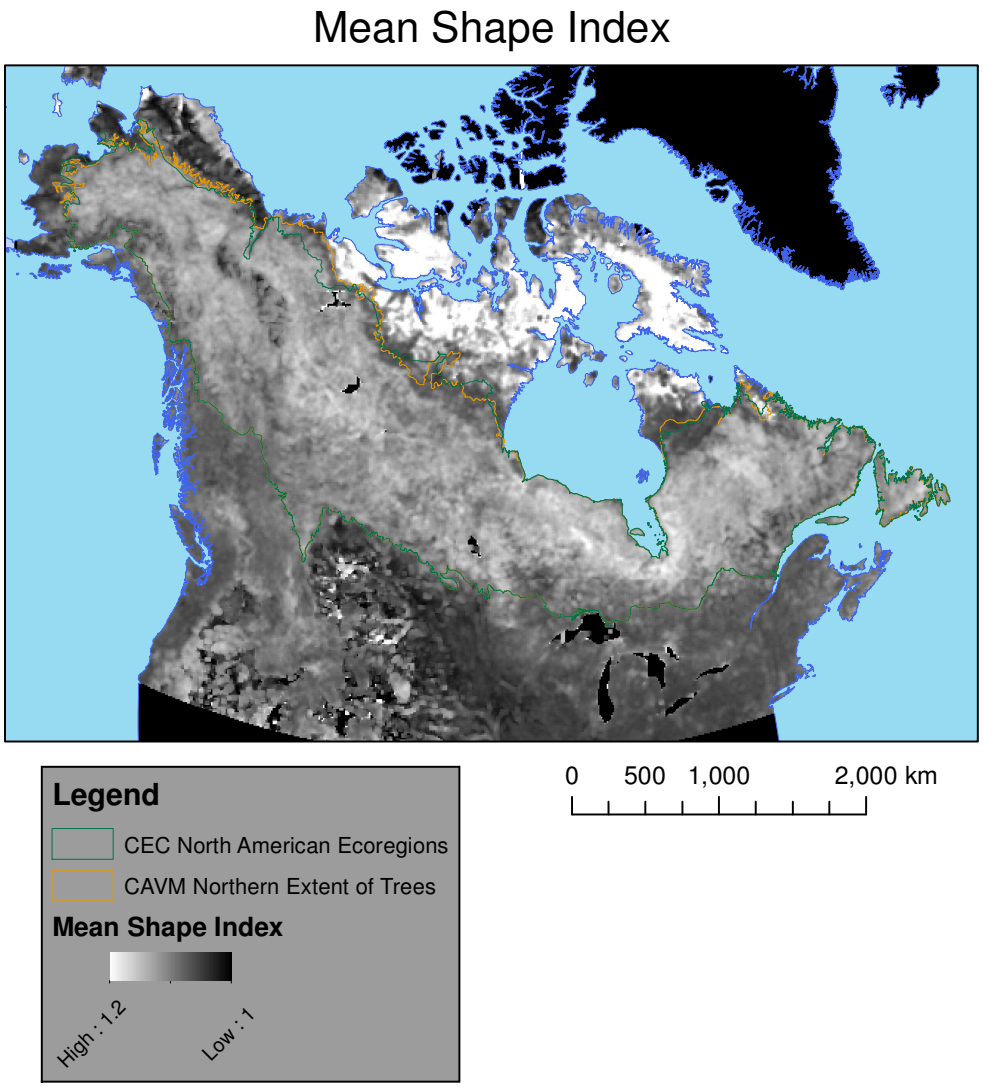

Figure 4.11. Mean shape index is less sensitive to patch size than perimeter-area ratio.

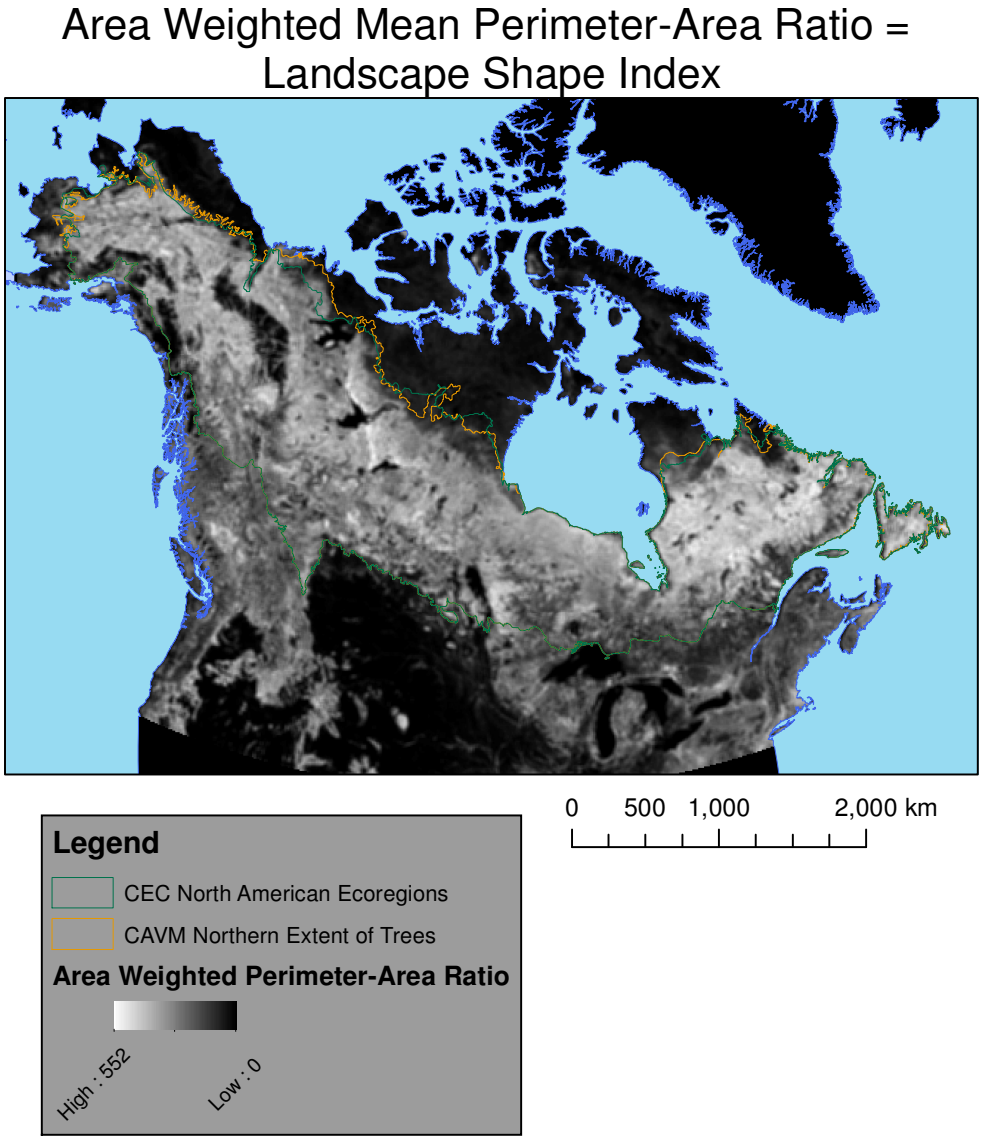

Figure 4.12. Landscape shape index is mathematically identical to the area weighted mean perimeter-area ratio.

way that the area weighted mean perimeter-area ratio/landscape shape index is calculated, the drop in perimeter length caused those tundra values to be significantly lower.

Fractal dimension was calculated using the log of perimeter and area as described in section 3.2.4.2. The resulting fractal dimension varied within the theoretical range of between 0 and 2 for a two dimensional image. The fractal dimension values within the boreal forest were relatively low indicating that the landscape was only moderately complex (Figure 4.13). All landscape fractal dimension was 0.78 while the class specific fractal dimensions were 0.65, 0.59, 0.58, 0.56, and 0.63 for the 0-25%, 25-50%, 50-75%, 75-100%, and water classes respectively.

4.3.1.3 Spatial Pattern and Diversity Metrics

The primary metrics for measuring the spatial pattern of pixels and patches in this study were the two pixel based metrics: contagion and percentage of like adjacencies, and the patch based metric patch cohesion. Patch richness and patch richness density were also calculated but had almost no variation across the study area.

Contagion was calculated for the full landscape as it is not class specific. Low values in the boreal forest indicated that the region had high levels of dispersion and interspersion of multiple land cover classes (Figure 4.14). Mountainous regions within the boreal forest, tundra to the north, and the Great Plains region to the south had much higher contagion values. These regions were dominated by one land cover class that tended to be aggregated into clumps rather than disaggregated or dispersed across the landscape. This result coincides with the earlier finding that the boreal forest region had broadly smaller mean land cover patches.

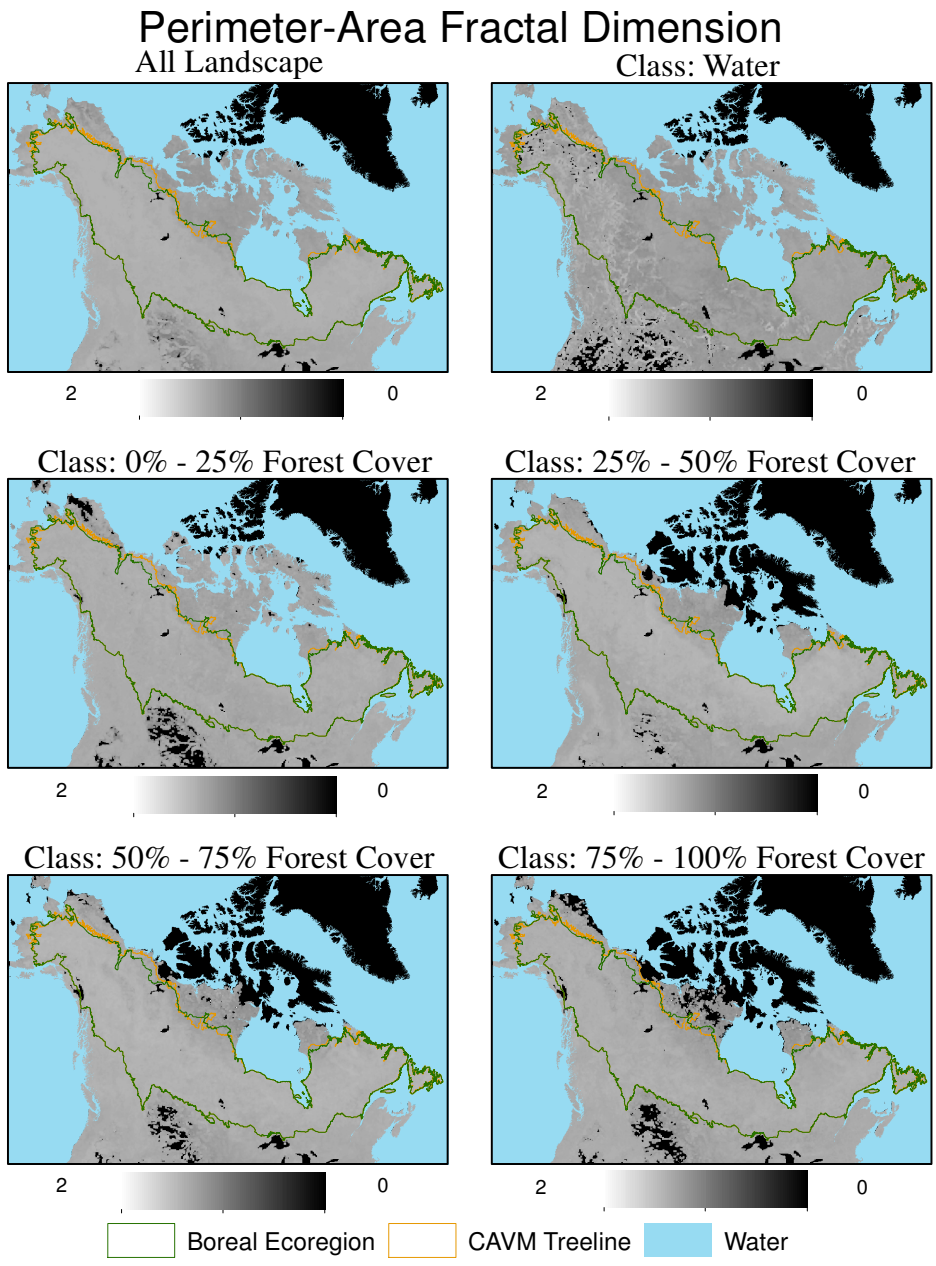

Figure 4.13. Perimeter-area fractal dimension is more sensitive to perimeter length than the shape index.

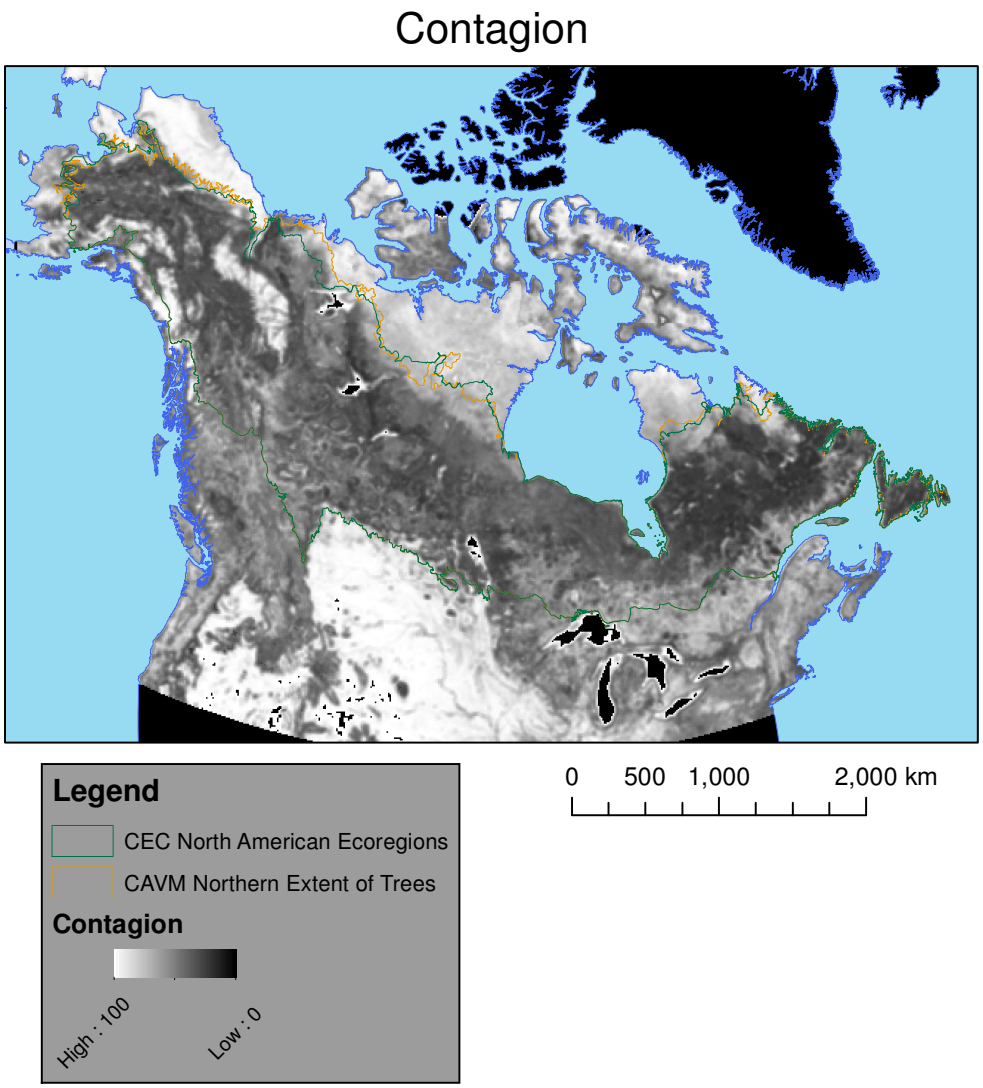

Figure 4.14. Contagion was broadly lower in the boreal forest as multiple forest cover types are dispersed and interspersed with each other.

Percentage of like adjacencies is a class specific version of the contagion metric therefore it was as expected that the all landscape map was very similar in its distribution to contagion (Figure 4.15). For the specific land cover classes, it only indicates the dispersion and not the interspersion of cover classes. When interpreting percentage of like adjacencies for specific classes, the percentage of landscape by the class must also be taken into account. When the percentage of like adjacencies metric for a class equals the class percentage of landscape area, that landscape is randomly dispersed. A higher percentage of like adjacencies than class percentage of landscape area indicates clustering of that particular class to a greater degree than random. Conversely, a lower percentage of like adjacencies than class percentage of landscape indicates nonrandom dispersion of pixels in the class. All values in Figure 4.16 were positive which indicated that none of the cover classes were dispersed more than a random degree. High values in Figure 4.16 indicated clustering of that land cover type and water tended to be the most clustered as the pixels were generally in lakes. The 0-25% cover class had broadly higher values within the boreal forest. This indicated that the unforested areas within the boreal forest tended to be clustered, possibly as a result of fires.

Similar to percentage of like adjacencies, patch cohesion index also requires that the class percentage of landscape area be taken into account. The maps of patch cohesion index indicated that patches of intermediate forest cover classes, 25-50% and 50-75% forest cover, were less connected to each other in the boreal forest than the other classes (Figure 4.17). When plotted against the class percentage of landscape area, each cover class showed different relationships. The scatter plots generated for each land cover class used only pixels within the boreal forest (Figure 4.18). In the water class plot, patch cohesion index increased very rapidly with increasing percentage of landscape to the percolation threshold. This indicated a highly

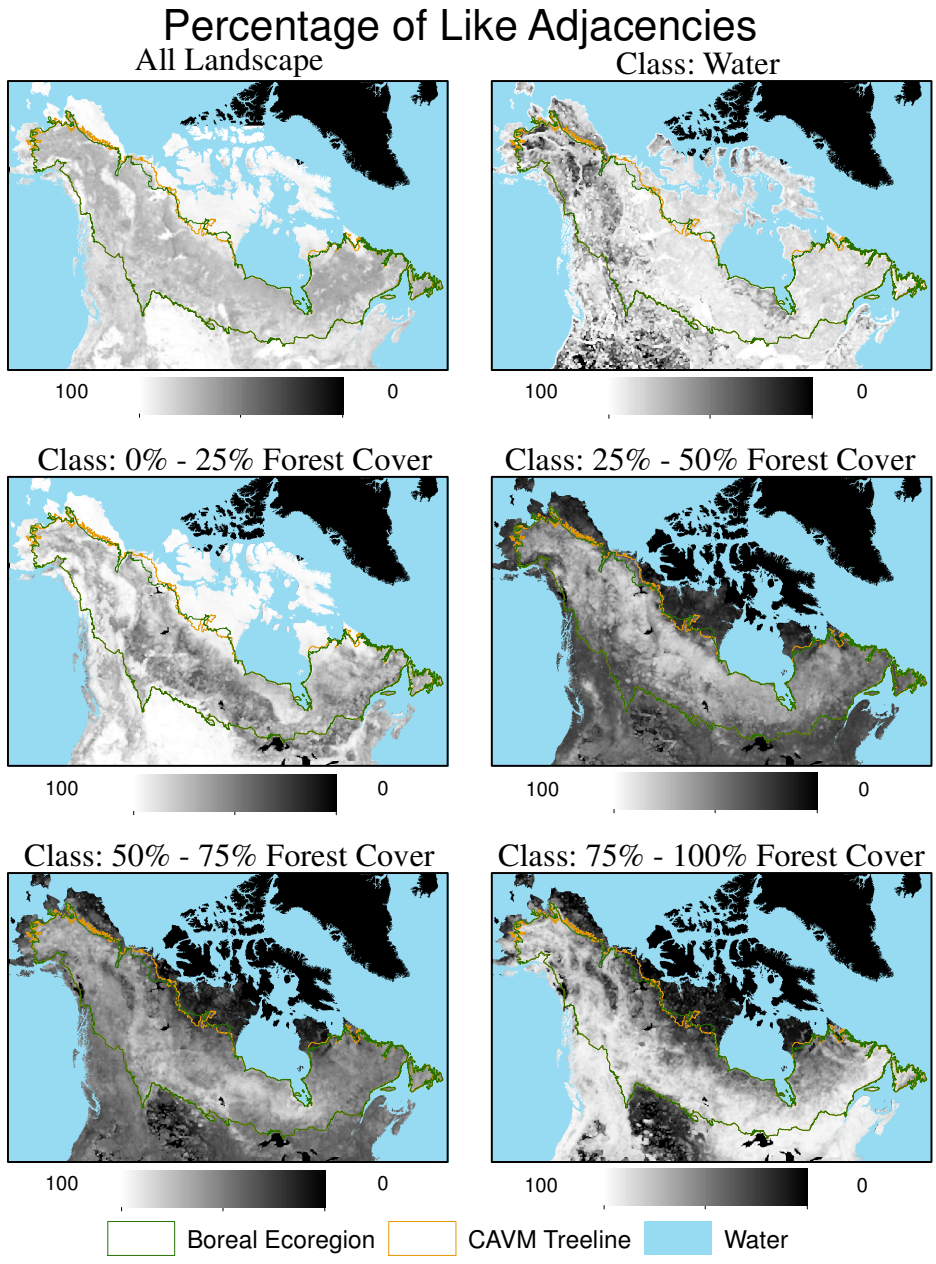

Figure 4.15. Percentage of like adjacencies is similar to contagion but for specific classes.

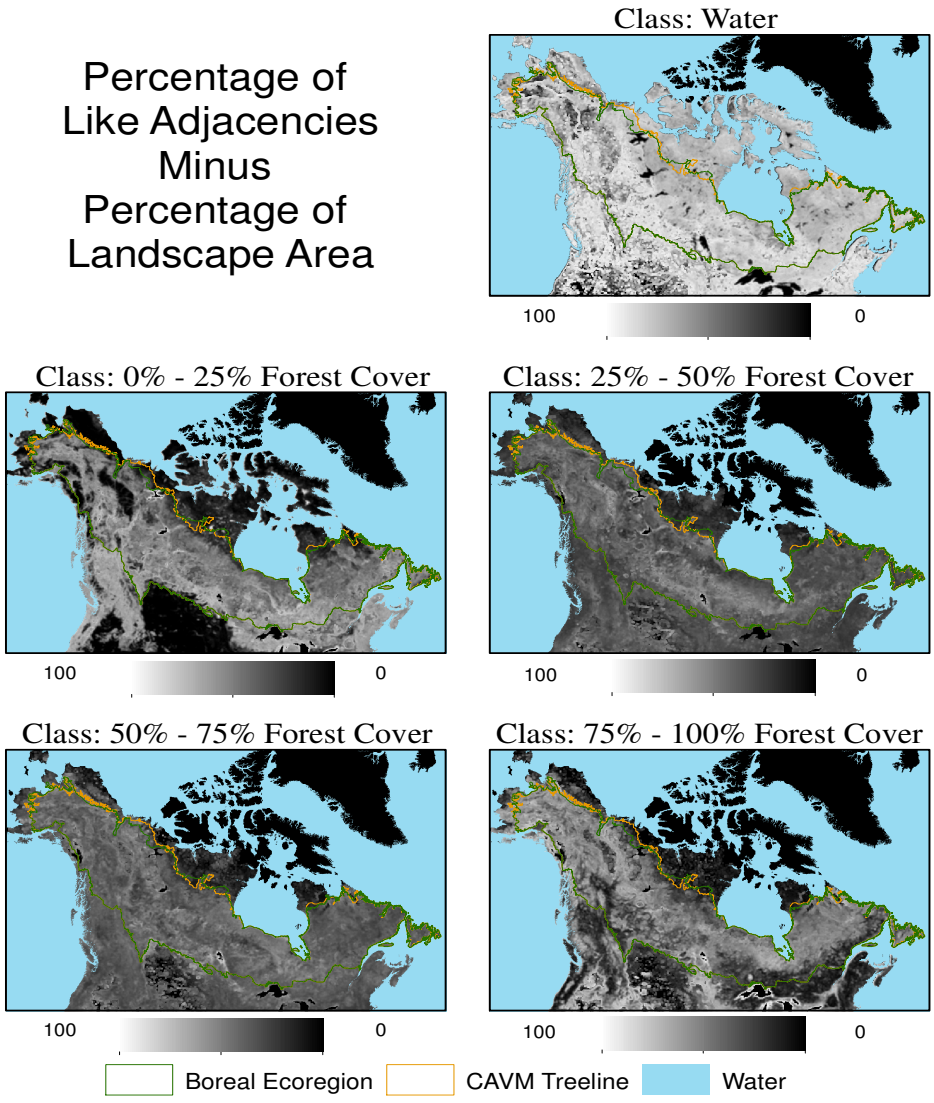

Figure 4.16. Clustered landscapes have a percentage of like adjacencies that is higher than the percentage of landscape area, the landscape is random when they are equal. In this figure, higher values indicate more clustering and lower values indicate a more randomly distributed landscape. There were very few negative numbers indicating that there were no dispersed to a greater than random degree.

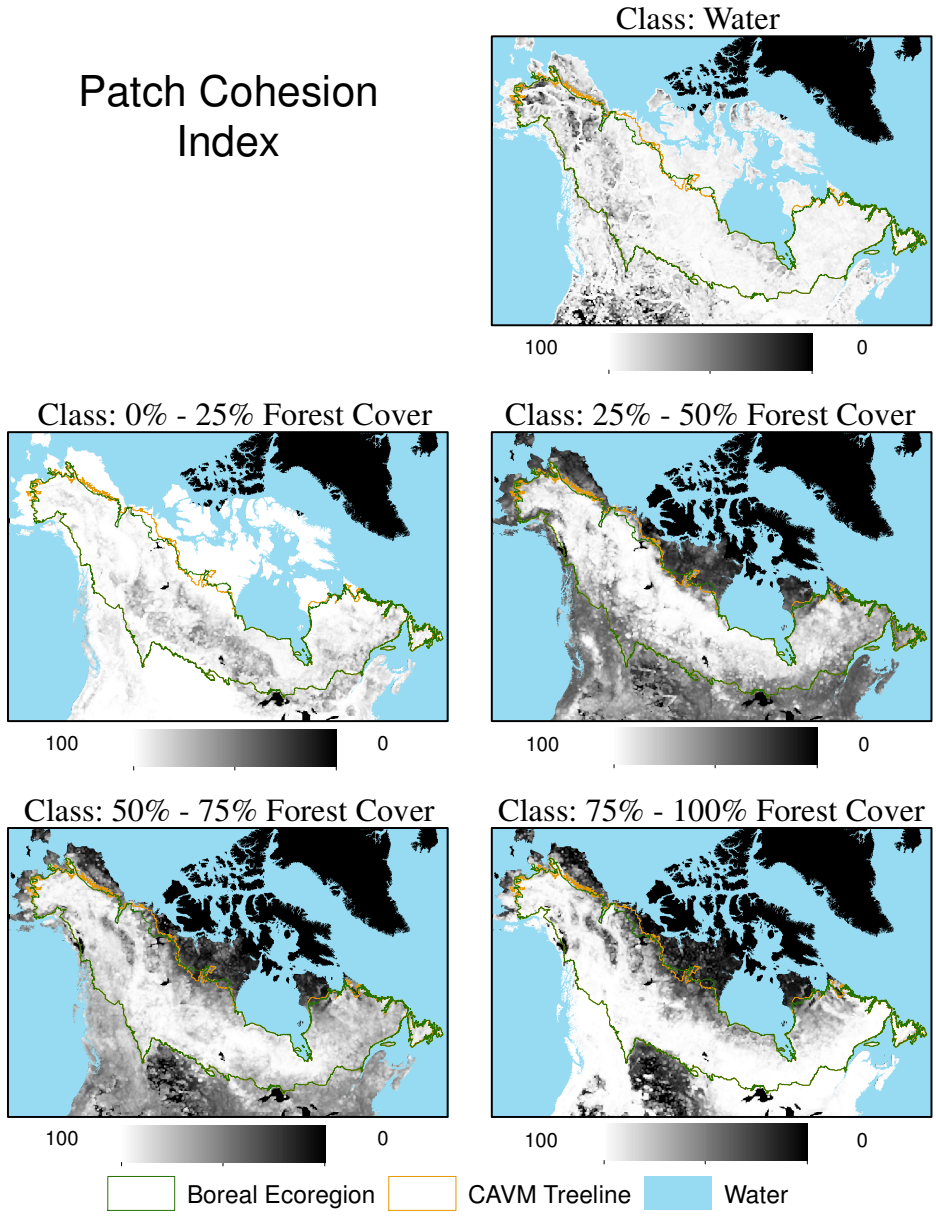

Figure 4.17. Patch cohesion for each forest cover class. The landscape reaches the percolation threshold as the parch cohesion approaches 100%.

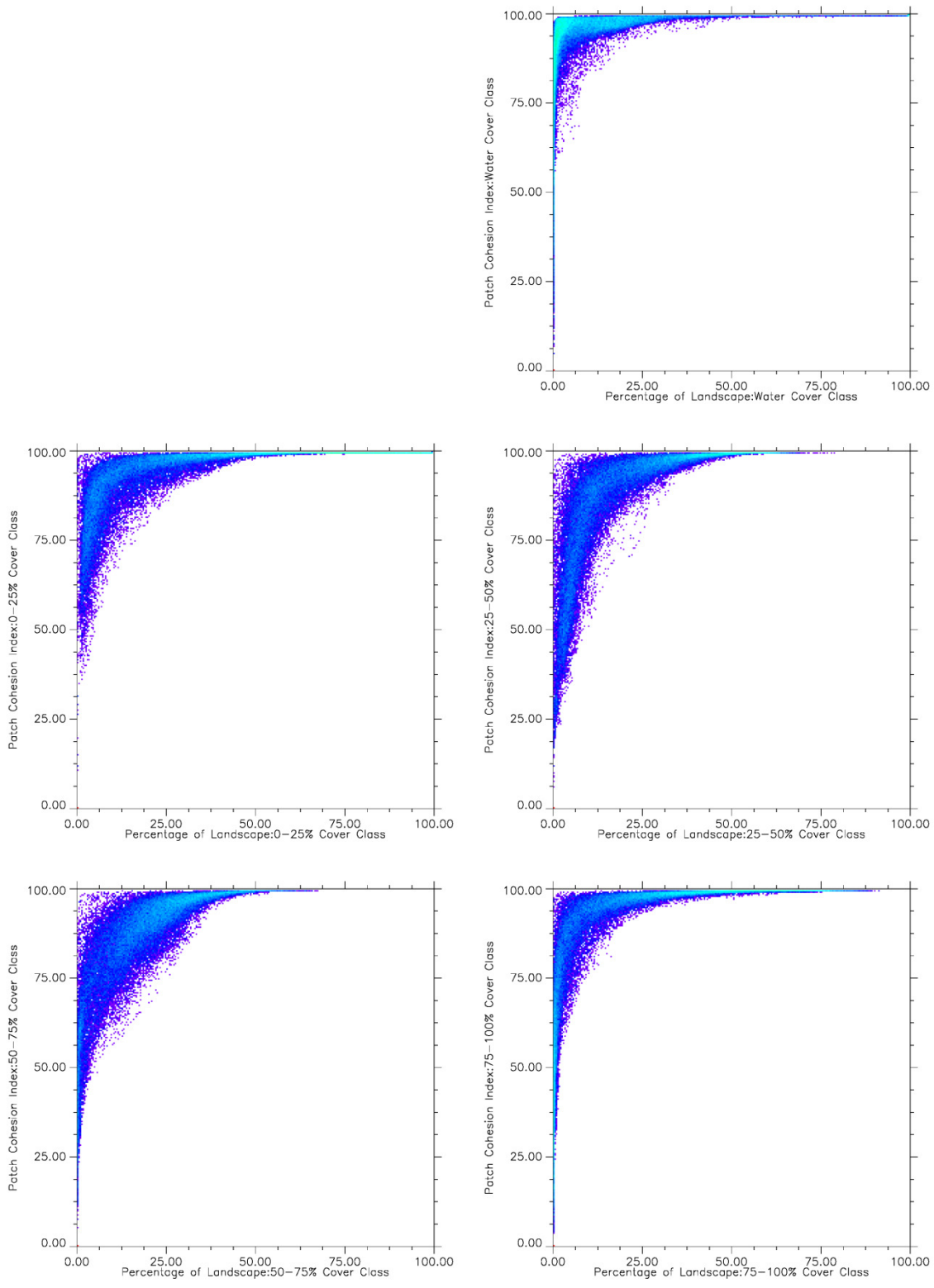

Figure 4.18. Scatter plots of percentage of landscape area and patch cohesion for each forest cover class. A steeper increase indicates a more clustered landscape.

clustered, clumpy landscape which makes sense given that the water patches are mostly lakes and rivers. A more gradual slope like the 50-75% cover class indicated a more dispersed and random landscape which agrees with findings from other metrics. More dispersed land cover classes required a higher percentage of landscape area to reach the percolation threshold which agrees with the percolation theory at the basis of the patch cohesion index.

The two most popular diversity metrics were both calculated for the full landscape as they were not class specific. Within the boreal forest, the values were 0.40 for Shannon's index and 0.21Simpson's index. The ranges were different, varying between 0 - 1.69 and 0 – 0.80 for Shannon's and Simpsons indices respectively, making the absolute values of the maps different but the spatial distributions were largely similar for both (Figures 3.19 and 3.20). The boreal forest was broadly more diverse than the surrounding regions.

4.3.2 Comparisons between Regions

There were eight boreal ecoregions, as defined by the CEC North American Ecoregions Dataset. Four tundra ecoregions and two temperate forest ecoregions were also included for quantitative comparison across metrics. The first metric for comparison is largest patch index (Figure 4.21). Tundra regions had significantly larger patches than the boreal forest and temperate forests. The temperate forests were slightly larger but not statistically distinguishable from boreal forests. Within the boreal forest, the Taiga Cordillera had the highest largest patch index values and the highest variability (50.7 ±35.2). This region, and the Boreal Cordillera which had the second highest values (36.7 ±28.2), contain the Mackenzie and Alaska mountain ranges which are largely unforested. The lowest largest patch index across all regions was the

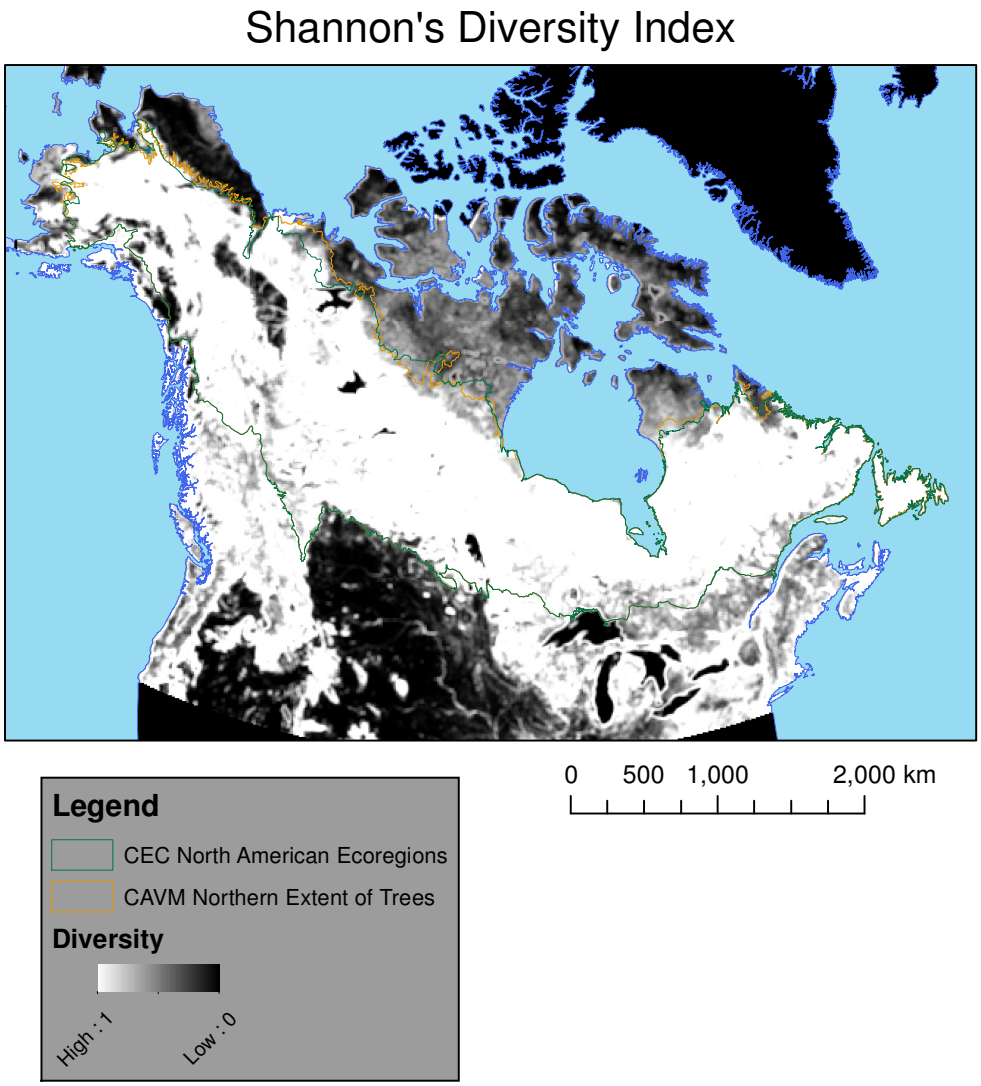

Figure 4.19. Shannon's diversity index is more sensitive to rare land cover types. Which land cover types are rare changes across the continent.

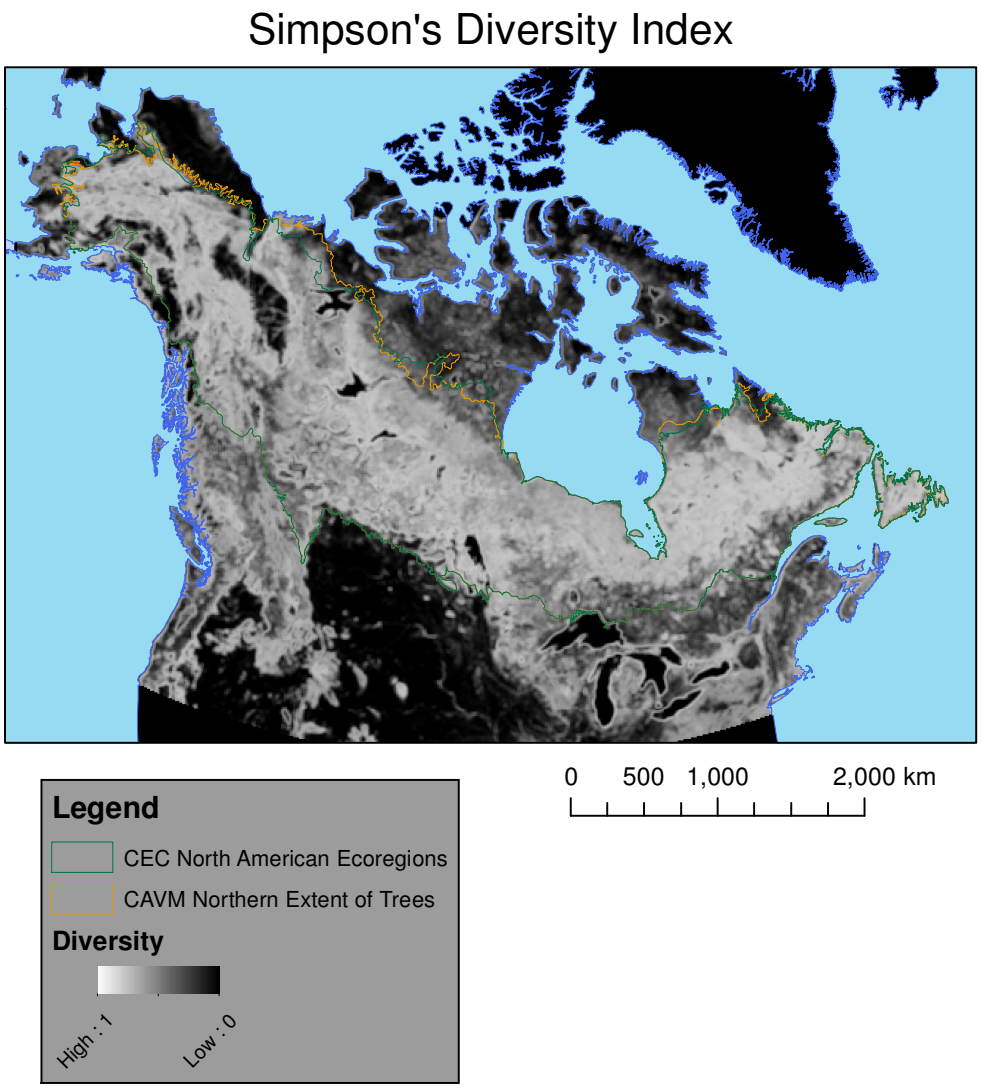

Figure 4.20. Simpson's diversity index is more sensitive to in landscapes that are dominated by a single land cover type.

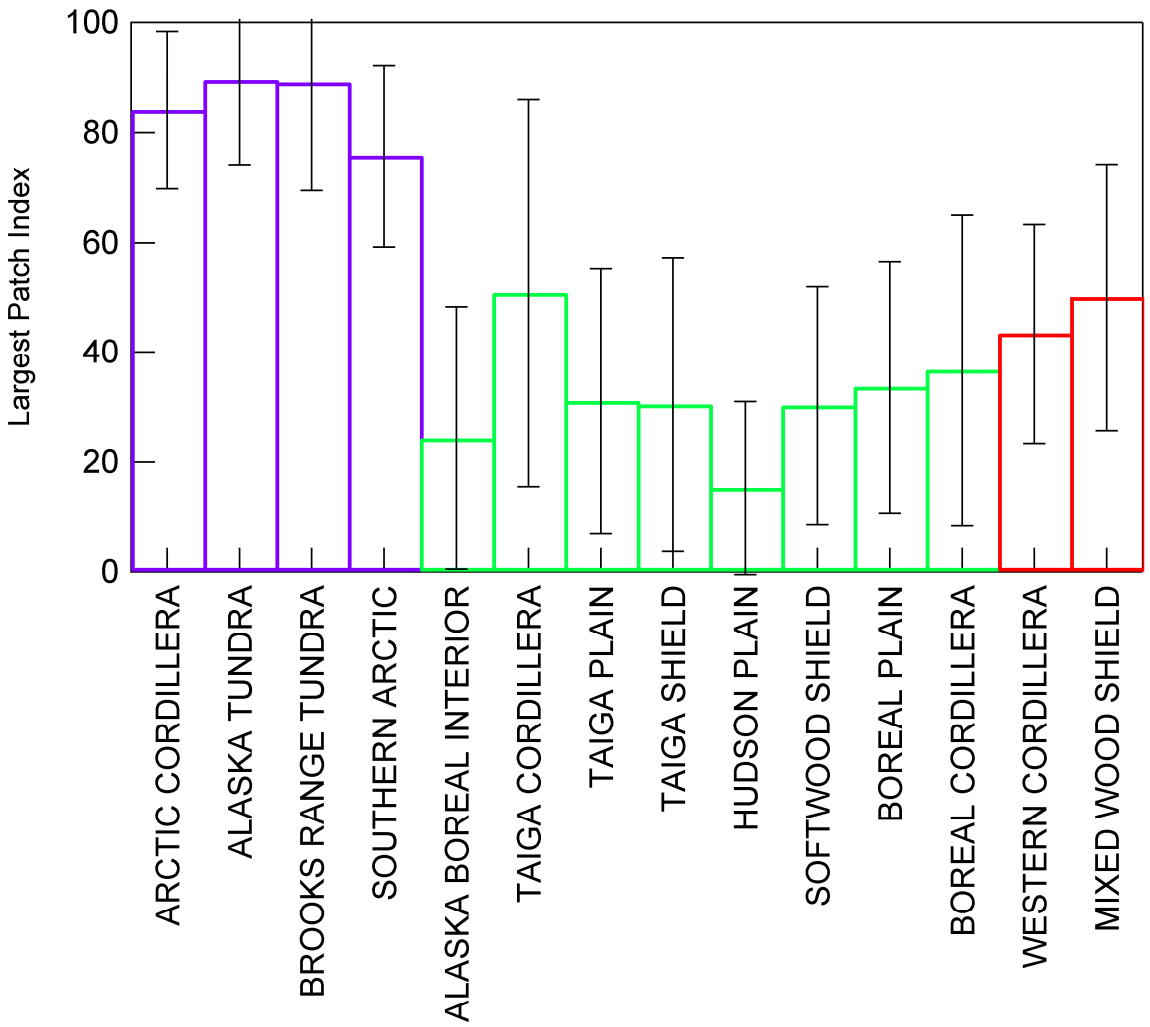

Figure 4.21 Largest patch index values across boreal and neighboring ecoregions. Tundra is shown is purple, boreal forests in green, and temperate forests in red. Error bars show the standard deviation.

Hudson Plain with a value of 15.3 ±15.8. This region and the Alaska Boreal Interior tend to have the smallest patches within the broader boreal forest region.

Fractal dimension was highest in the boreal forest and lowest in the tundra (Figure 4.22). This is consistent with other metrics which indicate a more complex landscape with high edge density in the boreal forest compared to neighboring regions. Variability within the boreal forest was relatively small except for the Taiga Cordillera region, which had lower values and higher variability than the rest of the boreal forest. The eight boreal forest regions together had a mean fractal dimension of 1.384 ±0.024. The Mixed Wood Shield region in Southeastern Canada had significantly lower fractal dimension (1.330 ±0.020) than the other temperate and boreal regions indicating a more homogeneous landscape with large patches of dense forest.

Patch cohesion must be computed for individual classes so Figure 4.23 contains the patch cohesion values for all four forest cover classes in each region. The tundra regions reached the percolation threshold for the 0-25% forest cover class with mean patch cohesion of 99.96 ±0.12. The tundra had low patch cohesion values for the other cover classes because these were only sporadically present in the region. The temperate forests also reached the percolation threshold in the 75-100% cover forest class with mean patch cohesion of 99.63 ±0.76. These temperate forests can therefore be considered continuous dense forest with patches of medium and less dense forests scattered within them. The boreal forest regions, on the other hand never reach the percolation threshold in any land cover class. The closest any region came was the Taiga Cordillera with 99.10 ±1.52 but this region, as discussed earlier, was not representative of the broader boreal forests. Across all of the forest cover classes, the boreal forest had broadly high patch cohesion values in the 80s and 90s, but no single forest cover class was ever dominant.

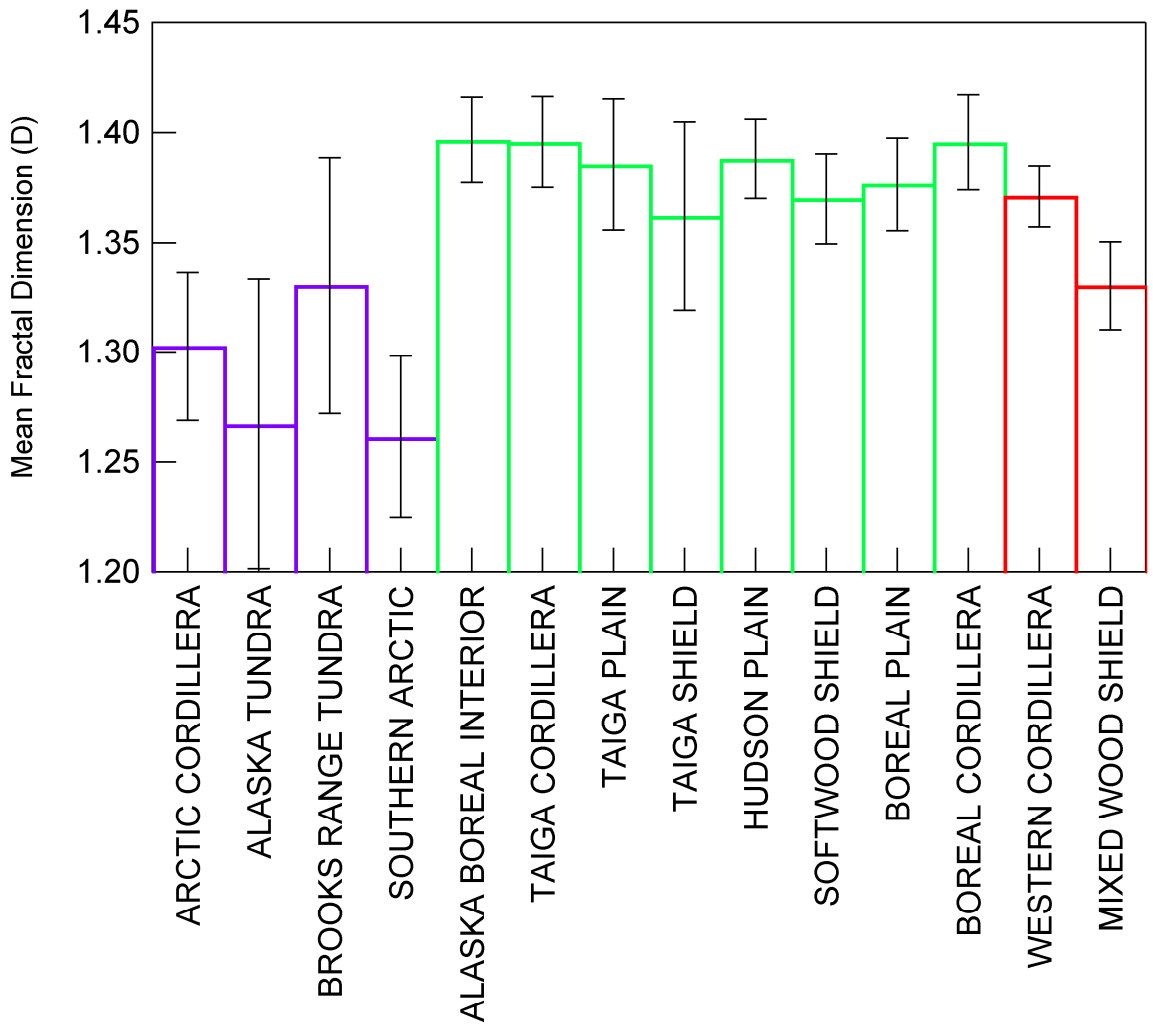

Figure 4.22. The mean fractal dimension of regions. Variability in fractal dimension within the boreal and temperate forests was low. The Mixed Wood Shield region was significantly different from other forested regions.

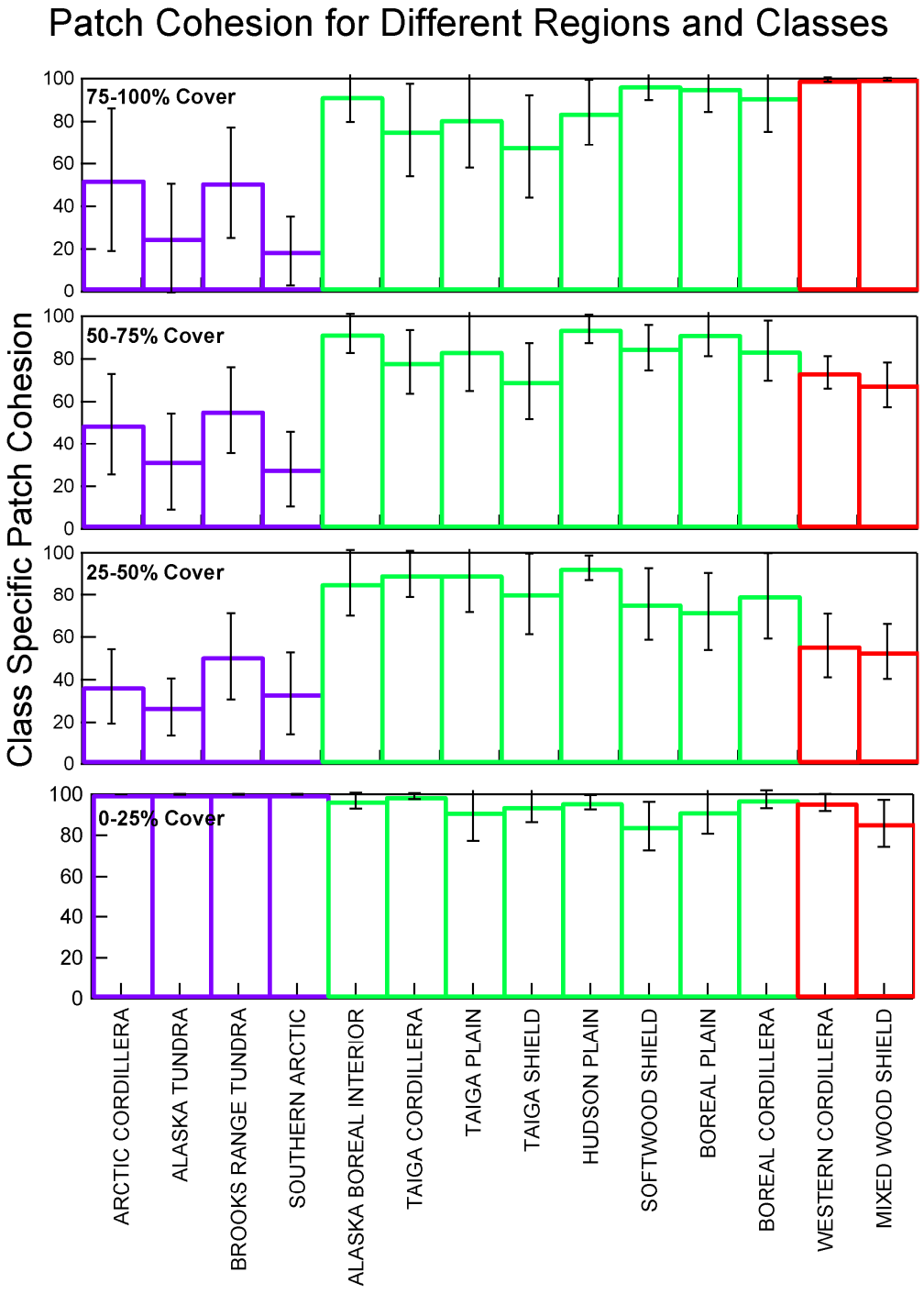

Figure 4.23. Class specific patch cohesion for each land cover class and region. The boreal forest does not reach the percolation threshold in any land cover class but comes close in the 0-25% class.

4.3.3 Boreal Treeline

The northern extent of trees, or boreal treeline, was represented in this study by two datasets from different sources. The Circumpolar Arctic Vegetation Map (CAVM) used the treeline as the southern extent of their dataset and the Commission for Environmental Cooperation (CEC) map of North American Ecoregions defined the border between several boreal and tundra ecoregions. Each treeline was divided into four regions: West Alaska, North Alaska, West Canada, and East Canada (Figure 4.24). These were buffered at 25 km intervals for 200 km on either side of the treeline and used to generate tables of zonal statistics for selected metrics.

Each metric was plotted for the buffers across the treeline for both the CEC and CAVM treelines (Figure 4.25). The dotted lines represent the values for CEC treeline buffers and the solid line represents CAVM treeline buffers. Each region is also represented by a different colored line. The X-axis represents distance from the treeline from South on the left to North on the right. Largest patch index increased across the treeline with the North Alaska region (green) experiencing the largest increase from 33.3 (±7.7) to 96.3 (±6.3) (Figure 4.25). Largest patch index was calculated for the full landscape rather than any one cover class.

Using class specific metrics can help identify the point where a particular class becomes dominant. Patch cohesion for the sparse 0-25% cover class increased across the treeline like the largest patch index but the tundra values were very similar between treeline datasets and regions (Figure 4.26). Patch cohesion was variable within the boreal forest for the 0-25% class but then converged to values close to a mean value of 99.94 ±0.12 above the treeline in all regions. This

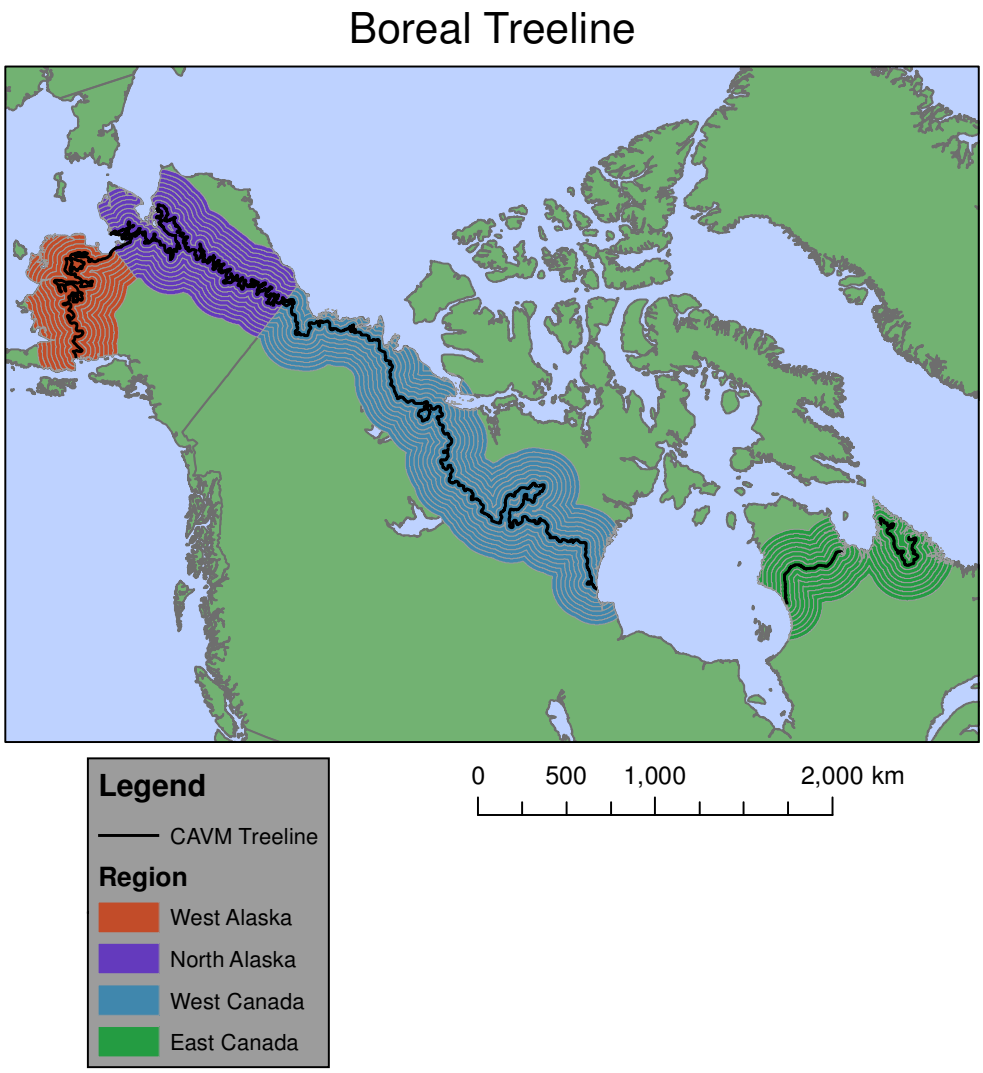

Figure 4.24. The four regions used in the treeline analysis are shown here. There are also eight buffers, each 25km wide on each side of the treeline. The CAVM treeline is shown here but the same buffers were applied to the CEC treeline as well.

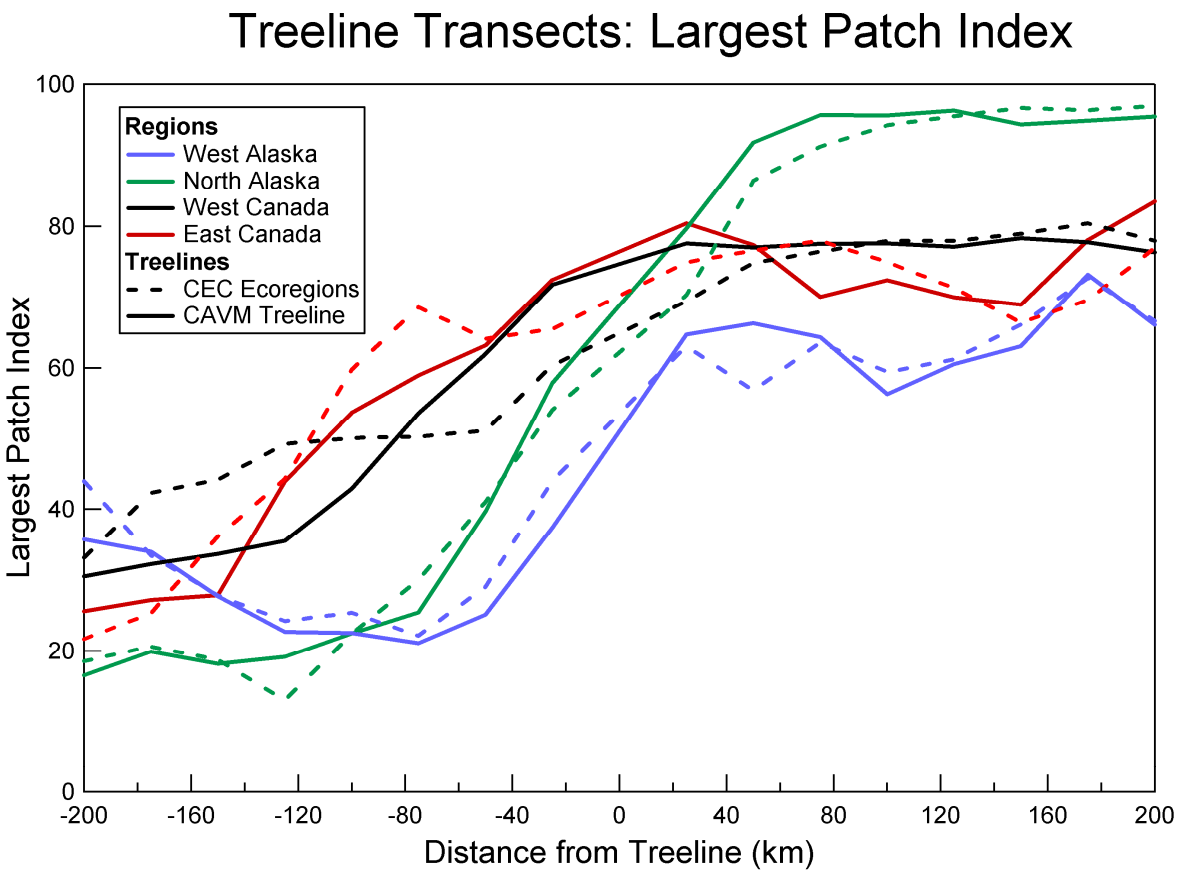

Figure 4.25. Largest patch index values across the treeline buffers. Each region is shown in a different color and the two treeline datasets are shown in dotted and solid lines.

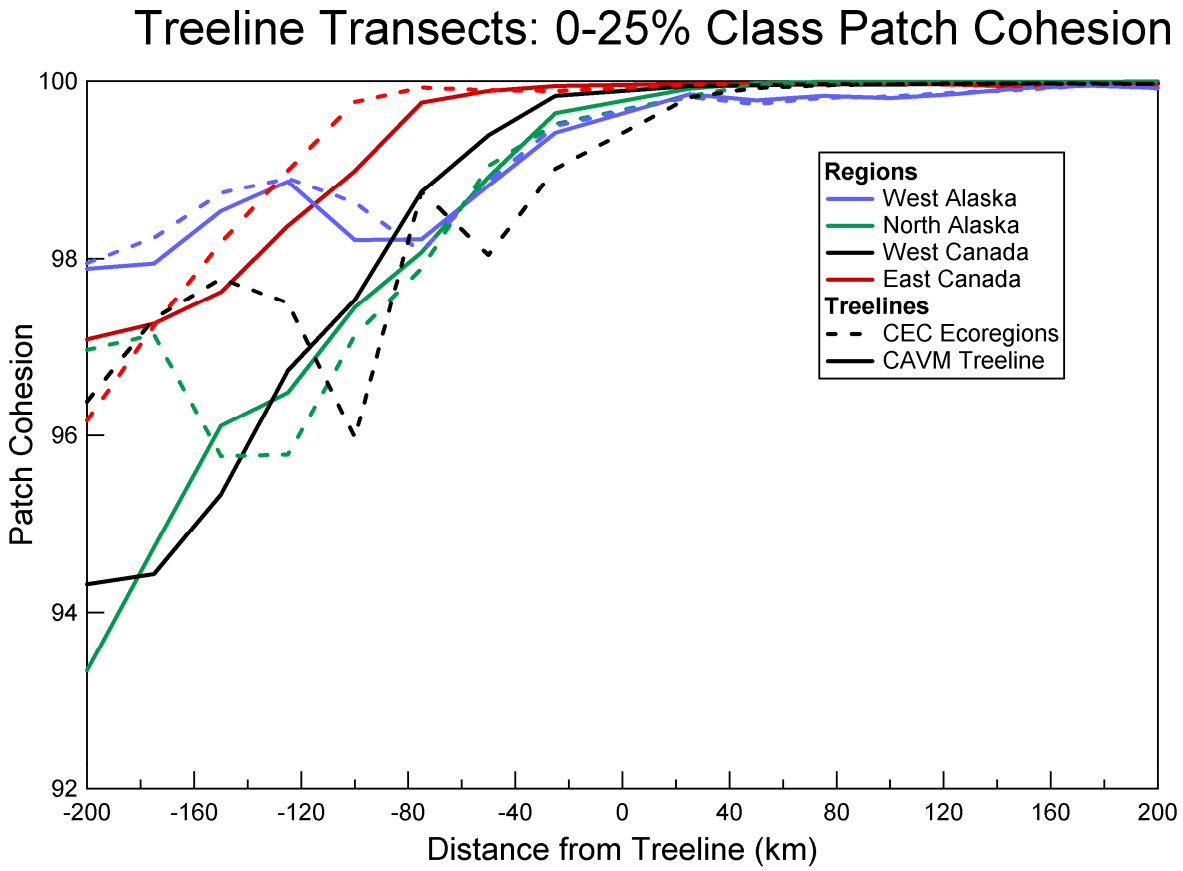

Figure 4.26. Patch cohesion values for the 0-25% cover class across the treeline buffers. Each region is shown in a different color and the two treeline datasets are shown in dotted and solid lines. The landscape tends to reach the percolation threshold for this cover class just south of both treeline estimates.

indicated that patch cohesion and the percolation threshold was a viable alternative method of mapping the boreal treeline.

A percolation threshold of 99.5% patch cohesion for the 0-25% cover class was selected based on the treeline transects in Figure 4.26. This threshold defines a limit where the class effectively forms one large patch that covers the entire landscape while the other classes are lightly dispersed throughout it without breaking it down. This new definition of the treeline improved on previous versions because it was uniformly applied across the continent, required no manual image interpretation, and was standard and repeatable. The original treelines mapped the northern extent of trees, meaning that there should not be any trees to the north of them. The patch cohesion treeline, on the other hand, mapped the southern extent of the tundra as a single cohesive landscape (Figure 27).

The resulting treeline included more areas, especially in central Canada, that would otherwise be considered boreal forest as it extends further south than either the CAVM or CEC treelines. When the three treelines were overlaid on top of the original Global Forest Cover 2000 dataset, the differences in the definitions were evident. In Alaska, the treelines were generally close together because the Brooks Range made a sharp boundary between the boreal and tundra regions (Figure 4.28). There were still details that were included in some treelines but not others like the Mackenzie Delta in the upper right of the figure. In the Taiga Shield and Hudson Plain regions of Canada, the patch cohesion based treeline diverged significantly from the other two (Figure 4.29). This region, as the name implies, was broadly taiga dominated and therefore marginally boreal to begin with. The patch cohesion based treeline classified the taiga as tundra

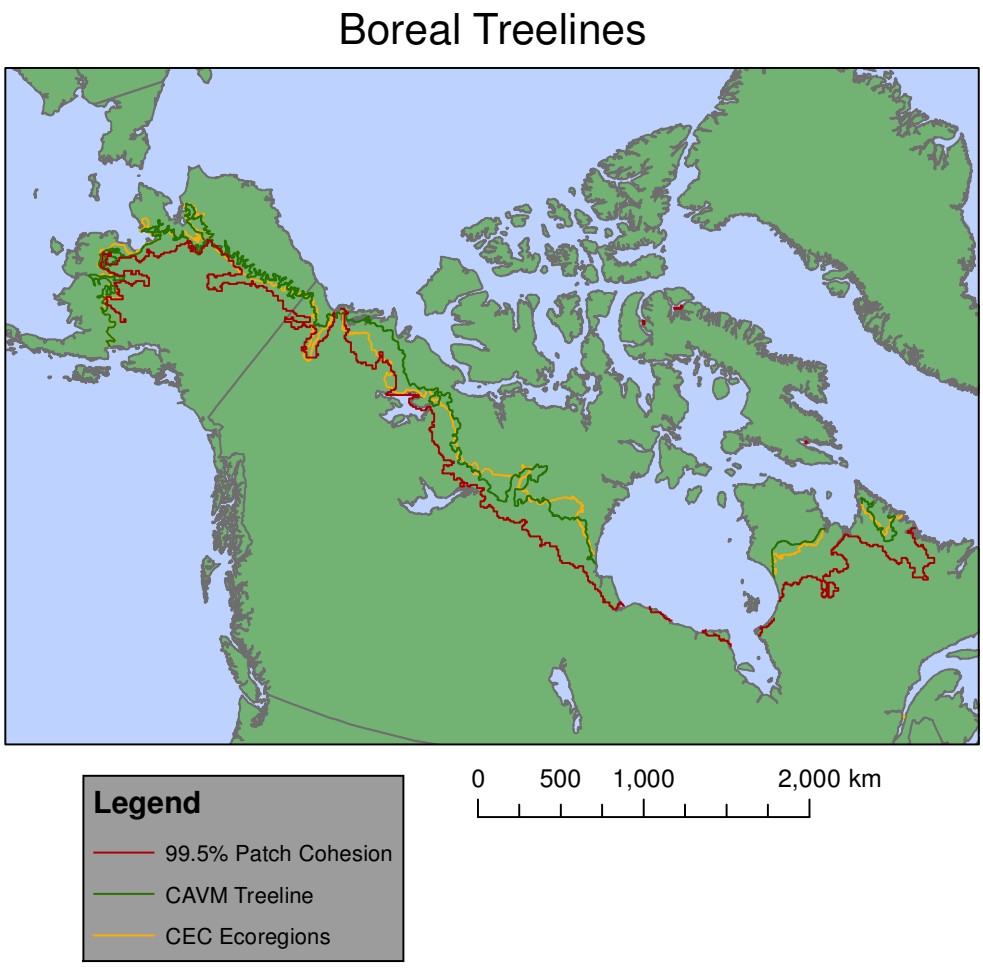

Figure 4.27. A new boreal treeline was generated using a patch cohesion threshold of 99.5% for the 0-25% cover class (shown in red). It is generally more south than the other estimates because of the taiga transitional zone which is particularly wide in Canada.

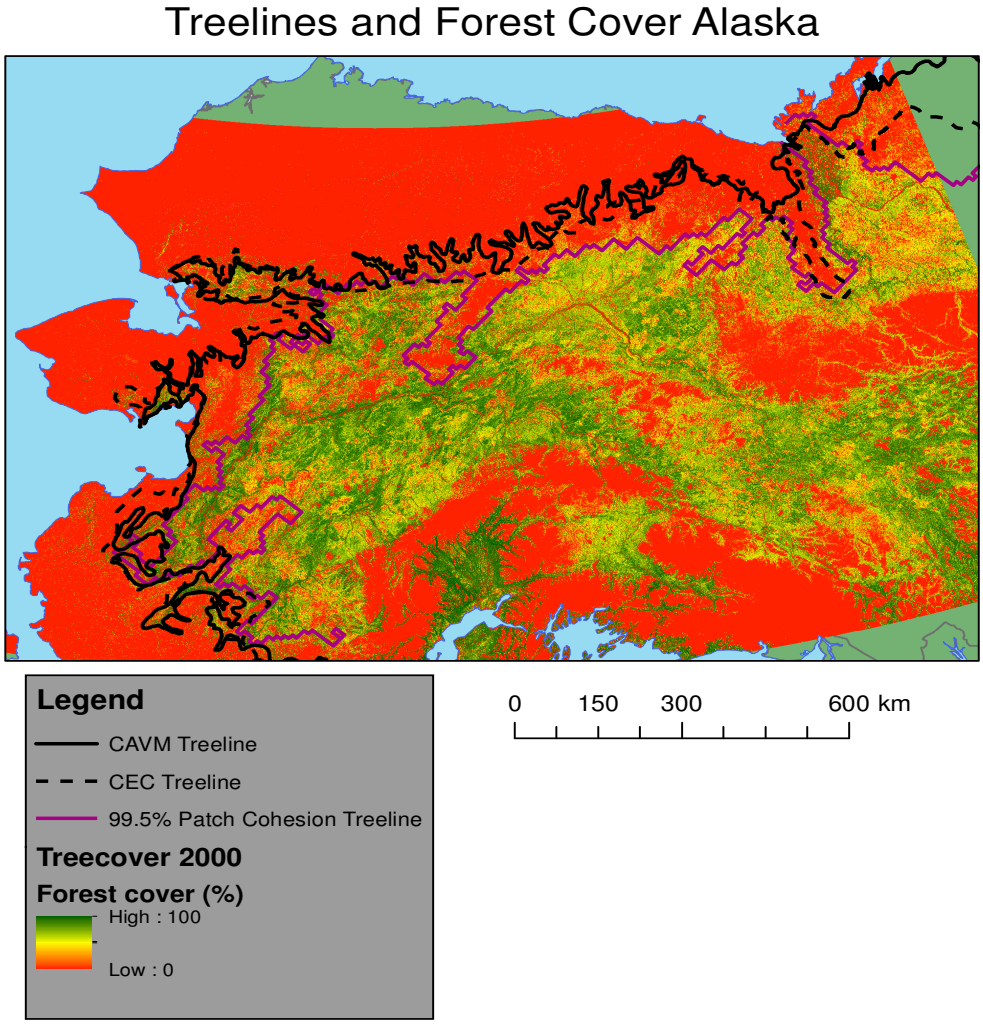

Figure 4.28. Three boreal treelines in Alaska. The CAVM and CEC treelines are shown in black solid and dashed lines respectively. The new treeline generated from patch cohesion data is shown in purple.

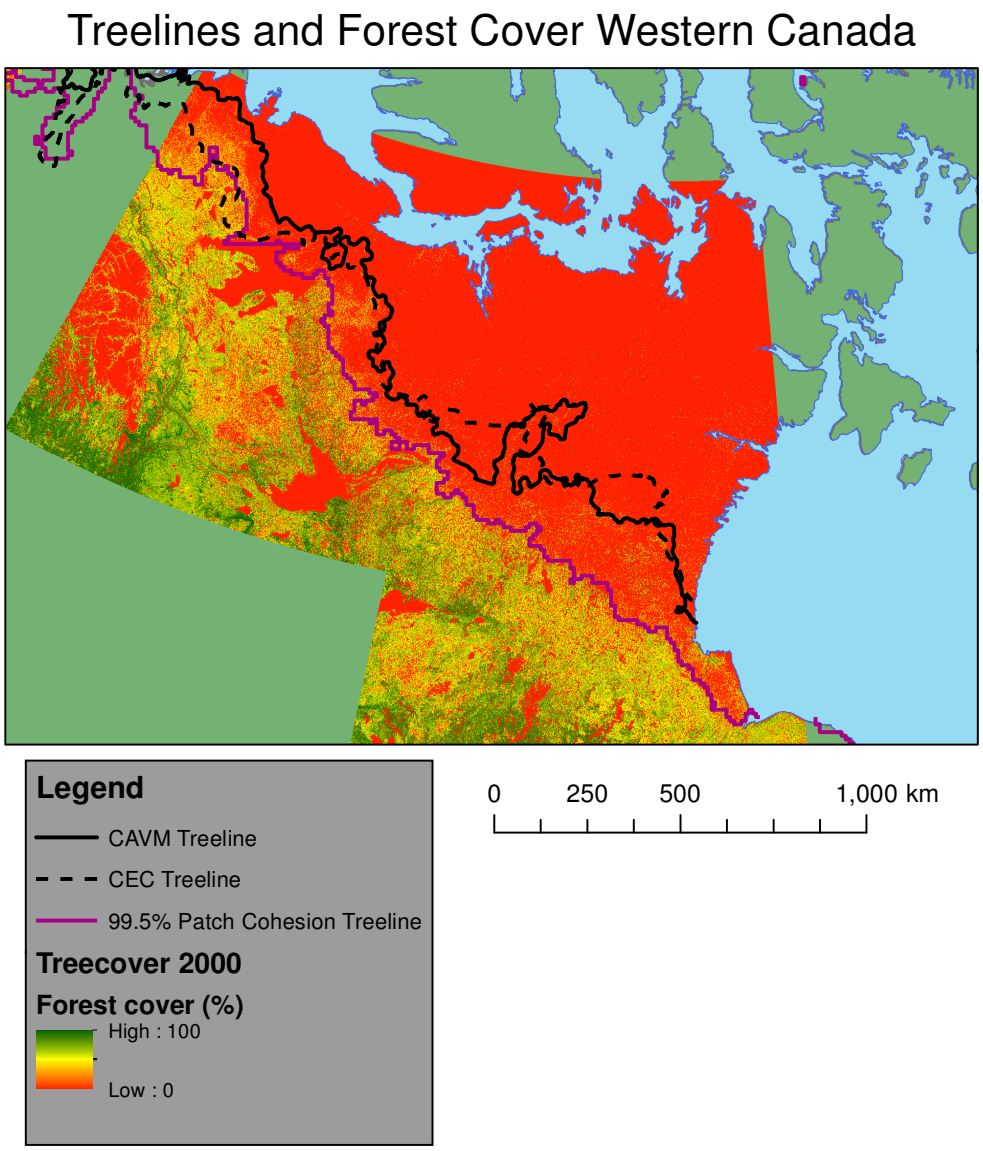

Figure 4.29. Boreal treelines in Western Canada had the greatest difference. The 99.5% Patch Cohesion treeline extended much farther south which excluded a large region of taiga from the boreal forest.

even though it included significant amounts of high forest cover pixels. Again, this highlights the difference in the definitions underlying each of these treelines.

4.4 Discussion

The boreal forest heterogeneity map produced here will provide many opportunities for research in the future. The analysis performed in this study only scratches the surface of the information contained in this new dataset. When selecting metrics to compute at the beginning of this study, I included more than I had initial plans for to allow further analysis and creative combinations of metrics. One such example was combining the class specific percentage of like adjacencies with the percentage of landscape area to map clustering and randomness in the landscape. Similar to the treeline analysis performed here, forest fire data, permafrost maps, and digital elevation models will be brought in to facilitate more analysis. Future studies will use these other datasets to measure the metrics in different regions and to assess the role of ecological processes in shaping these patterns. Fire, specifically will be covered in the next chapter.

Modelling studies need information about the land surface at high resolution. The boreal forest heterogeneity map allows models, with relatively coarse resolution, access to parameterized information about the fine scale patterns on the land surface. With this information, it will be possible to improve the representation of mesoscale processes, particularly those involving land-atmosphere interactions. One primary motivation for this study was to improve these models to better understand the role of the boreal forest in the global climate

system. Future models will better represent the complex spatial structure of and differences between the boreal forest, tundra, and taiga regions.

The high northern latitudes are generally represented by two biomes, the boreal forest to the south and the tundra to the north, but there is an important transitional zone between them known as the taiga. The Canadian Shield has extensive areas of taiga as the transition from boreal forest to tundra is not prescribed by mountains as it is in Alaska. The taiga region is difficult to define using traditional methods because it is grasslands with scattered trees and small forest stands giving it the components of both the boreal forest and tundra at the same time (Viereck et al. 1986). Thus taiga is generally only referred to in relative terms and mapped by manual image or map interpretation. One way to more precisely define the taiga could be to use the spatial patterns of those tundra and forest patches. Patch cohesion is particularly useful in this context because it identifies the connectedness of patches of different cover types. If one defined the taiga as primarily tundra with dispersed, disconnected patches of forest, grid cells with patch cohesion values above the percolation threshold for the tundra class and below the percolation threshold for forest class would fall within the definition. This is a novel approach to mapping the taiga that is robust and repeatable because it does not require human interpretation.

If a single border between the boreal forest and tundra is required without any transitional taiga zone, there are two datasets commonly used in research. The CAVM treeline and CEC Ecoregions borders both relied heavily on manual interpretation of satellite images and aerial photographs in their development. Comparing these treelines to the heterogeneity metrics mapped here help to understand the processes involved in treeline establishment in different regions across the continent.

The four analysis regions showed the same broad trends across the treeline but there were still significant differences. In general, West Alaska had the smallest difference across the treeline and North Alaska had the largest. These two regions have very different geographies which could help explain this difference (Figure 4.24). The treeline in North Alaska is largely prescribed by the Brooks Mountain Range which makes for a very well defined treeline compared to other regions. The treeline in West Alaska is actually oriented north-south, parallel to the coast, rather than running east-west like it does for most of the rest of North America. The processes limiting the growth of trees in Western Alaska are different than those in the north or in Canada (Viereck et al. 1983; Danby and Hik 2007; Liess et al. 2012). The two Canadian regions performed similarly as they were both part of the Canadian Shield and therefore had similar underlying geology despite being split by the Hudson Bay (Olthof and Pouliot 2010). Patch cohesion for the 0-25% cover class showed a large difference between classes within the boreal forest and almost identical values above the treeline (Figure 4.26). This pattern was specific to the patch cohesion metric as it saturates at the percolation threshold. The uniformity of patch cohesion in the tundra made it an effective way of defining the treeline.

While the forest cover classes used here were based on those used by the data producer (Hansen et al. 2013), there are many other forest cover thresholds and combinations of classes that could yield different results. One possibility would be to combine the two intermediate forest cover classes, 25-50% and 50-75% into one class as they performed similarly in many metrics. Another possibility would be to set aside the top 10% and bottom 10% of forest cover values into separate classes and keep the rest as one large intermediate class. The thresholds between classes could also be identified according to observed features in the landscape like fire scars or cleared forests.

Lastly, the next logical step will be to expand the map and analysis to include Eurasia which was excluded from this analysis. Because the processing of the raw forest cover data into rasters of heterogeneity metrics was completely automated, expanding into new regions would not require a great deal of effort. Many of these metrics could also be used, with little alteration, in temperate or tropical forests. For instance, mapping the different patterns and the kinds of landscapes that are produced by fire and logging in the amazon.

4.5 Conclusions

The boreal forest is a diverse and dynamic landscape. While not particularly diverse in plant species, the landscape is patterned with diverse land forms like lakes, meadows, and patches of forest in various stages of recovery from fire. This subtle variation is not often incorporated into climate models that tend to define the region as a solid carpet of trees. It was previously not possible to map the spatial pattern of land cover in the boreal forest because it required both high resolution maps of forest cover to be analyzed at a continental extent. The data and computational capacity are now available to perform this analysis and provide insight into the spatial structure of the boreal forests of North America.

This study produced a novel dataset that measured the spatial pattern of forest cover in the boreal region of North America. 34 landscape metrics and 33 land cover class specific metrics for five classes were calculated from a global forest cover dataset and gridded at 10km resolution. The final resolution and extent of analysis for each grid cell was selected to produce the finest resolution result maps possible while maintaining a large enough extent to calculate indices and avoid spatial autocorrelation issues.

The boreal forest had broadly smaller, more regularly shaped patches that were moderately clustered. It was more diverse than the tundra, unsurprisingly, but also more diverse than the more temperate hardwood forests to the southeast and southwest than the boreal forest. The high levels of dispersion and interspersion of small forest cover patches resulted in lower contagion values than surrounding regions. The mean fractal dimension for the boreal region was 1.384 ±0.024 which was significantly higher than the tundra and the temperate Mixed Wood Shield regions. The high fractal dimension indicates complex landscapes within the boreal forest. The Taiga Cordillera region generally diverged from the others as it was dominated by mountains. Patch cohesion for specific forest cover classes indicated that although the tundra and temperate forest regions reach the percolation threshold, the boreal forest never does. This indicates that there is no dominant forest cover type in the boreal forest. The boreal forest should therefore not be considered a continuous forest with patches of light and moderate density sprinkled throughout. Rather, it is a patchwork of forest patches that are too numerous and diverse for any of them to be considered dominant.

At the northern border of the boreal forest the sparse forest cover class did become dominant, with patch cohesion values above the percolation threshold at 99.96. The southward extent of the tundra dominated landscape was a better indicator for the border between the boreal and tundra ecosystems than the northern extent of individual trees, which has been used previously. The sparse cover class extended further south than previous treeline estimates, particularly in Canada. This was due to an extensive taiga transitional zone between the pure boreal and tundra regions on the Canadian Shield that should be taken into account in future analysis.

The analysis performed here was the first of many to come. This boreal forest heterogeneity map contains far more information waiting to be pulled out. The role of disturbance in setting and changing the patterns mapped here is of particular importance as these disturbance regimes are subject to rapid change with climate. Furthermore, the automated processes employed here can easily be expanded to incorporate the Eurasian boreal forest and even temperate and tropical forests in the future. The results now must be made available to the modelling community in a way that is useful and compatible with their models for maximum impact.

4.6 Appendices

Appendix A

```
#########################################################################
#          Process Raw FC Rasters
#########################################################################

folderpath = r"\\SHENGNAS\shenggroup\Evan\All_Raw_Data\test"
import arcpy
import os
arcpy.env.workspace = folderpath
from arcpy.sa import *
arcpy.CheckOutExtension("Spatial")


#Get a list of all of the files in the folder
filelist = os.listdir(folderpath)

for filename in filelist:
   if filename[:28] == "Hansen_GFC2014_treecover2000":    #_50N_060W.tif"
      print filename
      suffix = filename[29:]
      #print suffix
      datamask_prefix = r"\Hansen_GFC2014_datamask_"
      if os.path.exists(folderpath + datamask_prefix + suffix):
         print "Found " + folderpath + datamask_prefix + suffix
      else:
         print "No Datamask file found for the suffix " + suffix

      print "reclassifying Forest Cover Raster  " + suffix
      #open forest cover raster
      fc = arcpy.Raster(filename)

      #Reclassify forest cover raster
      FCremap = RemapRange([[-9,0,0],[0,25,0],[25,50,1],[50,75,2],[75,100,3]])
      FCreclass = Reclassify(fc, "Value", FCremap)
      del fc

      print "reclassifying Data Mask Raster  " + suffix
      #open datamask raster
      datamask = arcpy.Raster(datamask_prefix + suffix)

      #Reclassify the datamask
      DMremap = RemapValue([[0,0],[1,1],[2,5]])
```

```
        DMreclass = Reclassify(datamask, "Value", DMremap)
        del datamask

        print "Calculating new Raster  " + suffix
        #add the FC and DM rasters together to differentiate water from NoData
        final_FC = DMreclass + FCreclass
        del DMreclass, FCreclass

        #print "Saving New Raster  " + suffix
        #Save the resulting raster
        #final_FC.save(folderpath + r"\FC_reclass" + suffix)
        #del final_FC

        print "projecting Raster  " + suffix
        #project raster to Canada Conic
        arcpy.ProjectRaster_management(final_FC, "FC_reclass_proj.tif", \

r"\\SHENGNAS\shenggroup\Evan\FC_Data\60100caeac_301_reclass_lakes.tif", \
                                       "NEAREST", "30 Meters")

        del final_FC
        print suffix + " is completed"
```

Appendix B

```
#####################################################################
#          Mosaic and Break Down for Fragstats
#####################################################################

folderpath = r"\\SHENGNAS\shenggroup\Evan\All_Raw_Data\N_America"
import arcpy
import os
arcpy.env.workspace = folderpath
arcpy.env.overwriteOutput = True
from arcpy.sa import *
arcpy.CheckOutExtension("Spatial")

#Get the master fishnet at 10km.  It is already created and ready to go.
km_fishnet =
r"\\SHENGNAS\shenggroup\Evan\All_Raw_Data\Automated_forest_cover\10km_fishnet_CAN
.shp"
km_points =
r"\\SHENGNAS\shenggroup\Evan\All_Raw_Data\Automated_forest_cover\10km_fishnet_CAN
_labe_Joinl.shp"

#Get the 10deg fishnet
deg_fishnet =
r"\\SHENGNAS\shenggroup\Evan\All_Raw_Data\Automated_forest_cover\10deg_fishnet_CAN
2_Conic.shp"
arcpy.MakeFeatureLayer_management(deg_fishnet, 'raster_extents')

#Loop through the 10km fishnet in 50X50 grid steps
for x in range(0,14):
   for y in range(0,20):
      sql = '"column" >= ' + str(x*50) + ' AND "column" <= ' + str(((x+1)*50)+4) + \
           ' AND "row" >= ' + str(y*25) + ' AND "row" <= ' + str(((y+1)*25)+4)
      arcpy.MakeFeatureLayer_management(km_fishnet, 'temp_50x50', sql)

      arcpy.SelectLayerByLocation_management('raster_extents', 'INTERSECT', 'temp_50x50')

      #arcpy.CopyFeatures_management('raster_extents',
r"C:\Users\Evan\Desktop\temp50x25.shp")
      rasterlist = []
      prefix = "FC_reclass_proj"
      grids = arcpy.SearchCursor('raster_extents')#r"C:\Users\Evan\Desktop\temp50x25.shp")
      print str(x*50), str(y*25)
      print 'creating mosaic'
      arcpy.env.extent = ""
```

```
        arcpy.env.snapRaster = ""
        FC_mosaic =
arcpy.CreateMosaicDataset_management(r"D:\Workspace\Evan\Automated_forest_cover\temp_
mosaic.gdb", \
                "temp", "102001", 1, "8_BIT_UNSIGNED")  #Canada_Albers_Equal_Area_Conic
        raster_exists = False
        for grid in grids:
            print "Adding " + grid.suffix
            rasterlist.append(prefix + grid.suffix)
            if os.path.exists(folderpath+ "\\" + prefix + grid.suffix):
                print "Found " + prefix + grid.suffix
                arcpy.AddRastersToMosaicDataset_management(FC_mosaic, "Raster Dataset", prefix
+ grid.suffix, "", "",\
                    "UPDATE_OVERVIEWS", "", "", "", "", "", "","", "BUILD_PYRAMIDS",
"CALCULATE_STATISTICS")
                raster_exists = True
            else:
                print prefix + grid.suffix + " not found"
        del grids

        if raster_exists:
            print "Clipping"
            arcpy.Clip_management(FC_mosaic,"#",folderpath + "\exp" + str(x*50)+ "_" + str(y*25)
+ ".tif",\
                    "temp_50x50","255","ClippingGeometry","NO_MAINTAIN_EXTENT")

            print "Making UserPoints Raster"
            arcpy.MakeFeatureLayer_management(km_points, 'points_50x50', sql)
            arcpy.CopyFeatures_management('points_50x50', 'temp_points.shp')

            sub_ras = arcpy.Raster(folderpath + "\exp" + str(x*50)+ "_" + str(y*25) + ".tif")

            arcpy.env.extent = folderpath + "\exp" + str(x*50)+ "_" + str(y*25) + ".tif"
            arcpy.env.snapRaster = folderpath + "\exp" + str(x*50)+ "_" + str(y*25) + ".tif"


            print "point to raster"
            arcpy.PointToRaster_conversion('temp_points.shp',"FID_1","userpoints" + str(x*50)+
"_" + str(y*25) + ".tif",\
                "MOST_FREQUENT","NONE",sub_ras)
        del FC_mosaic
print "Done"
```

Appendix C

```
pro  Read_Fragstats_Results2_classes

restore,
'\\SHENGNAS\shenggroup\Evan\All_Raw_Data\Automated_forest_cover\Index_array.sav'
;restore,
'\\SHENGNAS\shenggroup\Evan\All_Raw_Data\Automated_forest_cover\Output_array.sav'

output = fltarr(678,470,35)

filelist = file_search('\\SHENGNAS\shenggroup\Evan\All_Raw_Data\N_America\', '*.class')
;class = ' water '
;class = ' 0-25 '
;class = ' 25-50 '
;class = ' 50-75 '
class = ' 75-100 '


for i = 0,n_elements(filelist)-1 do begin

  filename = filelist[i]
  print, filename

  b = read_ascii(filename, delimiter = ",", data_start = 1)
  b=b.field01
  s = size(b)
  bands = s[1]
  length = s[2]


  ;This whole thing gets the first column and converts into a vector of long integers
  get_lun, lun
  ;this gets rid of the header
  openr, lun, filename
  toss='g'
  readf, lun, toss

  for j = 0, length-1 do begin
    toss='g'
    readf, lun, toss
    toss = strsplit(toss, ',', /EXTRACT)
    point = toss[0]
    point = strsplit(point, '_', /EXTRACT)
    point = point[1]
```

```
    point = ulong(point)

    j_class = toss[1]
    if j_class EQ class then begin


    ;print, toss
    a = where(arr EQ point)
    a_col_row = col_row(a,arr)
    for k = 0,bands-1 do begin
      output[a_col_row[0], a_col_row[1],k] = b[k,j]
    endfor

    endif
  endfor
  close, lun
  free_lun, lun
  ;;;;;;;;;;;;;;;;;;;;;;;;;;;;;;;;;;;;;;;;;;;;;;;;;;;;;;;;;;;;;;;;;;;;;;;;;;;;;;;

endfor
save, output, filename =
'\\SHENGNAS\shenggroup\Evan\All_Raw_Data\Automated_forest_cover\Output_array_class_7
5_100 .sav'
end

FUNCTION col_row, sub, array
  sz = size(array)
  rows = floor(sub / sz[1])
  cols = 678 - (sub MOD sz[1])

  retarr = [cols, rows]

 return, retarr

 end
```

4.7 References

References

(CEC), C. f. E. C. (1997). Ecological Regions of North America. U. S. E. P. Agency.

Anderson, P. and L. Brubaker (1993). Holocene vegetation and climate histories of Alaska. . Global Climates Since the Last Glacial Maximum. K. J. Wright HE, Ruddiman WF, Street-Perrott FA, Bartlein P. Minneapolis, University of Minnesota Press**:** 386 - 400.

Balaguer-Beser, A., L. A. Ruiz, et al. (2013). "Using semivariogram indices to analyse heterogeneity in spatial patterns in remotely sensed images." Computers & Geosciences **50**: 115-127.

Baldocchi, D. D., B. B. Hicks, et al. (1988). "Measuring biosphere-atmosphere exchanges of biologically related gases with micrometeorological methods." Ecology **69**(5): 1331-1340.

Barrett, K., A. D. McGuire, et al. (2011). "Potential shifts in dominant forest cover in interior Alaska driven by variations in fire severity." Ecological Applications **21**(7): 2380-2396.

Baskent, E. Z. and G. A. Jordan (1995). "Characterizing spatial structure of forest landscapes." Canadian Journal of Forest Research **25**(11): 1830-1849.

Bastian, C. T., D. M. McLeod, et al. (2002). "Environmental amenities and agricultural land values: a hedonic model using geographic information systems data." Ecological Economics **40**(3): 337-349.

Benson, B. J. and M. D. MacKenzie (1995). "Effects of sensor spatial resolution on landscape structure parameters." Landscape Ecology **10**(2): 113-120.

Beringer, J., N. J. Tapper, et al. (2001). "Impact of Arctic treeline on synoptic climate." Geophysical Research Letters **28**(22): 4247-4250.

Birkett, C. M. and I. M. Mason (1995). "A New Global Lakes Database for a Remote-Sensing Program Studying Climatically Sensitive Large Lakes." Journal of Great Lakes Research **21**(3): 307-318.

Carson, C. E. and K. M. Hussey (1962). "The Oriented Lakes of Arctic Alaska." Journal of Geology **70**(4): 417-&.

CAVM_Team (2003). Circumpolar Arctic Vegetation Map, U.S. Fish and Wildlife Service, Anchorage, Alaska.

Cote, M. M. and C. R. Burn (2002). "The oriented lakes of Tuktoyaktuk Peninsula, western Arctic coast, Canada: A GIS-based analysis." Permafrost and Periglacial Processes **13**(1): 61-70.

Crapper, P. F. (1980). "Errors incurred in estimating an area of uniform land cover using Landsat." Photogrammetric Engineering and Remote Sensing **46**(10): 1295-1301.

Dalu, G. A., R. A. Pielke, et al. (2000). "Heat transport and weakening of atmospheric stability induced by mesoscale flows." Journal of Geophysical Research-Atmospheres **105**(D7): 9349-9363.

Danby, R. K. and D. S. Hik (2007). "Evidence of recent treeline dynamics in southwest Yukon from aerial photographs." Arctic **60**(4): 411-420.

DiMiceli, C. M., M.L. Carroll, R.A. Sohlberg, C. Huang, M.C. Hansen, and J.R.G. Townshend (2011). Vegetation Continuous Fields MOD44B. U. o. Maryland. College Park, Maryland, Global Land Cover Facility.

Dyrness, C. T., L. A. Viereck, et al. (1986). Fire in taiga communities of interior Alaska. Ecological series volume 57: forest ecosystems in the Alaskan taiga. K. Van Cleve, F. S. Chapin, P. W. Flanagan, L. A. Viereck and C. T. Dyrness. New York, Springer Verlag**:** 74-86.

Fahrig, L. (2002). "EFFECT OF HABITAT FRAGMENTATION ON THE EXTINCTION THRESHOLD: A SYNTHESIS*." Ecological Applications **12**(2): 346-353.

Foody, G. M. (2002). "Status of land cover classification accuracy assessment." Remote Sensing of Environment **80**(1): 185-201.

Frohn, R. C., K. M. Hinkel, et al. (2005). "Satellite remote sensing classification of thaw lakes and drained thaw lake basins on the North Slope of Alaska." Remote Sensing of Environment **97**(1): 116-126.

Gamon, J. A., K. F. Huemmrich, et al. (2004). "Remote sensing in BOREAS: Lessons leamed." Remote Sensing of Environment **89**(2): 139-162.

Gustafson, E. J. (1998). "Quantifying landscape spatial pattern: what is the state of the art?" Ecosystems **1**(2): 143-156.

Gutman, G., R. Byrnes, et al. (2008). "Towards monitoring land-cover and land-use changes at a global scale: The Global Land Survey 2005." Photogrammetric Engineering and Remote Sensing **74**(1): 6-10.

Hansen, M., P. Potapov, et al. (2013). "High-resolution global maps of 21st-century forest cover change." Science **342**(6160): 850-853.

Hansen, M. C., S. V. Stehman, et al. (2010). "Quantification of global gross forest cover loss." Proceedings of the National Academy of Sciences **107**(19): 8650-8655.

Harper, K. A., Y. Bergeron, et al. (2002). "Post-fire development of canopy structure and composition in black spruce forests of Abitibi, Quebec: A landscape scale study." Silva Fennica **36**(1): 249-263.

Honnay, O., K. Piessens, et al. (2003). "Satellite based land use and landscape complexity indices as predictors for regional plant species diversity." Landscape and urban planning **63**(4): 241-250.

Huang, H.-Y. and S. A. Margulis (2009). "On the impact of surface heterogeneity on a realistic convective boundary layer." Water Resources Research **45**(4): W04425.

Khorram, S., Ed. (1999). Accuracy Assessment of Remote Sensing-Derived Change Detection. Monograph Series. Bethesda, MD, American Society for Photogrametry and Remote Sensing.

Kolasa, J. and C. D. Rollo (1991). Introduction: the heterogeneity of heterogeneity: a glossary. Ecological heterogeneity, Springer**:** 1-23.

Kowarik, I. (2008). On the role of alien species in urban flora and vegetation. Urban Ecology, Springer**:** 321-338.

Kushla, J. D. and W. J. Ripple (1998). "Assessing wildfire effects with Landsat thematic mapper data." International Journal of Remote Sensing **19**(13): 2493-2507.

LaGro Jr, J. (1991). "Assessing patch shape in landscape mosaics." Photogrammetric Engineering and Remote Sensing **57**(3): 285-293.

Landsberg, J. J. and S. T. Gower (1997). Applications of physiological ecology to forest management. San Diego, Academic Press.

Larsen, J. A. (1980). The boreal ecosystem, Academic Press, New York, London etc.

Legendre, P. (1993). "Spatial autocorrelation: trouble or new paradigm?" Ecology **74**(6): 1659-1673.

Legendre, P., M. R. Dale, et al. (2002). "The consequences of spatial structure for the design and analysis of ecological field surveys." Ecography **25**(5): 601-615.

Lehner, B. and P. Döll (2004). "Development and validation of a global database of lakes, reservoirs and wetlands." Journal of Hydrology **296**(1-4): 1-22.

Levin, S. (1989). "Challenges in the development of a theory of community and ecosystem structure and function." Perspectives in ecological theory **242**: 255.

Levin, S. A. (1992). "The Problem of Pattern and Scale in Ecology: The Robert H. MacArthur Award Lecture." Ecology **73**(6): 1943-1967.

Li, H. and J. Reynolds (1995). "On definition and quantification of heterogeneity." Oikos: 280-284.

Liess, S., P. K. Snyder, et al. (2012). "The effects of boreal forest expansion on the summer Arctic frontal zone." Climate Dynamics **38**(9-10): 1805-1827.

Loranty, M. M., L. T. Berner, et al. (2013). "Vegetation controls on northern high latitude snow-albedo feedback: observations and CMIP5 model predictions." Global Change Biology: n/a-n/a.

Lovejoy, S. (1982). "Area-perimeter relation for rain and cloud areas." Science **216**(4542): 185-187.

Lyons, E. A., Y. Sheng, et al. (2013). "Quantifying sources of error in multitemporal multisensor lake mapping." International Journal of Remote Sensing **34**(22): 7887-7905.

MacDonald, G. M., A. A. Velichko, et al. (2000). "Holocene treeline history and climate change across northern Eurasia." Quaternary Research **53**(3): 302-311.

Mandelbrot, B. B. (1982). The Fractal Geometry of Nature. New York, W. H. Freeman and Company.

Mayer, H. J. and M. R. Greenberg (2005). "Using Integrated Geospatial Mapping and Conceptual Site Models to Guide Risk-Based Environmental Clean-Up Decisions." Risk analysis **25**(2): 429-446.

McGarigal, K., SA Cushman, and E Ene. (2012). "FRAGSTATS v4: Spatial Pattern Analysis Program for Categorical and Continuous Maps." 2014, from http://www.umass.edu/landeco/research/fragstats/fragstats.html.

McGlone, M. S. (1996). "When History Matters: Scale, Time, Climate and Tree Diversity." Global Ecology and Biogeography Letters **5**(6): 309-314.

Montesano, P. M., R. Nelson, et al. (2009). "MODIS tree cover validation for the circumpolar taiga-tundra transition zone." Remote Sensing of Environment **113**(10): 2130-2141.

Nagendra, H. (2002). "Opposite trends in response for the Shannon and Simpson indices of landscape diversity." Applied Geography **22**(2): 175-186.

Nowacki, G., P. Spencer, et al. (2001). Ecoregions of Alaska and Neighboring Terroitory. Reston, VA, USGS.

O'Neill, R., Krummel, JR, Gardner, RH, Sugi-hara, G., Jackson, B., DeAngelis, DL, and B. Milne, Turner, MG, Zygmunt, B., Christensen, SW, Dale, VH & Graham, RL (1988). Indices of landscape pattern. Landscape Ecology 1**:** 153–162.

O'Neill, R. V., K. H. Riitters, et al. (1999). "Landscape pattern metrics and regional assessment." Ecosystem health **5**(4): 225-233.

Oleson, K. W. and G. B. Bonan (2000). "The effects of remotely sensed plant functional type and leaf area index on simulations of boreal forest surface fluxes by the NCAR land surface model." Journal of Hydrometeorology **1**(5): 431-446.

Olthof, I. and D. Pouliot "Treeline vegetation composition and change in Canada's western Subarctic from AVHRR and canopy reflectance modeling." Remote Sensing of Environment **In Press, Corrected Proof**.

Olthof, I. and D. Pouliot (2010). "Treeline vegetation composition and change in Canada's western Subarctic from AVHRR and canopy reflectance modeling." Remote Sensing of Environment **114**(4): 805-815.

Osserman, R. (1978). "The Isoperimetric Inequality." Bulletin of the American Mathematical Society **84**(6): 1182-1238.

Ozdogan, M. and C. E. Woodcock (2006). "Resolution dependent errors in remote sensing of cultivated areas." Remote Sensing of Environment **103**(2): 203-217.

Pan, D., G. Domon, et al. (1999). "Temporal (1958–1993) and spatial patterns of land use changes in Haut-Saint-Laurent (Quebec, Canada) and their relation to landscape physical attributes." Landscape Ecology **14**(1): 35-52.

Pielke, R. A. and P. L. Vidale (1995). "The boreal forest and the polar front." Journal of Geophysical Research-Atmospheres **100**(D12): 25755-25758.

Pielou, E. C. (1975). Ecological diversity, Wiley New York.

Plotnick, R. E., R. H. Gardner, et al. (1996). "Lacunarity analysis: a general technique for the analysis of spatial patterns." Physical review E **53**(5): 5461.

Rey-Benayas, J. M. and K. O. Pope (1995). "Landscape Ecology and Diversity Patterns in the Seasonal Tropics from Landsat TM Imagery." Ecological Applications **5**(2): 386-394.

Riitters, K. H., R. O'neill, et al. (1995). "A factor analysis of landscape pattern and structure metrics." Landscape Ecology **10**(1): 23-39.

Riitters, K. H., J. D. Wickham, et al. (2000). "NATIONAL LAND-COVER PATTERN DATA: Ecological Archives E081-004." Ecology **81**(2): 604-604.

Ritters, K. and J. D. Wickham (1995). A Landscape Atlas of the Chesapeake Bay Watershed, DTIC Document.

Roy, D. B., M. O. Hill, et al. (1999). "Effects of urban land cover on the local species pool in Britain." Ecography **22**(5): 507-517.

Roy, P. S., B. K. Ranganath, et al. (1991). "Tropical forest type mapping and monitoring using remote sensing." International Journal of Remote Sensing **12**(11): 2205-2225.

Sawaya, K. E., L. G. Olmanson, et al. (2003). "Extending satellite remote sensing to local scales: land and water resource monitoring using high-resolution imagery." Remote Sensing of Environment **88**(1-2): 144-156.

Scheiner, S. M. (1992). "Measuring pattern diversity." Ecology: 1860-1867.

Schumaker, N. H. (1996). "Using landscape indices to predict habitat connectivity." Ecology **77**(4): 1210-1225.

Sellers, P., F. Hall, et al. (1995). "The Boreal Ecosystem-Atmosphere Study (BOREAS) - An Overview and Early Results from the 1994 Field Year." Bulletin of the American Meteorological Society **76**(9): 1549-1577.

Shannon, C. E. and W. Weaver (1949). "The mathematical theory of communication (Urbana, IL." University of Illinois Press **19**(7): 1.

Shortridge, A. M. (2004). "Geometric variability of raster cell class assignment." International Journal of Geographical Information Science **18**(6): 539-558.

Simpson, E. H. (1949). "Measurement of diversity." Nature.

Smith, F. E. (1972). "Spatial heterogeneity, stability, and diversity in ecosystems." Trans. Conn. Acad. Arts Sci **44**(30): 335.

Smith, L. C., Y. W. Sheng, et al. (2007). "A first pan-Arctic assessment of the influence of glaciation, permafrost, topography and peatlands on northern hemisphere lake distribution." Permafrost and Periglacial Processes **18**(2): 201-208.

Stauffer, D. and A. Aharony (1994). Introduction to percolation theory, CRC press.

Steyaert, L. T., F. G. Hall, et al. (1997). "Land cover mapping, fire regeneration, and scaling studies in the Canadian boreal forest with 1 km AVHRR and Landsat TM data." Journal of Geophysical Research-Atmospheres **102**(D24): 29581-29598.

Stow, D. A., A. Hope, et al. (2004). "Remote sensing of vegetation and land-cover change in Arctic Tundra Ecosystems." Remote Sensing of Environment **89**(3): 281-308.

Sturm, M., C. Racine, et al. (2001). "Climate change - Increasing shrub abundance in the Arctic." Nature **411**(6837): 546-547.

Sturm, M., J. Schimel, et al. (2005). "Winter biological processes could help convert arctic tundra to shrubland." Bioscience **55**(1): 17-26.

Thomas, J. W. and J. L. Parker (1979). Wildlife habitats in managed forests: the Blue Mountains of Oregon and Washington, USDA Forest Service Washington, DC, USA.

Tropek, R., O. Sedláček, et al. (2014). "Comment on “High-resolution global maps of 21st-century forest cover change”." Science **344**(6187): 981-981.

Turner, W. R. and E. Tjørve (2005). "Scale-dependence in species-area relationships." Ecography **28**(6): 721-730.

Viereck, L. A., C. T. Dyrness, et al. (1983). "Vegetation, soils, and forest productivity in selected forest types in interior Alaska." Canadian Journal of Forest Research-Revue Canadienne De Recherche Forestiere **13**(5): 703-720.

Viereck, L. A., K. Van Cleve, et al. (1986). Forest Ecosystem Distribution in the Taiga Environment. Forest Ecosystems in the Alaskan Taiga. K. Van Cleve, F. S. Chapin, P. W. Flanagan, L. A. Viereck and C. T. Dyrness. New York, Springer-Verlag**:** 22-43.

Wagner, H. H. and M.-J. Fortin (2005). "SPATIAL ANALYSIS OF LANDSCAPES: CONCEPTS AND STATISTICS." Ecology **86**(8): 1975-1987.

Wiens, J. A. (1989). "Spatial Scaling in Ecology." Functional Ecology **3**(4): 385-397.

Woodcock, C. E. and A. H. Strahler (1987). "The factor of scale in remote sensing." Remote Sensing of Environment **21**(3): 311-332.

Wu, J., W. Shen, et al. (2002). "Empirical patterns of the effects of changing scale on landscape metrics." Landscape Ecology **17**(8): 761-782.

Wu, J. G. (2004). "Effects of changing scale on landscape pattern analysis: scaling relations." Landscape Ecology **19**(2): 125-138.

Zeng, X. B. and R. A. Pielke (1995). "Landscape-Induced Atmospheric Flow and its Parameterization in Large-Scale Numerical Models." Journal of Climate **8**(5): 1156-1177.

Zhang, Y., W. J. Chen, et al. (2006). "Temporal and spatial changes of permafrost in Canada since the end of the Little Ice Age." Journal of Geophysical Research-Atmospheres **111**(D22): 14.

Chapter 5

Boreal Forest Heterogeneity Response to Fire and Lakes

Abstract

Wildland fire is the primary disturbance regime in the boreal forest because of its relatively rapid return cycle and the total area affected by it over time. Lakes are another important diver of landscape change in the region because of their areal extent and their sensitivity to changing climate via permafrost degradation. Together these two processes, wildfire and permafrost-driven lake change, are broadly responsible for the dynamic patterns on the boreal landscape. This is an important area of study because fire and lake processes are expected to change with climate in the future and because of the link between boreal forest heterogeneity and atmospheric circulation patterns. This study compares the observed regional variability in heterogeneity metrics including contagion with known distributions of fires and lakes in the boreal forest. The relationship between burned area and heterogeneity and lake area and heterogeneity were inconclusive. However, fire count and lake count were both related to contagion in opposite directions because of their different scales. Intensification of the boreal forest fire regime would likely lead to a more homogeneous landscape.

5.1 Introduction

The primary disturbance factor controlling vegetation structure and dynamics in the boreal forest is fire because it directly impacts a larger percentage of the region than any other disturbance. Wildfires in the boreal forest generally remove mature evergreen forests and replace them with grasslands and shrubs which generally return to evergreen forest (Van Cleve and Viereck 1981; Dyrness et al. 1986). Thus the fires are stand replacing (result in more evergreen forest after succession) and have a fire return time of approximately 80-150 years (Larsen 1997). Regular fires in central Alaska create a pattern of early, middle, and late successional vegetation in burn scars with carbon and energy fluxes that change with age (Kasischke et al. 2002; Liu and Randerson 2007; Lyons et al. 2008).

These regular fires are expected to increase in frequency, size, and severity due to drought stress, longer fire season, and higher temperatures (Flannigan et al. 1998; Kasischke and Turetsky 2006; Kasischke et al. 2010). Furthermore, the post fire successional trajectories are subject to change with climate and burn severity (Barrett et al. 2011). This could, in time, lead to a shift from evergreen needleleaf to deciduous broadleaf dominance with implications for albedo driven warming (Liu et al. 2005; Randerson et al. 2006; Lyons et al. 2008) and positioning of the Arctic frontal zone (Pielke and Vidale 1995; Liess et al. 2012). Since fires impact so much of the boreal forest so often, small changes to the disturbance regime could lead to rapid (decadal time scales) change to the landscape at the continental scale.

Lakes and wetlands are important because they are common in the boreal forest and also influence mesoscale atmospheric eddy fluxes (Pielke and Vidale 1995). While the distribution of high latitude lakes is dependent on glacial history, permafrost, and topography (Smith et al. 2007), only permafrost can change on decadal time scales. Responses of high latitude lakes to

melting permafrost has been observed in many cases but the nature of the change (increase or decrease in lake abundance) remains poorly understood (Osterkamp et al. 2000; Yoshikawa and Hinzman 2003; Smith et al. 2005).

The processes of fire disturbance and permafrost degradation are actively changing the nature of the boreal forest by redistributing plant functional types, lakes, and wetlands (Viereck 1973; Viereck 1983; Johnson 1992; Brown et al. 2002; Kasischke et al. 2002). These disturbance processes are subject to change along with climate and hold the potential for rapid change to the structure of the boreal forest (Payette et al. 2004; Jorgenson and Osterkamp 2005; Kasischke et al. 2010; Mann et al. 2012). Land cover and the processes that determine its distribution are the key to greater understanding of the high latitude environment.

5.1.1 Contagion

Many metrics were calculated in chapter four for the boreal forest but this section will concentrate on the contagion metric as it is particularly sensitive to dispersion and interspersion of multiple land cover classes. Contagion is relatively complicated to calculate but is included in the software package Fragstats as a landscape wide metric (McGarigal 2012). Contagion, as calculated by Fragstats, is expressed as a percentage by dividing the observed contagion by the maximum possible contagion with the given number of classes. Contagion approaches zero when patch types are maximally disaggregated, meaning that each pixel is a different patch type than its neighbors, and evenly interspersed, meaning that the patches are evenly distributed amongst each other. A chess board style distribution would yield a minimum contagion because the black and white squares, pixels, are perfectly disaggregated and interspersed. High contagion

values indicate that the pixels are aggregated into large clusters of the same type. Contagion is related to percentage of like adjacencies and inversely related to edge density.

This landscape heterogeneity metric is particularly useful because it is sensitive to the size, shape, and orientation of land cover patches, and also the diversity of land cover types that are near each other. This makes it particularly interesting for mapping the boreal forest. The result is also relatively simple to understand as low values represent a more complex heterogeneous landscape and high values represent a simpler, more homogeneous landscape.

5.2 Methods

Heterogeneity metrics were calculated for the North American boreal forest as discussed extensively in Chapter 4. The original Global Forest Cover 2000 dataset included water as a land cover class and was therefore used to represent lakes (Hansen et al. 2013). Fire perimeter datasets were available from the United States and Canadian governments. The Alaska Fire History Database is maintained by the US Bureau of Land Management (BLM) and contains fires in Alaska dating back to 1927 (French et al. 1995). The accuracy of the Alaska fire dataset varies over time and is broadly unreliable before 1950 when the mapping procedures were standardized. Similarly for Canada, the Canadian National Fire Database (CNFD) is maintained by Natural Resources Canada (2013).

The two datasets were merged and aggregated to the same 10km resolution as the heterogeneity results rasters according to area burned and number of fires present in each grid cell. The area burned and number of fires were both normalized relative to the grid cell area (100 km^2) so when averaged for each region, the relative areas of the regions would not influence the data. Thus burned area was expressed as a percent of grid cell burned and number

of fires as fire density or number of fires per grid cell. Only fires between 1950 and 2000 were included in both Alaskan and Canadian fire maps. Fires before 1950 were unreliable in both datasets and fires after 2000 would not be included in the forest cover dataset as it was generated from circa 2000 Landsat data. Also, 50 years is approximately half of the average fire return interval for the boreal forest. This means that forests that burned before 1950 could be mature enough to burn again and should be considered background forests. Several newer fires in the datasets did burn over the top of older burn scars indicating that even relatively young stands have enough accumulated fuel that they are capable of sustaining a wildfire. The water layer in the Global Forest Cover 2000 dataset was also aggregated to same 10km resolution for lake area and number of lakes.

5.3 Results

Contagion was broadly lower in the boreal forest than neighboring regions (Figure 5.1). The mean contagion values for tundra (shown in purple), boreal forest (shown in green), and temperate forests (shown in red) were 84.42 ±11.05, 45.82 ±14.75, and 55.43 ±10.21 respectively. The boreal forest and temperate forests had similar contagion values except for the Taiga Cordillera region of the boreal forest. As discussed in Chapter 4, this region was an outlier in the boreal forest due to the Mackenzie Mountain Range which is largely unforested. This region was excluded from the analysis because it was not representative of the broader boreal forest.

The distribution of burned area and fire density were similar between regions except for the Boreal Plain and Western Cordillera, which had relatively higher fire density than burned area (Figure 5.2). The tundra had almost no fires, which was to be expected. Lake area and lake

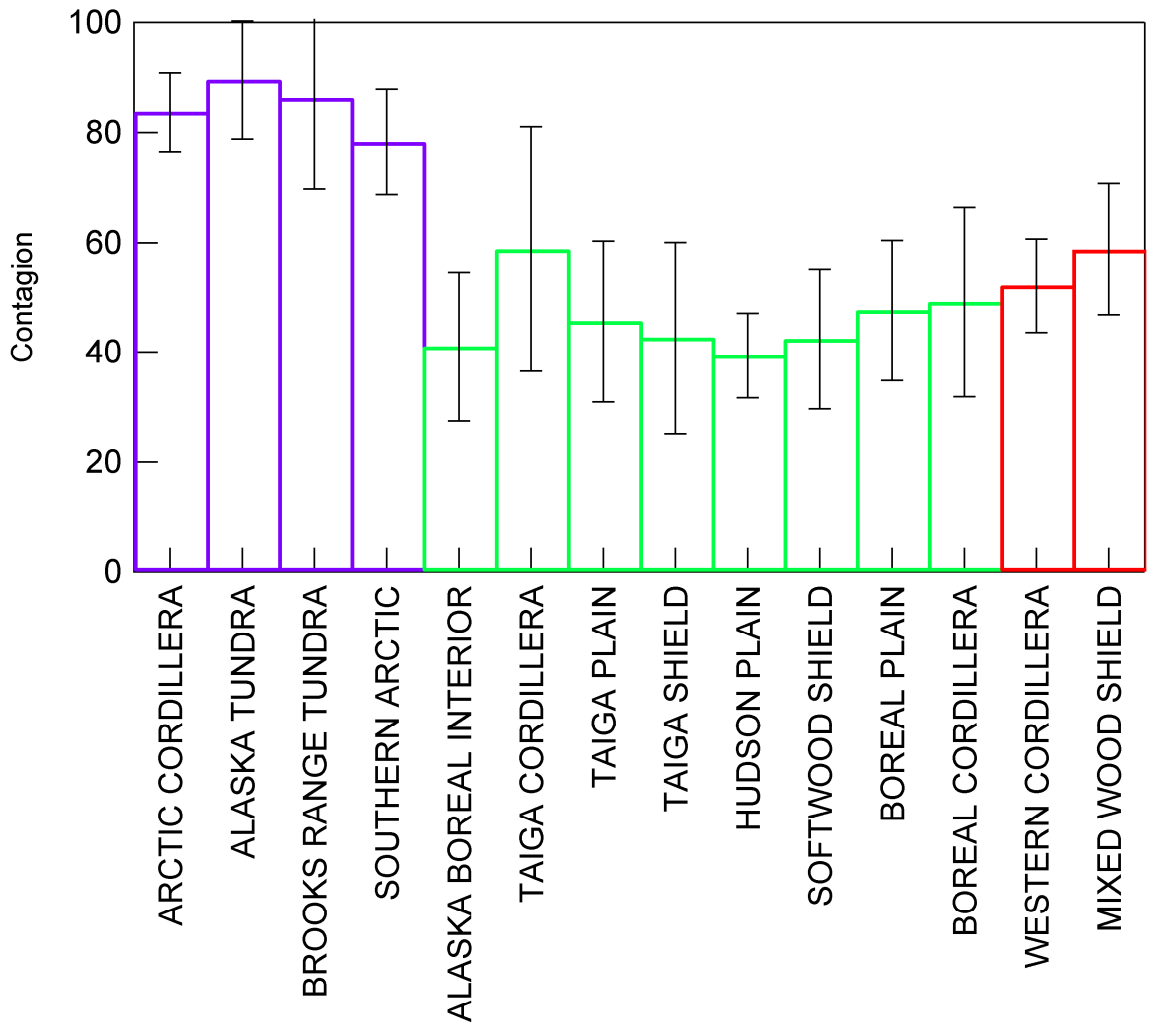

Figure 5.1 Contagion across the boreal forest and neighboring tundra and temperate forest regions. Contagion is lower in the boreal forest because many different forest cover classes are interspersed among each other.

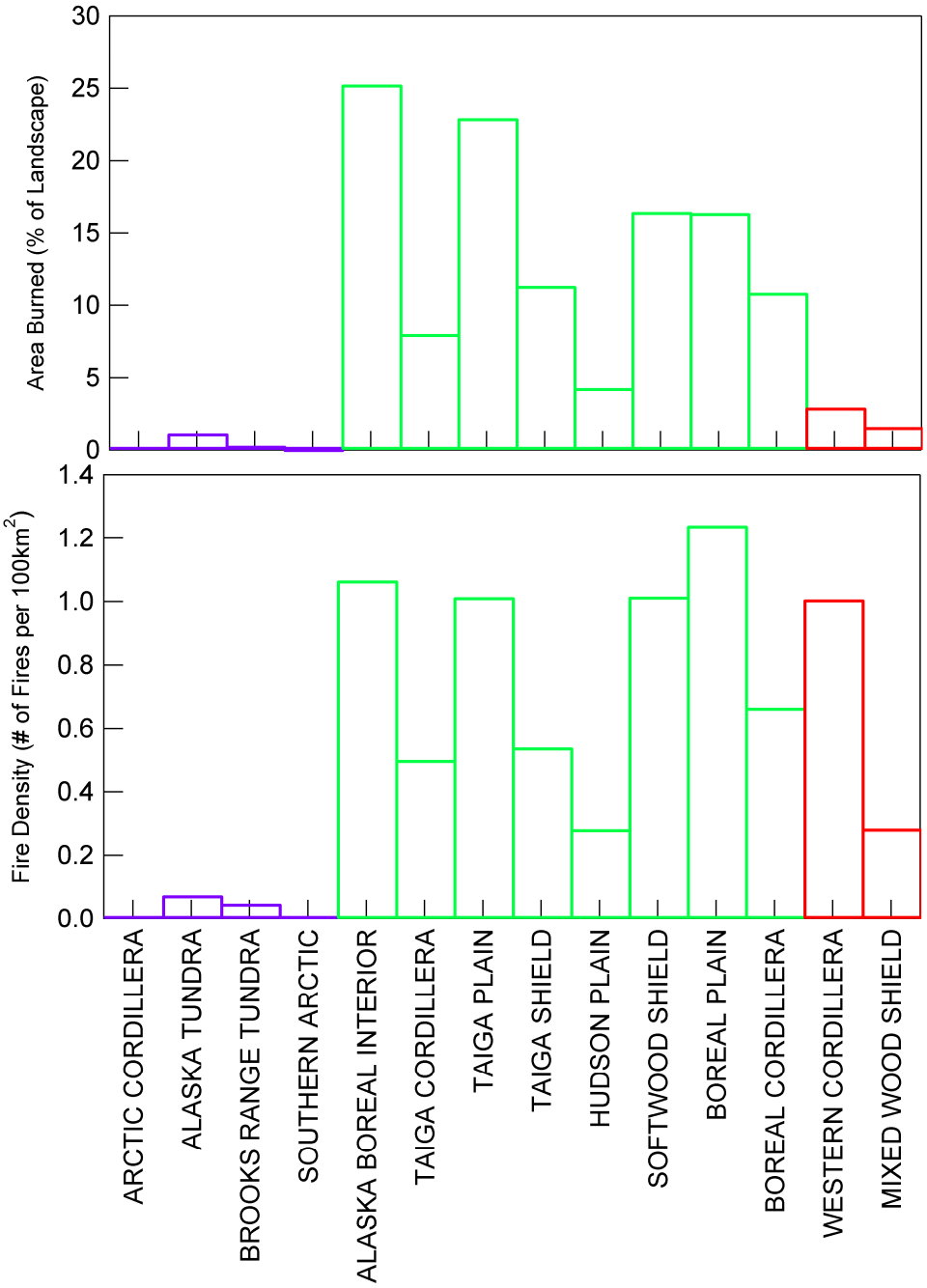

Figure 5.2 Burned area and number of fires in the boreal forest and neighboring regions.

density were more different from each other (Figure 5.3). The Taiga Plain and Taiga Shield regions had high lake area but low lake density indicating a small number of relatively large lakes. The Hudson Plain, on the other hand, had high lake density and low lake area indicating a large number of small lakes. The tundra regions generally had large lake areas and densities except for the Brooks Range Tundra which is a mountainous region.

Contagion and the four explanatory variables were compared for seven regions within the boreal forest only. The mountainous Taiga Cordillera region was not included in the analysis because it was not representative of the boreal forest. Comparing burned area and lake area to contagion was inconclusive as there was no statistically significant relationship between the variables. Fire and lake density, on the other hand, had relatively weak but still statistically significant relationships with contagion (Figure 5.4). Contagion increased with increasing fire density (p-value = 0.388) and decreased with increasing lake density (p-value = 0.078).

The opposite relationships of fire and lakes with contagion were caused by the scale difference between the two processes. The boreal forest had an average of 0.83 fires per 100 km^2 which burned 15.35% of the landscape. These fires were large and rare, at least over the 100 km^2 extent of a single grid cell. Lakes on the other hand were far more numerous than fires with a mean density of 1130.91 lakes per 100 km^2 even though they covered less of the landscape than fires with 9.48% coverage. This scale difference drove the divergent response of contagion to fire and lake density. As the number of large fires increased in a grid cell, many small forest patches were combined into large homogeneous burn, thus increasing contagion. Lakes on the other hand, were much smaller than the forest cover patches so as they increased, they tended to break them up rather than combine them together, decreasing contagion.

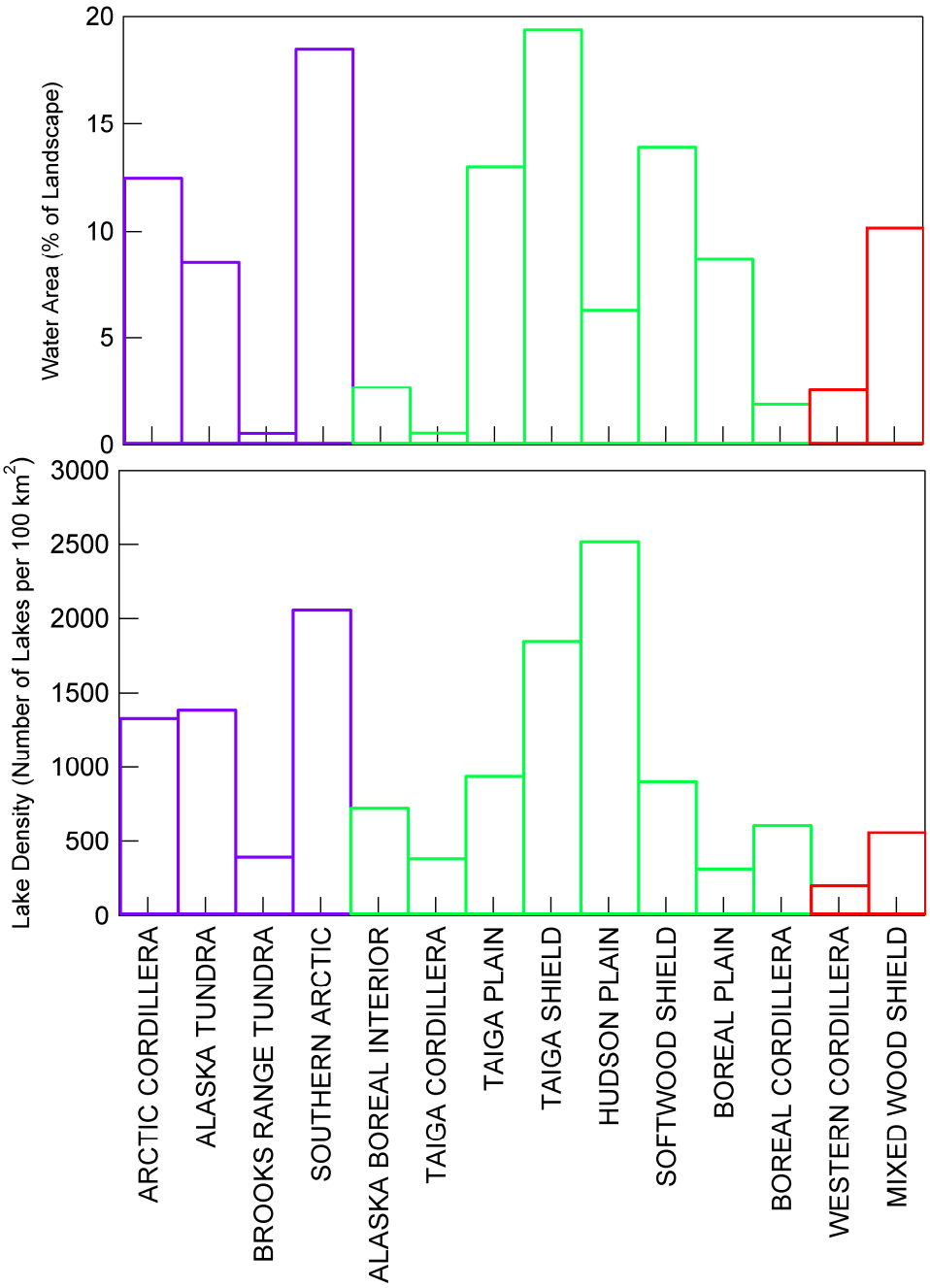

Figure 5.3 Lake area and number of lakes for the boreal forest and neighboring regions.

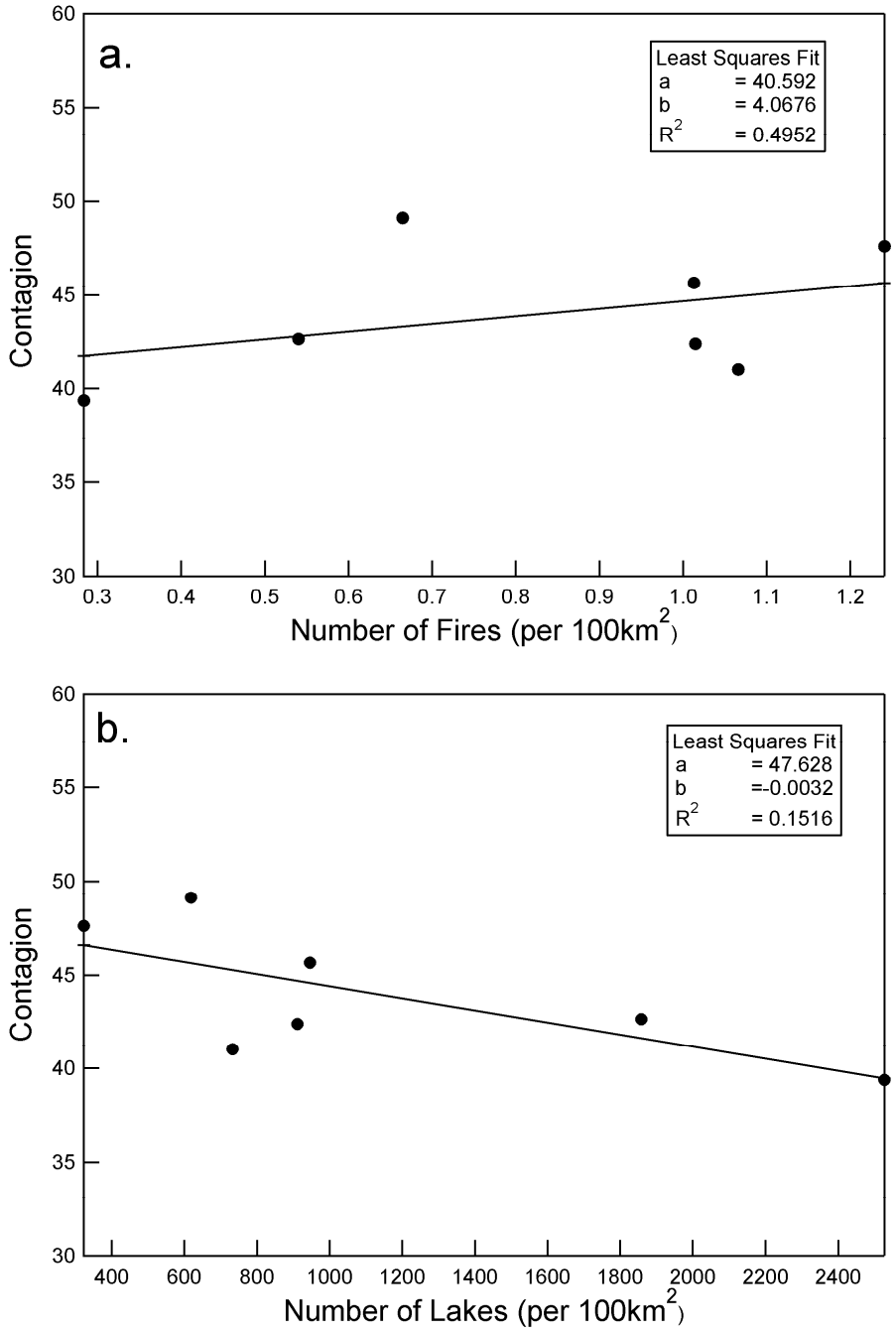

Figure 5.4 Contagion plotted with linear regression lines for (a) and number of lakes (b) for the boreal forest only.

5.4 Discussion

Boreal forest fires are expected to become more numerous, larger, and more severe with climate change (Kasischke et al. 2010; Mann et al. 2012). All of these factors would lead to an increase of contagion and decrease of heterogeneity in the boreal forest. Increased numbers of fires would increase contagion by replacing small patches of diverse forest cover classes with large homogeneous patches. Similarly, larger fires would cover a greater portion of the landscape and amplify this effect. Furthermore, the severity of fires, or depth of burning, has been shown to impact the post fire successional trajectories of recovery (Epting and Verbyla 2005; Johnstone and Kasischke 2005; Hollingsworth et al. 2013). Increased severity also tends to favor deciduous tree species post-fire. Ultimately, the expected changes to the boreal forest fire regime will likely produce a more homogeneous boreal forest landscape.

While boreal forest fires tend to be much larger than the pre-existing forest cover patches, lake sizes tend to follow a power law distribution (Lehner and Döll 2004; Hinkel et al. 2005; Smith et al. 2007). This means that there are many small lakes while large lakes are rare. It is likely that there are even more lakes that are smaller than the detection threshold for the Landsat based forest cover dataset (Lyons et al. 2013).

One potential issue with the lakes used in this study is that they were generated as a simple water cover class for the Global Forest Cover 2000 dataset and were not necessarily intended for this use. For instance, the dataset included rivers which could have influenced patch size and shape metrics. A high resolution lakes map that was purposely generated to focus on lakes would be a better analysis tool. On the other hand, from a forest heterogeneity perspective, rivers and lakes are not particularly different, so their inclusion could be seen as a benefit.

According to the results from Chapter three, the unburned forest and the oldest fires were largely indistinguishable in terms of heterogeneity. Due to the rapid growth of intermediate successional species like deciduous trees, the heterogeneity effects of forest fire appear to be relatively short-lived. A different, more recent, burned area class could have a more significant forest heterogeneity response. The other findings from Chapter three were that the younger, recently burned stands tended to have larger, more regularly shaped, and clustered patches and that coincides with the results here as well. All three of those metrics: patch size, shape index, and patch density, are related to contagion with patch size and shape index positively correlated and patch density inversely related (McGarigal 2012).

The linear relationships reported here for fire and lake density vs contagion could be an oversimplification of a set of more complex relationships as aggregating to and comparing regions downplayed the importance of outlier features. The two different relationships could also be manifestations of the same process at different scales. For instance, a small fire would likely have similar influence on contagion as a small lake, and a large lake would have similar influence as a fire of the same size. If the processes that determine the size distribution or spatial patterns of lakes or fires change significantly in the future, the relationships that those features have with forest heterogeneity will likely change as well.

Rapid changes to the spatial structure of the boreal forest driven by climate change are likely given the already observed trends in the fire regime. These changes will influence regional to global climate and may involve positive or negative feedbacks to amplify or dampen further warming. The changes will also simply alter the face of the boreal forest to something fundamentally different. This is an important impact of climate change in and of itself that should not be understated.

5.5 Conclusions

This study compared the distributions of fires and lakes across the boreal forest with the heterogeneity metric contagion. Contagion is a useful metric because it is sensitive to many aspects of landscape heterogeneity. This one metric is an efficient way to represent landscape heterogeneity. High values indicate a clustered, homogeneous landscape while low values indicate more complexity and diversity of land cover types. Contagion in the boreal forest was significantly lower than in the tundra indicating that different forest cover patches in the boreal landscape were more disaggregated and interspersed with each other. Fires and lakes were distributed unevenly throughout the boreal forest regions with much higher numbers of lakes than fires.

Landscape heterogeneity broadly increased, contagion decreased, with higher numbers of lakes and heterogeneity decreased, contagion increased, with higher numbers of fires. There was not strong relationship between burned are or total lake are with contagion. These opposite reactions were the result of the different scales that fires and lakes operate in. Fires are generally larger than the pre-existing forest patches while lakes are much smaller.

The relationships between fires, lakes and the spatial structure of the boreal forest are important to understand as the fire regime is already beginning to shift due to climate change. Fires especially are expected to become more numerous, larger, and more severe in the future which would lead to a more homogeneous boreal forest. Because of the rapid fire return time and large area burned per year, these changes can occur over a large area at decadal time scales.

5.6 References

Alaska Fire History (1950 - 2005).

(2013). Canadian National Fire Database. C. F. Service. Northern Forestry Center, Edmunton, Alberta, Canadian Forest Service.

Barrett, K., A. D. McGuire, et al. (2011). "Potential shifts in dominant forest cover in interior Alaska driven by variations in fire severity." Ecological Applications **21**(7): 2380-2396.

Brown, J., O. J. F. Jr., et al. (2002). Circum-Arctic Map of Permafrost and Ground-Ice Conditions. Version 2. N. S. a. I. D. Center. Boulder, Colorado USA.

Dyrness, C. T., L. A. Viereck, et al. (1986). Fire in taiga communities of interior Alaska. Ecological series volume 57: forest ecosystems in the Alaskan taiga. K. Van Cleve, F. S. Chapin, P. W. Flanagan, L. A. Viereck and C. T. Dyrness. New York, Springer Verlag**:** 74-86.

Epting, J. and D. Verbyla (2005). "Landscape-level interactions of prefire vegetation, burn severity, and postfire vegetation over a 16-year period in interior Alaska." Canadian Journal of Forest Research-Revue Canadienne De Recherche Forestiere **35**(6): 1367-1377.

Flannigan, M. D., Y. Bergeron, et al. (1998). "Future wildfire in circumboreal forests in relation to global warming." Journal of Vegetation Science **9**(4): 469-476.

French, N. H. F., E. S. Kasischke, et al. (1995). "Mapping The Location Of Wildfires In Alaskan Boreal Forests Using AVHRR Imagery." International Journal Of Wildland Fire **5**(2): 55-62.

Hansen, M., P. Potapov, et al. (2013). "High-resolution global maps of 21st-century forest cover change." Science **342**(6160): 850-853.

Hinkel, K. M., R. C. Frohn, et al. (2005). "Morphometric and spatial analysis of thaw lakes and drained thaw lake basins in the western Arctic Coastal Plain, Alaska." Permafrost and Periglacial Processes **16**(4): 327-341.

Hollingsworth, T. N., J. F. Johnstone, et al. (2013). "Fire severity filters regeneration traits to shape community assembly in Alaska's boreal forest." PloS one **8**(2): e56033.

Johnson, E. A. (1992). Fire and Vegetation Dynamics: Studies from the North American Boreal Forest, Cambridge University Press.

Johnstone, J. F. and E. S. Kasischke (2005). "Stand-level effects of soil burn severity on postfire regeneration in a recently burned black spruce forest." Canadian Journal of Forest Research-Revue Canadienne De Recherche Forestiere **35**(9): 2151-2163.

Jorgenson, M. T. and T. E. Osterkamp (2005). "Response of boreal ecosystems to varying modes of permafrost degradation." Canadian Journal of Forest Research-Revue Canadienne De Recherche Forestiere **35**(9): 2100-2111.

Kasischke, E. S. and M. R. Turetsky (2006). "Recent changes in the fire regime across the North American boreal region - Spatial and temporal patterns of burning across Canada and Alaska." Geophysical Research Letters **33**(9): L09703, doi:09710.01029/02006GL025677.

Kasischke, E. S., D. L. Verbyla, et al. (2010). "Alaska's changing fire regime - implications for the vulnerability of its boreal forests." Canadian Journal of Forest Research-Revue Canadienne De Recherche Forestiere **40**(7): 1313-1324.

Kasischke, E. S., D. Williams, et al. (2002). "Analysis of the patterns of large fires in the boreal forest region of Alaska." International Journal of Wildland Fire **11**(2): 131-144.

Larsen, C. P. S. (1997). "Spatial and temporal variations in boreal forest fire frequency in northern Alberta." Journal Of Biogeography **24**(5): 663-673.

Lehner, B. and P. Döll (2004). "Development and validation of a global database of lakes, reservoirs and wetlands." Journal of Hydrology **296**(1-4): 1-22.

Liess, S., P. K. Snyder, et al. (2012). "The effects of boreal forest expansion on the summer Arctic frontal zone." Climate Dynamics **38**(9-10): 1805-1827.

Liu, H. and J. T. Randerson (2007). "Interannual variability of surface energy exchange depends on stand age in a boreal forest fire chronosequence." Journal of Geophysical Research-Biogeosciences **In press.**

Liu, H. P., J. T. Randerson, et al. (2005). "Changes in the surface energy budget after fire in boreal ecosystems of interior Alaska: An annual perspective." Journal of Geophysical Research **110**: Art. no. D13101.

Lyons, E. A., Y. F. Jin, et al. (2008). "Changes in surface albedo after fire in boreal forest ecosystems of interior Alaska assessed using MODIS satellite observations." Journal of Geophysical Research-Biogeosciences **113**(G2).

Lyons, E. A., Y. Sheng, et al. (2013). "Quantifying sources of error in multitemporal multisensor lake mapping." International Journal of Remote Sensing **34**(22): 7887-7905.

Mann, D. H., T. S. Rupp, et al. (2012). "Is Alaska's Boreal Forest Now Crossing a Major Ecological Threshold?" Arctic Antarctic and Alpine Research **44**(3): 319-331.

McGarigal, K., SA Cushman, and E Ene. (2012). "FRAGSTATS v4: Spatial Pattern Analysis Program for Categorical and Continuous Maps." 2014, from http://www.umass.edu/landeco/research/fragstats/fragstats.html.

Osterkamp, T. E., L. Viereck, et al. (2000). "Observations of thermokarst and its impact on boreal forests in Alaska, USA." Arctic Antarctic and Alpine Research **32**(3): 303-315.

Payette, S., A. Delwaide, et al. (2004). "Accelerated thawing of subarctic peatland permafrost over the last 50 years." Geophysical Research Letters **31**(18).

Pielke, R. A. and P. L. Vidale (1995). "The boreal forest and the polar front." Journal of Geophysical Research-Atmospheres **100**(D12): 25755-25758.

Randerson, J. T., H. Liu, et al. (2006). "The impact of boreal forest fire on climate warming." Science **314**(5802): 1130-1132.

Smith, L. C., Y. Sheng, et al. (2005). "Disappearing Arctic lakes." Science **308**(5727): 1429-1429.

Smith, L. C., Y. W. Sheng, et al. (2007). "A first pan-Arctic assessment of the influence of glaciation, permafrost, topography and peatlands on northern hemisphere lake distribution." Permafrost and Periglacial Processes **18**(2): 201-208.

Van Cleve, K. and L. A. Viereck (1981). Forest succession in relation to nutrient cycling in the boreal forest of Alaska. Forest Succession: Concepts and Application. D. C. West, H. H. Shugart and D. B. Botkin. Berlin, Springer**:** 185-211.

Viereck, L. A. (1973). "Wildfire in the taiga of Alaska." Quaternary Research **3**: 465-495.

Viereck, L. A. (1983). The effects of fire in black spruce ecosystems of Alaska and northern Canada. The Role of Fire in Northern Circumpolar Ecosystems. R. W. Wein and D. A. MacLean. Chichester, John Wiley and Sons**:** 201-220.

Yoshikawa, K. and L. D. Hinzman (2003). "Shrinking thermokarst ponds and groundwater dynamics in discontinuous permafrost near Council, Alaska." Permafrost and Periglacial Processes **14**(2): 151-160.

Chapter 6

Summary and Conclusions

The boreal forest is a diverse and dynamic landscape. While not particularly diverse in plant species, the landscape is patterned with diverse land forms like lakes, meadows, and patches of forest in various stages of recovery from fire. This subtle complexity is often not taken into account in regional to global scale climate studies as they generally treat the boreal forest as a giant homogeneous carpet of trees wrapping around the sub-Arctic. These spatial patterns and heterogeneities in the boreal landscape are actually very important to the region's interactions with the broader climate and fundamental to its continued existence.

This dissertation first investigated the landscape heterogeneity and rates of land cover change in a sub-region within the boreal forest using Landsat satellite data and fire scar maps. Between 1992 and 2009, up to 35% of the landscape underwent some land cover change and that change was predominantly caused, either directly or indirectly, by fire. Because so much of the area of the boreal forest is impacted by fire over a relatively short time period, there are few, if any, pure, undisturbed, climax forests. This is a fundamentally different way of thinking about forests than those in temperate or tropical regions. Rather than searching for an undisturbed forest stand to represent the broader boreal forest as a field site or to parameterize surface fluxes in a model, the entire changing landscape must be taken into account. The boreal forest is in a constant state of flux which makes it particularly susceptible to climate change. Rapid changes to the spatial structure of the boreal forest driven by climate change are likely given the already observed trends in the fire regime. These changes will influence regional to global climate and

may involve positive or negative feedbacks to amplify or dampen further warming. The changes will also simply alter the face of the boreal forest to something fundamentally different. This is an important impact of climate change in and of itself that should not be understated.

Within recent burn scars, less than 22 years old, the landscape heterogeneity and pattern was very different from older burn scars as forest patches in recent burns tend to be larger, more regularly shaped, and densely packed than unburned stands. Those recently burned areas were rapidly colonized by early and mid-successional plants like grasses and mixed forest stands and their heterogeneity metrics approached their previous values but the creation of dense "mature" forest stands is much slower.

Based on those preliminary, small scale results, I went on to produce a novel dataset that measured the spatial pattern of forest cover in the boreal region of North America. This involved 34 landscape metrics and 33 land cover class specific metrics for five classes were calculated from a global forest cover dataset and gridded at 10km resolution. The final resolution and extent of analysis for each grid cell was selected to produce the finest resolution result maps possible while maintaining a large enough extent to calculate indices and avoid spatial autocorrelation issues. The value of this dataset will outlive this dissertation as continuing analysis will find more useful information in the future. First, the heterogeneity rasters were aggregated to regions within and neighboring the boreal forest.

The boreal forest had broadly smaller, more regularly shaped patches that were moderately clustered. It was more diverse than the tundra, unsurprisingly, but also more diverse than the more temperate hardwood forests to the southeast and southwest than the boreal forest. The high levels of dispersion and interspersion of small forest cover patches resulted in lower

contagion values than surrounding regions. The mean fractal dimension for the boreal region was 1.384 ±0.024 which was significantly higher than the tundra and the temperate Mixed Wood Shield regions. The high fractal dimension indicated complex landscapes within the boreal forest. Patch cohesion for specific forest cover classes indicated that although the tundra and temperate forest regions reach the percolation threshold, the boreal forest never did. There was no dominant forest cover type in the boreal forest. The boreal forest should therefore not be considered a continuous forest with patches of light and moderate density sprinkled throughout. Rather, it is a patchwork of forest patches that are too numerous and diverse for any of them to be considered dominant. This result supports the earlier conclusion that there were no truly "mature" climax forests in the boreal forest because of the rapid fire return interval.

At the northern edge of the boreal forest the 0-25% forest cover class did become dominant, with patch cohesion values above the percolation threshold at 99.96%. The southward extent of the tundra dominated landscape was used as an indicator for the location of the border between the boreal and tundra ecosystems. This proved to be a superior definition for this border than the northern extent of individual trees, which has been used previously. The sparse cover class extended did further south than previous treeline estimates, particularly in Canada. This was due to an extensive taiga transitional zone between the pure boreal and tundra regions on the Canadian Shield. This region was previously included in the boreal forest because there were small clusters of trees but the new patch cohesion threshold method considers this region to be tundra.

The relationships between fires, lakes and the spatial structure of the boreal forest are important to understand as the fire regime is already beginning to shift due to climate change.

Landscape heterogeneity broadly increased, contagion decreased, with higher numbers of lakes and heterogeneity decreased, contagion increased, with higher numbers of fires. There was not strong relationship between burned are or total lake are with contagion. These opposite reactions were the result of the different scales that fires and lakes operate in as fires are generally larger than the pre-existing forest patches while lakes are much smaller. Fires especially are expected to become more numerous, larger, and more severe in the future which could rapidly lead to a more homogeneous boreal forest.

The analysis performed in this dissertation was the first of many to come. This boreal forest heterogeneity map contains far more information waiting to be pulled out. The automated processes employed here can easily be expanded to incorporate the Eurasian boreal forest and even temperate and tropical forests in the future. For maximum impact, the results now must be made available to the modelling community in a way that is useful and compatible with their models. These, and other challenges, remain and inspire me to continue pushing forward to improve our understanding of the dynamic and vital boreal forest.